The Dissertation Committee for Nazmus Sakib
Certifies that this is the approved version of the following Dissertation:

Towards a better understanding of bitumen chemistry, microstructure, and rheology

Committee:

Amit Bhasin, Supervisor

Gaylon Baumgardner

Adalberto L. Faxina

Maria G. Juenger

Navid Saleh

Towards a better understanding of bitumen chemistry, microstructure, and rheology

by

Nazmus Sakib

Dissertation

Presented to the Faculty of the Graduate School
of The University of Texas at Austin
in Partial Fulfillment
of the Requirements
for the Degree of

Doctor of Philosophy

The University of Texas at Austin

December 2018

I dedicate this work to my family.

Acknowledgments

I want to thank my supervisor, Dr. Amit Bhasin for guiding me through the long path of doctoral degree. It has been a great privilege to work with him. He helped me to develop not only as a researcher but as a better person.

I want to thank my friends, both in USA and Bangladesh, who helped me and my family to get through the tough times. In times of need, We always found our friends in Austin with us, for which we are ever grateful.

I want to thank the great state of Texas and The University of Texas at Austin for enabling me to pursue my goals and for offering unparalleled opportunity for my development. I also want to thank the city of Austin and Austinites for their warm hospitality.

I want to thank the government and the people of Bangladesh for supporting my pursuit of education. I am forever indebted to the sacrifices made by the people of Bangladesh for my betterment.

I want to thank my parents who supported me in every step of my life and made countless sacrifices for my well-being. I also thankful to my parent-in-laws who encouraged and supported us to go through many tough times.

Finally, I want to thank my wife, Nitu and my daughter, Inaaya. My wife's encouragement was my source of hope which helped me to pass the challenging times. I am ever grateful for her incomparable sacrifices for the family. My daughter has been the best thing in my life. She is the source of joy and happiness that refresh us everyday and give meaning to our lives.

Abstract

Towards a better understanding of bitumen chemistry, microstructure, and rheology

Nazmus Sakib, Ph.D.

The University of Texas at Austin, 2018

Supervisor: Amit Bhasin

Bitumen is the residua of fractional distillation of crude oil. It generally consists of complex and a diverse variety of organic molecules and other heteroatoms. The nature and interactions between these molecules dictate the engineering properties of the bitumen. One of the attributes used to classify and examine these diverse constituent molecules is based on their relative polarities. Typically a bitumen is classified into four polarity based fractions, namely saturates, aromatics, resins and asphaltenes (SARA) using physical separation by precipitation and chromatography. Such separations require specialized equipment and expertise. In this study, two new fast and repeatable techniques of chromatography using disposable and inexpensive parts were developed. One of these methods was then used to fractionate a large set of bitumens in order to compare the constitution of the bitumens based on these fractions to their rheological, mechanical, and microstructural properties. Results show that parameters based on bitumen stiffness and tensile strength correlate well with these fractions. Similar relationship with more time dependent parameters was not conclusive. Microscopic observation of surface microstructures indicates similarity among bitumens from the same producer. There was also a good correlation between SARA parameters and surface microstructure for bitumens from the same producer. However, this relationship

was unique for each producer and not global suggesting that other factors related to the crude source need to be considered as well.

Contents

List of Tables

List of Figures

Chapter 1

Introduction

Bitumen is one of the most important engineering materials in the world. It is estimated that there are about 2.7 million miles (about 9 million lane miles) of paved road in United States, of which 94% has bituminous surface layers (FHWA 2016). Bitumen can be derived from oil sands or by refining of crude oils, the latter being the most common source of paving bitumen. During refining of crude oil, lighter fractions such as diesel, gasoline, kerosene, jet fuel are extracted by fractional distillation. After removal of lighter bottom residual fractions such as gas oil (for creating lighter fuel by hydrocracking), the remaining residua is usually further modified and/or processed and sold as bitumen. Compositional characteristics of a bitumen vary widely depending on the source of the crude oil, processes used to fractionate the crude oil, and post-processing of the residua to produce bitumen. For example, USA and Arabian crude oils generally have less density and are rich in lighter fractions while Mexican and Canadian crude oils tend to be rich in heavier fractions. Even within a similar geological zone, crude composition can vary significantly from one source to another.

Classification of paving bitumen is typically done based on its ability to withstand common distresses that it may be exposed to during its service life without rendering the pavement to premature failure. Bitumen is a viscoelastic material which indicates that loading time and temperature have a significant effect on bitumen behavior. Bitumen selection and qualification process for use in a pavement relies on a few mechanical tests and associated parameters, mostly based on rheology. This is done with an intent to avoid two most common types of distresses: permanent deformation and low temperature cracking. Bitumen is more susceptible to permanent deformation at increased temperature, reduced aging, and slower traffic speeds (or standing traffic). A high temperature grade is typically assigned to the bitumen based on stiffness and viscoelastic behavior. This high temperature grade indicates the maximum temperature the bitumen can experience in a pavement without becoming susceptible to rutting. As pavement temperatures fall, flexible pavements develop thermal stresses. A properly selected bitumen can 'relax' and dissipate these thermal stresses before they exceed its tensile strength

and result in transverse cracking. The thermal stresses are directly related to the stiffness of the bitumen and inversely related to the rate at which the bitumen can relax. These properties are used to determine the low temperature grade of the bitumen, which indicates the lowest temperature at which the bitumen can be used in the field without becoming susceptible to transverse cracking. These two temperatures (high and low grade) are the basis of Performance Grading (PG) which dictates the climatic temperature range within which a given bitumen can be used. There are also other tests to capture bitumen physical properties, some of which are incorporated into different agencies' specification. These tests capture creep-recovery characteristics, tensile strength, elastic recovery of bitumen, among others.

Many of these tests and parameters associated with the Performance Grading or PG framework (as of this writing) are shown to have a weak relationship with actual field performance (Delgadillo et al. 2006, D'Angelo 2009, Batista et al. 2017, Hajj and Bhasin 2017). In addition, bitumen producers, contractors, and agencies are keen to utilize new modifiers and extenders such as polymers, bio-binder, reclaimed asphalt in order to reduce life-cycle cost and adverse environmental impact. While these modified bitumens meet the specification benchmarks, their field performance was understandably less predictable (Batista et al. 2017). In fact, lack of such correlation made way for additional tests (PG plus) such as multiples stress creep recovery test. Despite these efforts, catching up with the current stream of inventions of new products such as polymers, nano-materials, bio-binders, rejuvinators, is very challenging.

Bitumen is a blend of a very large variety of predominantly complex organic molecules. Therefore, it is common practice to examine the chemical characteristics of bitumen on the basis of attributes such as relative polarities of molecules, size distribution, ionic character, and functional group concentrations. It is also important to emphasize that on a comparatively micro-scale, bitumen is known to be microscopically heterogeneous. Bitumen surface usually has certain structures known as 'bee' structures (Loeber et al. 1996, Claudy et al. 1992). Ramm et al. (2016) also shown that bitumen has bulk microstructures and these structures can potentially dictate temperature dependent properties of bitumen. Therefore, it can be deduced that chemical composition also influences microstructures which was

the subject of several past studies (Schmets et al. 2010, Menapace et al. 2016, Jahangir et al. 2015, Nahar 2016). On a macro-scale, chemistry can potentially influence bitumen properties including, but not limited to, properties that dictate the PG grade of a bitumen. Recognizing the significance of chemical composition, several previous studies correlated parameters based on chemical composition to performance benchmarks of bitumen with various degrees of success (Weigel and Stephan 2018, Stangl 2010, Pauli and Branthaver 1998, Isacsson and Zeng 1997, Baumgardner 2012, Hajj et al. 2017) . However, due to restrictive technological issues, both microstructure and chemical evaluation of bitumen were limited to few samples of bitumen by most researchers.

The theme of this dissertation is to address the challenges of understanding bitumen chemistry and the influence of chemistry on properties evaluated at different length scales (micro and macro). The following sections of this dissertation are arranged in the order that goes from method development and verification to utilizing the newly developed methods toward advancing current understanding of the aforementioned relationships. The dissertation is organized in form of three separate papers which make up Chapters 2 to 4. Organization of the succeeding sections is discussed below.

The second chapter of this dissertation details two new techniques of bitumen fractionation into four chemical species (commonly known as SARA). Basis of both of these methods lies on existing theories for chromatographic separation of bitumen but one used liquid chromatography and the other used thin layer chromatography. These techniques, compared to existing practices, offered faster fractionation of bitumens, reduced cost of setup and operation, better repeatability and consistency due to use of commercially available consumable parts and overall safer practice due to reduced consumption of solvents. The results from the proposed methods and an established procedure (ASTM D4124) were compared semi-quantitatively for verification.

The third chapter is on the creation of a dataset involving about 100 bitumen samples in different aging conditions. These samples were subjected to chemical fractionation using the liquid chromatographic method (TexSARA), which is one of the two methods described in Chapter 2. A matrix of different physical and mechanical tests was performed on these bitumens. Data obtained

from these tests and chemical fractionation information were compared and a prediction model was developed for some of the mechanical properties.

The fourth chapter offers a discussion on bitumen microstructure and its relation with bitumen chemistry. A recent microscopy method, which offers fast and easy imaging on bitumen microstructure, enabled microstructure imaging of unaged and short-term aged bitumens. Chemical makeup of these bitumens are known using the method described in Chapter 2. The microstructure images were qualitatively and quantitatively analyzed to observe the effect of aging and source dependency as well as identification of unusual bitumens. Comparison of the quantitative parameters and chemical fractions helped to develop a better understanding of this interrelationship.

The fifth chapter summarizes the observations made in previous chapters and outlines potential researches that may follow this current work.

Chapter 2

Estimating polarity-based distribution of bitumen using simplified chromatographic techniques [1]

2.1 Overview

The chemical composition of bitumen dictates its rheological properties as well its expected performance in an asphalt mixture. Amongst the different attributes that can be used to describe the chemistry of any given bitumen, the distribution of its constituent molecules based on polarity is strongly related to the bitumen's microstructure and engineering properties. However, quantifying this distribution is a time consuming technique with multiple variations. Generally, bitumen is subdivided into asphaltenes and maltenes. The latter is further divided into three more fractions: saturates, aromatics and resins. This paper reviews the basic principles of liquid chromatography and presents a simplified technique for asphaltene-maltene separation and two new methods for maltene fractionation.

The two methods for maltene fractionation are based on chromatographic principles. The first method applies the thin layer chromatographic technique combined with optical fluorescent densitometry for separation and quantification.

The second method utilizes solid phase extraction (SPE) cartridges, which are commercially available in pre-packed standard units and allow rapid and repeatable testing when used as a mini liquid chromatography column. Both methods are scalable to quantify more than three maltene fractions. The proposed methods were semi-quantitatively validated using ten bitumens with known polar fractions.

The simplicity, the minimal requirement of capital equipment, and the monitoring time makes the proposed method an attractive option for use as a routine test to create a sizable database of bitumen fingerprints based on their polarity.

[1] Substantial part of this chapter has been published in the International Journal of Pavement Engineering. Sakib, N. and Bhasin, A., (2018). "Measuring polarity-based distributions (SARA) of bitumen using simplified chromatographic techniques". *International Journal of Pavement Engineering*.

2.2 Introduction

The chemical makeup of bitumen dictates its engineering properties and ultimately its field performance when used in an asphalt mixture. Despite its significance, a detailed description of the chemical composition of bitumen is particularly challenging because it contains innumerable and complex molecular structures that vary by crude oil source, refining process, and the batch of crude oil. A more practical approach is to characterize bitumen chemistry based on different attributes such as elemental composition, acid-base characteristics, types and abundance of functional groups, molecular size distribution, and polar characteristics.

Among these, the distribution of molecules based on their polarity (herein after referred to as polarity-based distribution for brevity) has been shown to have a strong relationship with engineering properties and performance of bitumen in a mix (Redelius and Soenen 2015, Soenen et al. 2006, Isacsson and Zeng 1997, Santagata et al. 2009).

Chromatographic separation of bitumen has been utilized since 1970's typically dividing bitumen into four polarity based fractions: saturates, aromatics, resins and asphaltenes (commonly abbreviated as SARA fractions) (Jewel et al. 1972, Corbett 1969). Saturates, aromatics, and resins are also collectively referred to as maltenes. It must be emphasized here that these four polar fractions are not discrete entities in any given bitumen but rather discretization of a continuous spectrum of polar molecules (Redelius 2000). Chromatographic techniques are commonly used with bitumen samples to obtain polarity-based distributions such as SARA. The following section review some of these methods.

2.3 Background

Asphaltenes are generally separated as precipitates from the dissolution and filtration of bitumen in a nonpolar solvent (ASTM D6560 2012, ASTM D4124 2009, ASTM D2007 2016, ASTM D3279 1997). Choice of the non-polar solvent varies between standards but most methods use heat (under reflux) to dissolve the bitumen (maltene) into solution.

After separating asphaltenes and maltenes, the latter are further separated us-

ing liquid or thin layer chromatography. There are several variations of liquid chromatographic (LC) methods which involve different chromatographic mediums, such as Attapulgus clay, alumina, amino-silane, cyano-silane, silica gel, glass beads, Polytetrafluoroethylene (PTFE) (Boysen and Schabron 2015, ASTM D4124 2009, ASTM D3279 1997) as well as different elution solvents (elutants) and proportions. One of the most commonly used standards, ASTM D4124, utilizes a 70-cm long and 1.5-cm diameter closed glass liquid chromatography column which is manually packed with calcined Alumina.

Another common practice is the use of thin layer chromatography (TLC) for separation followed by quantification using Flame Ionization Detector (FID) (Karlsen and Larter 1991, Wan et al. 1992, Vela et al. 1995, Suzuki 1972). A standard silica gel-coated rod is spotted with bitumen solution and developed using different solvents to separate bitumen fractions spatially. The rod is then placed in a device (e.g. Iatroscan) which 'burns' the organics with a hydrogen flame to measure eluted fractions accumulated at different spots on the rod (IP469 2006). This TLC-based method uses a small amount of material and offers fast analysis.

Several researchers have studied quantitative SARA fractionation through TLC-densitometry. Cebolla and his colleagues made important contributions to establish TLC-Densitometry as viable quantification technique (Cebolla et al. 1999, 2002, 2003, 2016, Matt et al. 2002). Cebolla et al. (1999) used TLC to separate lubricant and gas oil into SARA fractions followed by quantification through fluorescence scanning using a commercial TLC scanner. They utilized berberine sulfate impregnated plates for saturate identification. In another noteworthy work, Matt et al. (2003) applied HPTLC on gas oil with densitometric quantification. The authors used three types of thin layer chromatography plates (berberine impregnated, regular and caffeine impregnated) to evaluate gas oil fractions using a commercial TLC Scanner.

Kharrat et al. (2007) noted that differences in solvent type, solvent quantity, column size, material, temperature (as suggested by different standards and methods) yield widely different bitumen fractions despite all being called SARA. Apart from the lack of a universal standard, current SARA fractionation methods pose a number of practical challenges as well:

1. long testing time per bitumen sample (regular column LC),

2. large sample and solvent requirement (regular column LC),

3. excessive loss of lighter fractions (TLC-FID),

4. expensive setup (TLC-FID and Densitometry with commercial TLC scanner), and

5. extended monitoring and supervision (asphaltene separation, regular column LC).

These practical concerns limit the use of fractionation tests on a routine basis particularly in laboratories not specializing in analytical chemistry (Boysen and Schabron 2015, Fan and Buckley 2002). These challenges, combined with multiple disparate definitions of SARA, prohibit researchers from constructing a sizable database of bitumen fractions and investigating the correlation with performance and engineering properties on a larger and global scale.

2.4 Scope

The focus of this study was to overcome the aforementioned challenges and develop low-cost, fast and repeatable alternative test methods that can be used on a routine basis by materials engineers to quantify polar characteristics of different bitumen. The ultimate and long-term goal of this research initiative is to facilitate development of a database of bitumen properties that cover both engineering and chemical properties.

The first part of the paper describes the rationale and development of a method to separate asphaltene and maltenes. The second part of the paper presents the rationale and development of two different procedures to separate maltenes into saturates, aromatics and resins (although the procedure is easily scalable to quantify more than three fractions).

One of these two methods is based on thin-layer chromatography (TLC) combined with densitometry or photographic quantification. The other method is based on liquid chromatography and utilizes commercially available pre-packed solid phase extraction (SPE) cartridges. To summarize, this study engages in the development of a method for asphaltene separation and two new methods for

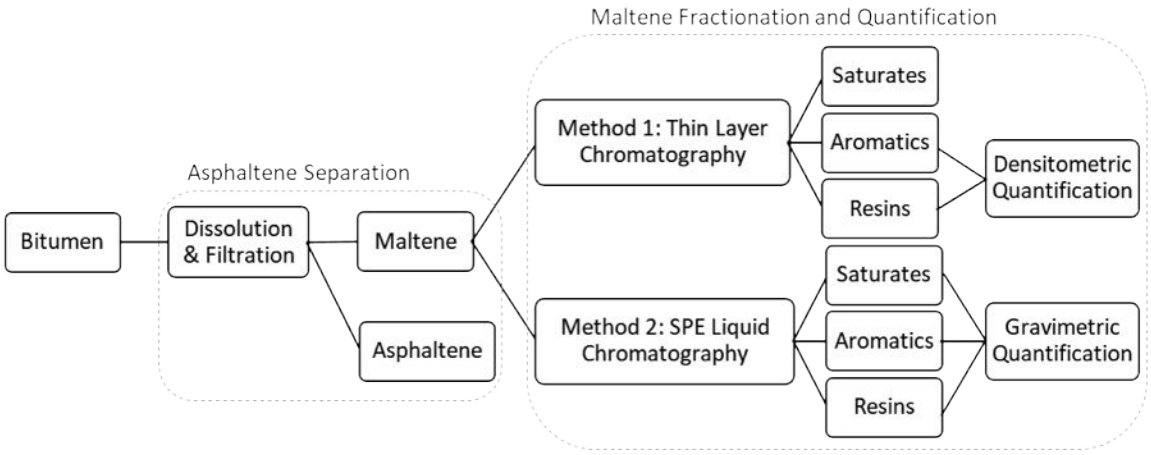

Figure 2.1: Organization of the current research

maltene fractionation into three (or more) sub-fractions along with quantification of each fraction.

Figure 2.1 presents a flowchart showing the research steps.

Before proceeding, it is important to emphasize that the authors are aware of the disparate definitions of SARA in practice and literature. The primary purpose of this study was not to introduce “yet another" definition and method for SARA, although that was a necessary byproduct. Rather, the primary goal was to develop an efficient procedure that can be used with a large number of bitumens on a routine basis.

2.5 Materials

Two base bitumens (PG64-22 and PG67-22) were separated into SARA fractions using ASTM D4124 (2009) as a part of a previous study (Sultana 2014). Each of the separated fraction was used to ‘spike’ the corresponding base bitumen and to create two sets of four new bitumens. The ‘spiked’ bitumens had fractions that were about 34% more than their original proportion (relative to other unchanged fractions). These ten bitumens with previously known SARA fractions were acquired and used as the basis of this study (Table 2.1).

It should be recognized that the methods proposed in this study are different

from ASTM D4124. Therefore, although a a quantitative match cannot be expected, the viability of the proposed method can be demonstrated via a semi-quantitative comparison.

Table 2.1: SARA fractions in percentage of the two base and eight 'spiked' bitumens according to ASTM D4124 (Sultana 2014).

Bitumen		Saturates	Aromatics	Resins	Asphaltenes
Bitumen 1 (PG 64-22)	Base bitumen	14.5	42.7	24.8	18.2
	Saturate-spiked	18.6	40.7	23.6	17.4
	Aromatic-spiked	12.7	50.0	21.6	15.9
	Resin-spiked	13.4	39.4	30.7	16.8
	Asphaltene-spiked	13.7	40.2	23.3	23.0
Bitumen2 (PG 67-22)	Base bitumen	15.1	43.0	19.6	21.8
	Saturate-spiked	18.8	41.1	18.8	20.8
	Aromatic-spiked	13.3	49.6	17.3	19.2
	Resin-spiked	14.2	40.5	24.2	20.5
	Asphaltene-spiked	14.1	40.3	18.4	26.6

2.6 Asphaltene-Maltene Separation

The initial step of bitumen fractionation involves separation of asphaltenes from maltenes. This section presents the literature and theory relevant to asphaltene separation along with the explanation for the choices that were made during method development.

2.6.1 Rationale for Choice of Solvent

The separation of asphaltenes and maltenes involves dissolving the bitumen into a non-polar solvent followed by filtration of the precipitated asphaltene. The key attributes of several different standards are summarized below:

1. 1:10 w/v solution in *n-pentane* swirled in a warm water bath dissolved; filtered using rapid filter paper (ASTM D2007 2016)

2. 1:100 w/v solution in *iso-octane* prepared under reflux for 3-4 hours; filtered using a medium porosity (10-15 μm pore size) Buchner funnel filter (ASTM D4124 2009).

3. 1:30 w/v solution in *n-heptane* prepared under reflux for 60 minutes; filtered using a Whatman Grade 42 (2.5 μm pore) filter paper (ASTM D6560 2012)

4. 1:100 w/v solution in *n-heptane* prepared under reflux for 20 minutes; filtered using a glass microfiber filter pad with 1.5 μm pore size (ASTM D3279 1997).

Several variations of the above mentioned methods can also be found in the literature (Schabron and Rovani 2008, Schabron et al. 2010).

It is evident from the aforementioned summary that different standards call for different solvents, ratios, filter sizes and filter medias.

The solvents determine the threshold value of polarity of the asphaltene that would be precipitated. It is important to briefly review solubility parameters and their effect on asphaltene precipitation in order to better understand the precipitation process.

For a given solvent, Hildebrand (1936) proposed a single parameter solubility factor (δ_T) based on liquid cohesion energy and molar volume. Hansen (1967, 2007) divided that single factor into three Hansen Solubility Parameters (HSP): dispersion interaction (δ_D MPa$^{1/2}$), dipole interaction (δ_P MPa$^{1/2}$), and hydrogen-bonding interaction (δ_H MPa$^{1/2}$). Relative solubility between two substances is estimated by the 'distance' between corresponding HSPs in three-dimensional space (created by three HSP parameters), represented by R_a. Theoretically, there is a spherical zone around each substance in HSP-space within which any solvent (meaning, HSP parameters of the solvent lying within the sphere) will dissolve the substance. The radius of this sphere is referred to as the interaction radius (R_0). The ratio of R_a to R_0 is referred to as the relative energy difference (RED). A RED$\leq$1 indicates a good solvent for a given substance and vice versa. This theory can be extended to a mixture of solvents where the resulting solubility is the weighted sum of solubility of the solvents according to their volume fraction.

Tables 2.2 and 2.3 represent a compilation of measured HSP values for a typical asphaltene specimen and HSP parameters for the solvents of interest, respectively. HSP values of a representative asphaltene (and its parent bitumen and maltene)

Table 2.2: HSP of bitumen, asphaltene and maltene (Redelius 2004)

Material	δ_D MPa$^{0.5}$	δ_P MPa$^{0.5}$	δ_H MPa$^{0.5}$
Bitumen	18.4	3.9	3.6
Maltene	17.7	5.8	2.5
Asphaltene	19.6	3.4	4.4

come from Redelius (2004). He used 48 solvents to find the solubility parameters of asphaltene and maltene fraction of a Venezuelan crude where the fractions were derived from partial dissolution in heptane (Table 2.2). These parameters were used to estimate typical RED values for common solvents as seen in Table 2.3. As a side note, it is important to recognize that these parameters were derived using a maltene, where the definition of the maltene itself was contingent on the solution used to obtain it.

Table 2.3 illustrates the relative ability of different solvents to dissolve asphaltenes and maltenes.

For example, RED values for aromatic hydrocarbons are very close to each other and lie on the margin of the solubility sphere; hence they can not be chosen. In case of cyclic alkanes, the difference between RED values for asphaltene versus maltene (Δ_{RED}) is about 0.5-0.6 which may not be adequate to delineate these two fractions. However, they can be considered as potential candidates. On the other hand, n-alkanes have the highest value for Δ_{RED}, which makes them an excellent candidate for asphaltene separation. Readers may note that maltenes have a RED value that is greater than 1.0, indicating that maltenes may not completely dissolve in these solvents. As such, some maltene may also precipitate along with asphaltene. The extent of such precipitation and consequently the asphaltene content will vary with the choice of solvent. This is a systematic bias inherent to this procedure.

The choice of a solvent from these alkanes cannot be resolved using solubility factor alone; hence practical considerations such as boiling point, vapor pressure, toxicity, flammability, and autoignition temperature should all be considered in solvent selection. While many of the parameters are very similar, low boiling points and high vapor pressure make n-hexane less desirable. Between n-heptane and iso-octane, the former was chosen because of its more prevalent use in the literature, therefore allowing some level of comparison.

Table 2.3: RED parameters of asphaltene and maltenes for different non-polar solvents and relevant solvent information

Solvents	δ_D	δ_P	δ_H	RED Values		
				Asphaltene	Maltene	Δ
Class: Alkane						
iso-Octane	14.3	0.0	0.0	2.3	1.4	0.9
n-Hexane	14.9	0.0	0.0	2.1	1.3	0.8
n-Heptane	15.3	0.0	0.0	1.9	1.2	0.7
Class: Cyclic Alkane						
Dimethyl Cyclohexane	16.1	0.0	1.1	1.6	1.0	0.6
Cyclohexane	16.8	0.0	0.2	1.5	1.0	0.5
Class: Aromatic						
Benzene	18.4	0.0	2.0	0.9	0.9	0.0
Xylene	17.6	1.0	3.1	0.9	0.7	0.2
Toluene	18.0	1.4	2.0	0.8	0.7	0.2

Note: δ is in units of $MPa^{0.5}$

2.6.2 Asphaltene Separation Method

Dissolution

The process of dissolving bitumen usually involves heating and stirring it with the solvent for a period of time that can vary from 20 minutes to 3 hours (depending on the standard being used) at a temperature near the boiling point of the solvent, followed by 2-3 hours for cooling and flocculation. As n-heptane is volatile, combustible, and toxic, the process is done under reflux. This necessitates a temperature-controlled heating plate, reflux equipment and accommodation such as Erlenmeyer flask, Allihn reflux condenser and cooling water supply. The following method was developed and utilized to minimize space, equipment, and operator supervision time.

In order to simplify the asphaltene separation process and reduce operator supervision, dissolution of bitumen into the solvent was carried out at room temperature using the procedure described below.

A small amount of bitumen (≈ 0.5 gram) was weighed to a precision of 0.01 mg and placed in a wide-mouthed jar with septa along with a PTFE coated magnetic stirrer bar. The solvent (n-heptane) was poured into the jar at 1:100 w/v ratio of added bitumen. Air was drawn out of the jar through the septa using a syringe to minimize oxidation. Then, the jar was placed on the stirrer and stirred at about 120 rpm. The amount of bitumen and solvent can be proportionately changed depending on the required amount of maltene and number of replicates desired; it is possible to use between 0.1 gram to 1.0 gram bitumen to make 10 ml to 100 ml solution.

Filtration

A working procedure was established for asphaltene separation with the use of disposable syringe PTFE filters. This saves significant amount of material and time.

Similar methods have been used by Fan and Buckley (2002) and Rogel et al. (2016).

After dissolution, 10 ml of solution (while being stirred) was drawn into a syringe and a pre-weighed syringe filter was placed on the tip of the syringe. Thermo

Scientific™ Titan3™ PTFE hydrophobic syringe filters of 0.2μm pore size were used for asphaltene separation. PTFE was chosen as the filtration medium over cellulose or glass microfiber (as in ASTM D3279) due to a concern of adsorption of other fractions on glass fibers or cellulose as indicated by Boysen and Schabron (2015), Guo et al. (2017). Then, the solution was pushed through the PTFE filter and the filtrate was collected in pre-weighed glass bottles.

The filter was air-purged with 20 ml air using a syringe followed by 5 ml n-heptane, followed by another 20 ml air to flash any hold-up solution in the filter. Thumb pressure was required to pass the solution through the filters which are rated for 90 psi pressure.

Maltene was recovered from the filtered solution by heating at 120°C for 45 minutes under nitrogen purge. The residual maltene was weighed and the amount of asphaltene was resolved gravimetrically.

The process was repeated four more times, with 10 ml solution extracted each time, consuming the 50 ml solution that was prepared. Further, the entire process was repeated at least one more time with a different operator. Note that for routine use, depending on the number of replicates desired, fewer samples can be drawn, dried and weighed.

2.6.3 Semi-quantitative Validation of the Asphaltene Separation Process

Figure 2.2 presents the asphaltene content measured using the proposed method with PTFE syringe filters and ASTM D4124 method as used by Sultana (2014). The observed asphaltene yields are higher for the proposed method compared to the values from ASTM D4124. However, as mentioned before, this comparison is semi-quantitative at best. In particular, there are two factors that differentiate these two methods. First, the pore size of the PTFE syringe filter (0.2 μm) is much smaller than that of the medium fritted glass filter (10-15 μm) that is used in ASTM D4124. This is in addition to the fact that the filtering medium was also different (silica vs PTFE). Second, this study used a slightly more polar solvent (n-heptane) while ASTM D4124 prescribes the use of iso-octane. These two factors contribute to the overall increase in asphaltene content. However, asphaltene fractions of the bitu-

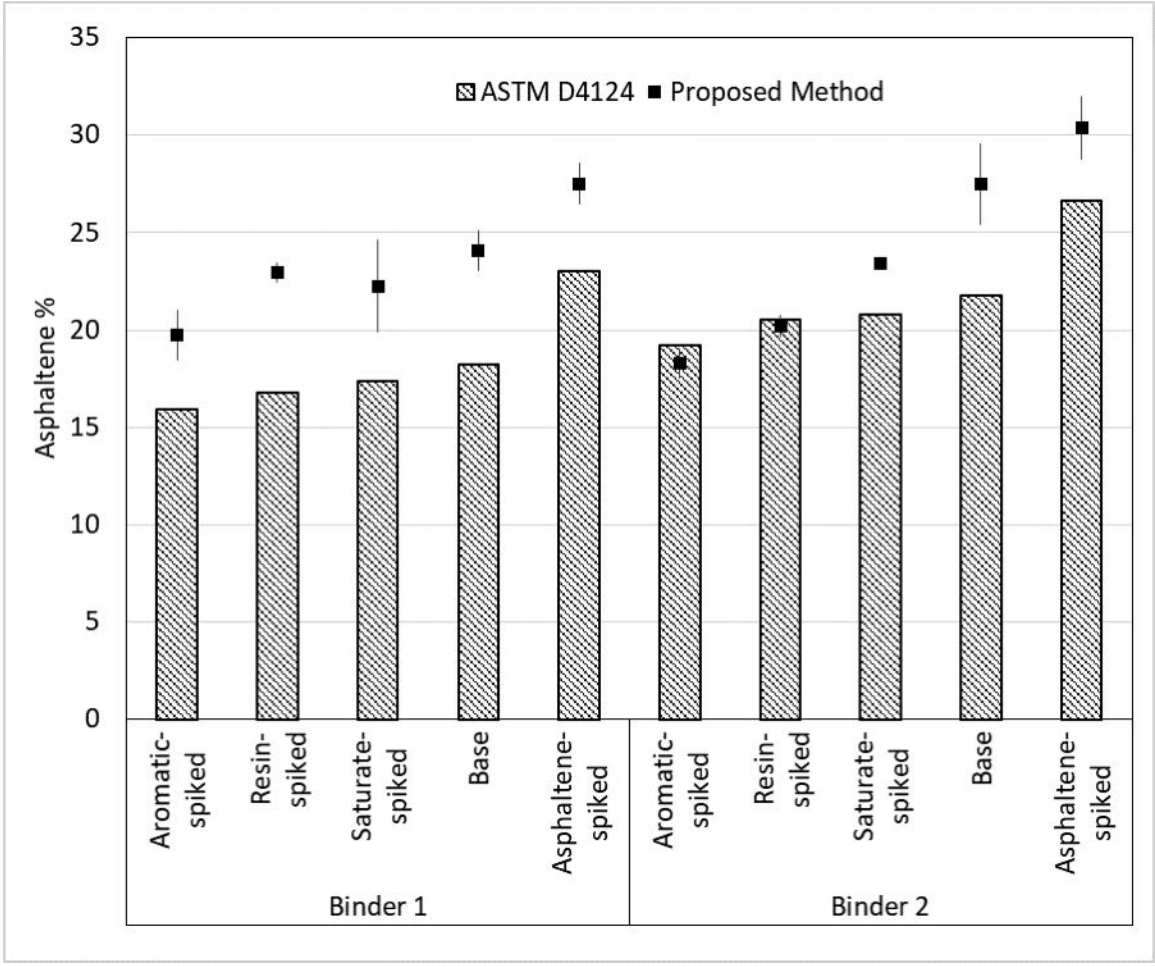

Figure 2.2: Asphaltene content measured using syringe filters in the proposed method and ASTM D4124; Error bars show one standard deviation, above and below.

mens, when considered relative to each other, show a trend that is consistent with ASTM D4124. In particular, the two asphaltene spiked bitumens showed relatively higher asphaltene content as expected.

In contrast to some other available methods, it takes about 20 minutes of operator time to conduct the actual filtration and uses small amount of solvent. Also note that multiple samples can be run concurrently and the only limitation is the number of magnetic stirrers for a scale-up operation.

2.7 Maltene Fractionation

A maltene fraction is typically subdivided into three more fractions: Saturates, Aromatics and Resins (S-A-R), in order of increasing polarity. It should be recognized that while maltenes are typically divided into three sub-fractions, it is also possible to fractionate the maltene into more than three fractions by suitable choice of solvents.

In fact, while the method described in the following paragraphs aims to separate maltenes into three fractions, the same approach can easily be scaled using additional solvents to achieve additional fractions.

2.7.1 Review and Rationale for Choice of Method

S-A-R separation typically employs normal-phase liquid chromatography with a stationary phase of polar silica gel or aluminum oxide. Diluted bitumen is placed on the stationary phase and eluted using different solvents (mobile phase). The primary mechanism in a chromatographic separation is the variation of competitive attraction of different bitumen molecules between the stationary and mobile phase. That is, if any fraction of bitumen is relatively more 'compatible' with the mobile phase than the stationary phase, that fraction will get dissolved into and elute along with the mobile phase. The authors consider that a more detailed discussion on mechanism of chromatographic separation is not within the scope of this paper as the process is well-established; however, the rationale for the choice of solvents will be discussed in detail.

There are two major chromatographic methods that are commonly used for S-A-R separation: liquid chromatography and thin-layer chromatography (TLC).

While both are very similar in principle, these two methods offer different levels of accuracy, efficiency and convenience for the user. After separation of fractions, quantification of each fraction is also different for each approach. In LC, gravimetric quantification is commonly used along with evaporative light scattering detection technique (ELSD). For TLC, different hyphenated techniques are available, such as mass spectrometry (MS), flame ionization detection (FID), and densitometry. Some other more esoteric methods for this purpose are Fourier Transform Infrared Spectroscopy (FTIR), Raman, Matrix Assisted Laser Desorption/Ionization (MALDI), Direct Analysis in Real Time (DART) etc.

In summary, to develop a working process of S-A-R separation, several choices need to be made:

1. the chromatographic method,
2. mobile phase (solvents),
3. stationary phase,
4. elution process, and
5. quantification method and calibration.

The following sections discuss these steps in more detail.

Chromatographic Methods

The most common practice for maltene fractionation is to use liquid column (LC) chromatography. Regular column chromatography requires a long glass tube to be packed to a specified density with a stationary phase material such as Attapulgus clay, alumina, amino-silane, cyano-silane, activated silica gel, glass beads or PTFE. (Boysen and Schabron 2015, ASTM D4124 2009, ASTM D3279 1997). Generally, a solution of maltene is added to the column which is then eluted using different solvents. The elute collection of specific fractions is triggered at specific time intervals or by presence (or absence) of fluorescence at specific UV wavelengths. Each elution product is subsequently dried and measured. While column chromatography is the most common method for S-A-R fractionation, it is a time-consuming and supervision-intensive process, which makes it onerous for use on a routine basis outside of laboratories specially equipped for such analysis.

The first method that is proposed for S-A-R quantification is the use of thin layer chromatography (TLC). Generally, TLC uses a plate overlaid with silica gel, which constitutes the stationary phase. The plate is 'spotted' with maltene solution and then placed in a jar with a specified solvent. Due to capillary action, the solvent rises along the plate and elutes the compatible bitumen components with it. In a multiple development process, multiple solvents are used in succession and each solvent is allowed to traverse a specified length. Each solvent front (and its proximity) contains different fractions of bitumen.

As an alternative to the TLC, another method based on solid-phase extraction (SPE) was developed for maltene fractionation. SPE is an attractive option for S-A-R separation because SPE cartridges, which can be used as disposable mini-LC columns, are commercially available and pre-packed to specific density. This reduces reproducibility issues and saves significant time and material requirement that is usually consumed for cleaning, packing and eluting LC columns.

It should be noted that both methods (TLC and SPE) are based on the same basic principle as liquid column chromatography. However, the focus of this research was primarily two fold:

1. develop S-A-R separation method(s) that can be used for routine tests with low capital cost and high throughput; and

2. semi-quantitatively validate the proposed test methods by cross-verification with each other as well as with ASTM D4124.

Choice of Mobile Phase and Stationary Phase

As mentioned earlier, the relative affinity of different bitumen components towards stationary and mobile phase dictates the separation process. Solvent strength appropriate for a given adsorbent system or solid phase depends on the relative solvent-solute (adsorbed) interaction and solvent-adsorbent interaction (Gocan 2005). There are several theories that help classify solvent selection options including, but not limited to, solubility parameter model, Snyder's solvent selectivity triangle, solvatochromic parameter model etc. (Poole 2015). Advanced models such as linear solvation energy relationship (LSER) account for as many as five different solvent-strength contributing variables.

While Hansen and Hildebrand solubility parameters (Hansen 1967, Hildebrand 1936) focus on solubility strength of solvents, they do not account for adsorbed solute-solvent interactions for use in chromatography. However, Hansen Solubility Parameters can provide a qualitative overview to compare different solvent sets. Table 2.4 contains Hansen parameters for some of the relevant solvents (and solvent blends) (Hansen 2007).

Unlike LC, there is no standard that dictates solvents for bitumen to be used in TLC as a stand-alone procedure. However, one of the most common hyphenated technique, TLC-FID, uses IP469 as a standard. While some researchers have fully or partially used the set of solvents proposed by IP469, other solvents sets have been used as well (Masson et al. 2001, Vela et al. 1995, Fan et al. 2002). This section describes the rationale for selecting a solvent-set that can be used for the proposed chromatographic methods and comparing the proposed set with existing standards of IP469 and ASTM D4124. While it is possible to adapt any of the LC or TLC solvent sets (or variations thereof) for fractionation, it was considered that having a similar set of solvents as IP469 will allow potential cross-method verification opportunity in future.

Table 2.4 shows that n-heptane is used for all cases to elute saturates. However, Toluene is introduced in the later part of saturate separation in ASTM D4124. Toluene and 80:20 Toluene:n-heptane are not very different from each other based on their Hansen Parameters although the pure form is slightly more polar. In addition, ASTM D4124 requires 50:50 Toluene:Methanol elution to follow 100% Toluene elution. This elution process should elute more polar fraction from maltene compared to 80:20 Toluene:n-heptane. On the other hand, 90:10 DCM:Methanol (95:5 in IP469) is more polar than 100% Tricholoroethylene. Slight departure from the IP469 recommended blend had to be made for separation of resins because 95:5 DCM:Methanol solution (as in IP469) was not eluting all remaining maltene fractions (i.e. resins) from the plate spot (in TLC) and cartridges (in SPE). Increasing the methanol (polar-heavy component) by 5% (total 10%) solved this issue. In summary, the solvent set selected for maltene fractionation is very similar to IP469 with a slight difference during the final resin elution step.

Two additional differences between the traditional LC (ASTM D4124) and TLC (using rods with Iatroscan or sheets as in this case) or SPE must be noted. First,

Table 2.4: Hansen parameters of the solvents used in proposed SPE and TLC methods as well as in IP469 and ASTM D4124

Procedure	Solvent	δ_D	δ_P	δ_H	δ_{Tot}
	Saturates				
TLC, SPE, IP469	n-heptane	15.3	0.0	0.0	15.3
ASTM 4124	n-heptane	15.3	0.0	0.0	15.3
	Toluene*	18.0	1.4	2.0	18.2
	Aromatics				
TLC, SPE, IP469	80:20 Toluene:n-heptane	17.5	1.1	1.6	17.6
ASTM 4124	Toluene	18.0	1.4	2.0	18.2
	50:50 Toluene:Methanol*	16.4	6.9	12.2	21.5
	Resins				
TLC, SPE	90:10 DCM:Methanol	17.8	6.9	7.7	20.6
IP469	95:5 DCM:Methanol	18.0	6.6	6.9	20.4
ASTM D4124	Trichloroethylene	18.0	3.1	5.3	19.0

Note: * The second solvent is introduced following the first on a continuous basis

with traditional LC, the eluting solvent is changed after the elute changes its character based on UV detection, whereas, in case of SPE, TLC or TLC-FID the eluting solvents are changed in discrete predetermined steps based on volume (or capillary rise). Second, the adsorbent used for ASTM D4124 is calcined alumina while the adsorbent for proposed methods is silica gel. Due to these important differences, the comparison between these methods can be semi-quantitative at best. It must also be emphasized that the authors did consider calcined alumina or Alumina-B for TLC plates and SPE cartridges. In fact, several preliminary tests conducted during the development of these procedures showed a strong match between SPE method and ASTM D4124. However, Alumina-B cartridges or plates are not as readily available or as standardized as silica gel. For this reason, the latter was chosen as the stationary phase.

2.7.2 Development and Quantification of Chromatographic Plates for TLC

This section presents details for the TLC based procedure. After separation of asphaltenes, the maltenes in n-heptane were dried and weighed as a part of asphaltene measurement process. Then, n-heptane was added again to maltenes at 2 mg/ml (w/v) ratio to re-dissolve maltenes. For routine use, it is possible to only dry two of the 10 ml maltene samples to determine the asphaltene content and use two other 10 ml samples to further dilute with n-heptane and achieve this target concentration. All solvents (n-heptane, toluene, dichloromethane, and methanol) were HPLC-grade.

An EMD Millipore aluminum-backed silica-gel plate was used. The plates were 20 cm$\times$20 cm and the pore size was 60Å, yielding a specific surface area of 520 m^2/g. The plates are pre-treated by the manufacturer to exhibit green fluorescence at 254 nm wavelength. A coarse filter-paper-lined development tank was utilized for TLC plate development to ensure controlled environment (this is basically a glass tank the size of the TLC sheet). The TLC plate was spotted with 10 μL maltene solution using a Fisherbrand^{TM} Elite^{TM} Adjustable-Volume Pipetter. A total of 11 spots were made on each plate. The spots were placed at 15 mm distance from each other and 25 mm from the edges.

'Spotting' the TLC plates needs special attention as a very slow application can result in fast evaporation of solvent and creation of a dense maltene ring on the plate. Also, pushing the pipette tip to the TLC plate restricts the solution from coming out and can damage the fragile silica gel near the spot. A uniform spot on the plate is important for proper chromatography and subsequent quantitative analysis. A few practice spots made using a holder or support are important for fast and repeatable results. There are commercial plate spotting devices available that can produce automated spots or bands. This can help repeatability to some extent. However, one of primary goals of this study was to develop a low-cost setup for SARA fractionation. Hence, automated spotters that are typically a high cost capital equipment were not used.

After air-drying the spots, the plate was placed in a development chamber and developed with three solvents (mobile-phase) sequentially: 100% n-heptane, 80% toluene-20% n-heptane mix, and 90% dichloromethane-10% methanol mix. About

100 ml solution of the desired solvent was poured into the tank which provided about 10 mm solution depth. Before developing the plate, the chamber was primed and saturated with the mobile phase's vapor. To achieve this, the chamber was lined with a P8-grade coarse filter paper that was soaked with and dipped into the mobile phase. The chamber was allowed to saturate with the vapors for 30 minutes before each development. After saturation, the plate was put in the tank for development and the solvent front to traverse a specific distance. The target distance was marked on the edge of TLC plate with a pencil. The TLC plate was removed from the chamber immediately after the solvent front reached the mark. The following development distances, measured from the center of the spot, were used:

1. Saturate elution (100% n-heptane): 120 mm
2. Aromatic elution (80% toluene-20% n-heptane): 60 mm
3. Resin elution (90% dichloromethane-10% methanol): 35 mm

After each development the plates were air-dried in a horizontal position. The fractions of bitumen were spatially separated corresponding to the mobile development phase used and distance traveled by each of the mobile phase. Since bitumen molecules comprise a distribution of polar fractions, it does not result in discrete spots; rather spots with high concentration of eluted fractions followed by a streak are generally observed.

The 'saturates' portion is invisible due to its transparency; aromatic and resin streaks are visible under white light and more clearly against UV-fluorescent backlight. One of the advantages of using this procedure was that up to 11 spots or samples could be developed using a single TLC plate at the same time.

Quantification of maltene fractions using TLC

Densitometric quantification using UV fluorescence was employed to quantify S-A-R fractions. The TLC plates are produced with fluorescent material which emits green light under shortwave ultraviolet light. Densitometric analysis is based on the principle that the eluted opaque fractions of maltene reduce the fluorescent

backlight intensity and the area of reduced intensity is related to the quantity of the eluted materials that is deposited in that area.

Fluorescent densitometric analysis requires a camera with sufficient resolution, a shortwave UV source to activate fluorescence and a dark chamber where photography can take place under controlled and constant lighting conditions. In a bare-bone configuration, it is possible to use a smart-phone camera, hand-held UV lamp and shoe-box type darkroom for analysis (Yu et al. 2016). On the higher end, commercial TLC scanners that offer much more sophisticated analysis over a wide range of UV wavelengths are also available (Jarne et al. 2015). Popovic and Sherma (2014) compared four types of densitometric analysis. Three of these were commercially available devices designed for TLC analysis and the fourth was a phone camera coupled with ImageJ. Results obtained in all methods showed good correlation (R^2 >0.97).

For this study, a Syngene G:BOX Chemi XX6 was used which was fitted with 254-nm UV-lamp for fluorescence imaging. This or similar single UV wavelength image acquisition devices are substantially more inexpensive and easier to operate compared to FID devices. One of the issues encountered with imaging was spatially non-uniform lighting condition across the plate. To resolve this, images of different streaks/spots were taken at the exact same place to make them comparable. In addition, the plate was covered with a dark paper except for the area being photographed so that fluorescence from other areas does not affect the image of the area of interest.

The images of individual streaks were analyzed using an open source image analysis software ImageJ. A threshold value was used to distinguish between the background and aromatic/resin streaks. This threshold rendered the image into a binary format where the area containing bitumen fraction (aromatic/resin) appears as white and the background appears as black. Figure 2.3 shows a photograph of streaks before and after image processing. The integrated density of each fraction streak was computed. This value of integrated density serves as a quantitative estimate of the specific fraction at that location.

A limitation that was recognized during the development of this method was that variation in the UV source size, shape and intensity, incidence distance and angle, as well as batch-wise variation of fluorescent response from the TLC plate

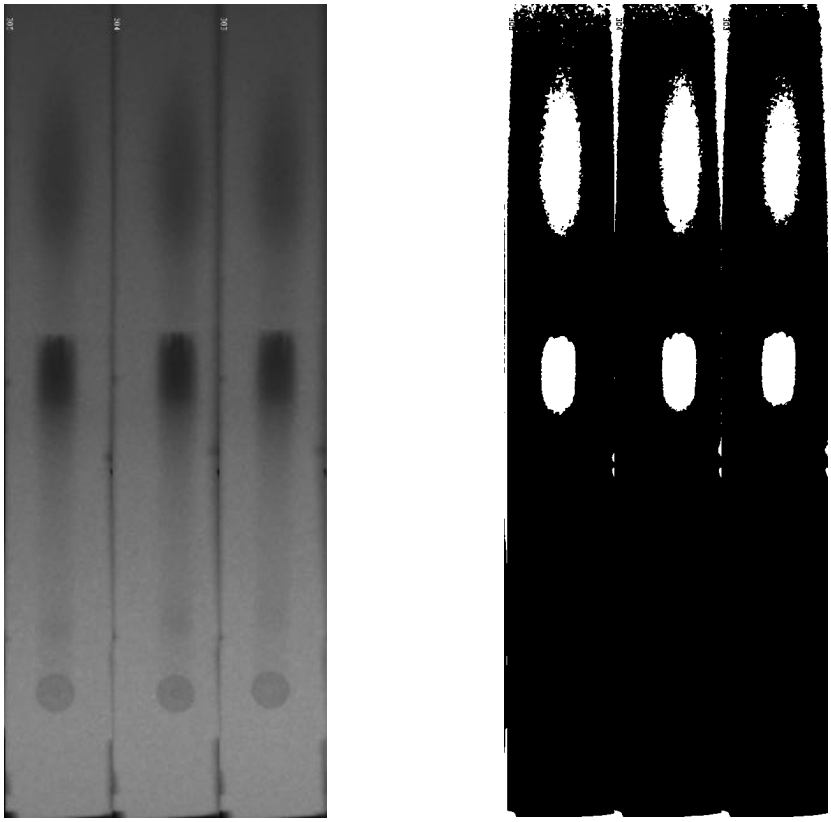

(a) (b)

Figure 2.3: TLC plate image showing before (a) and after (b) image analysis

could result in different values of threshold and variability of the densitometric parameter. However, the results were found to be repeatable when the same setup was used. For this reason, in future, the authors anticipate that a standard solution or bitumen can be used to calibrate inter-laboratory results.

2.7.3 Maltene Fractionation Using SPE

Fractionation of maltenes using SPE started with the maltene obtained from separation of asphaltene from the bitumen and n-heptane solution. Similar to the TLC methods discussed earlier, a solution of 3.33 mg/ml maltene/n-heptane (w/v) ratio was prepared for fractionation using SPE.

Supelclean normal-phase SPE cartridges (syringe-type) were obtained from Sigma-Aldrich. These cartridges had 5 g silica gel packed inside a polypropylene syringe

Figure 2.4: Liquid Chromatography using silica-gel SPE cartridges and vacuum manifold; three SPE cartridges showing phases of Aromatics separation

with 45 μm particle size which provided 60Å pore size (same as TLC plate), yielding 475 m^2/g specific surface. Typically, the maximum allowable dosage on the cartridge is 5% (0.15 g). However, the dosage was kept to 1% by administering 15 ml of prepared maltene solution which contained approximately 50 mg maltene.

The cartridges were mounted on a vacuum manifold which allowed multiple extractions to be carried out simultaneously (Figure 4.3). Vacuum was applied to drive the mobile-phase through the packed silica and the eluted material was collected in the vials placed in the manifold under the syringe.

The SPE cartridges were first primed with 20 ml n-heptane. Then, 15 ml maltene solution was applied to the cartridge followed by 10 ml n-heptane flush. The elution products up to this point were collected in a pre-weighed vial; the col-

lected fraction was deemed as 'saturates' dissolved in n-heptane. After this step, the same cartridge was moved to the next location/vial and 25 ml of 80:20 (v:v) Toluene:n-heptane solution was pushed through the cartridge. This portion of the elute was regarded as 'aromatics'. In the next and final step, the mobile phase was prepared with 25 ml of 90:10 (v:v) dichloromethane and methanol solution. This solvent eluted 'resin' fraction and the syringe was allowed to run dry under vacuum. The flow rate of the solvent through the SPE cartridge was adjusted so that it took approximately two to three minutes for each elution. The total time taken to perform the three elution steps was approximately 15 minutes. The speediness of this process makes it possible to process several bitumen a day. The collected solutions were then oven-dried under nitrogen purge and weighed to measure maltene fractions gravimetrically. Note that the solvent amounts for elution were determined based on several trials that were conducted following the same procedure as above; in these trials elution was carried out using the solvent in smaller increments of 5 ml to determine the point at which 95% by mass of each fraction was eluted.

2.8 Semi-Quantitative Verification of Proposed methods

2.8.1 TLC vs. ASTM D4124 LC

Previously separated maltenes from the 10 bitumen samples (2 base and 4 derivatives from each) were used to spot TLC plates which were subsequently developed and analyzed using the process described in previous section. Five replicate (spots) for each maltene sample were prepared. Integrated density at the expected locations of aromatic and resin fractions were calculated and compared with respect to the values based on ASTM D4124 (Sultana 2014) (Figure 2.5). The four plots represent comparisons between TLC and LC for different maltene fractions as well as the combined general trend.

Notable observations from Figure 2.5 are as follows:

1. The spiked bitumens, such as aromatic-spiked and resin-spiked (represented in dotted boxes in Figure 2.5a and 2.5b, respectively), show distinctively higher integrated density values compared to other bitumens in each base

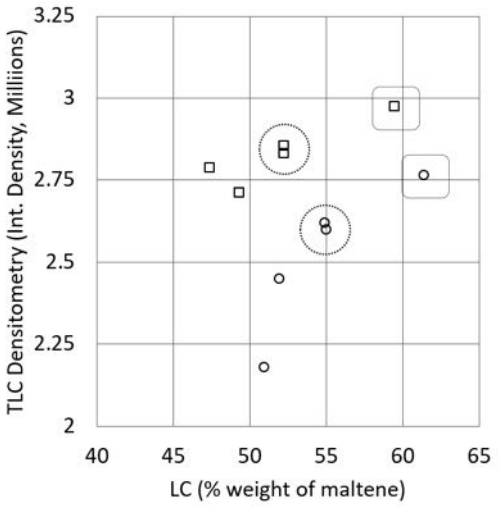

(a) Aromatic fraction of maltenes; 'Aromatic-spiked' bitumens are shown in dotted boxes.

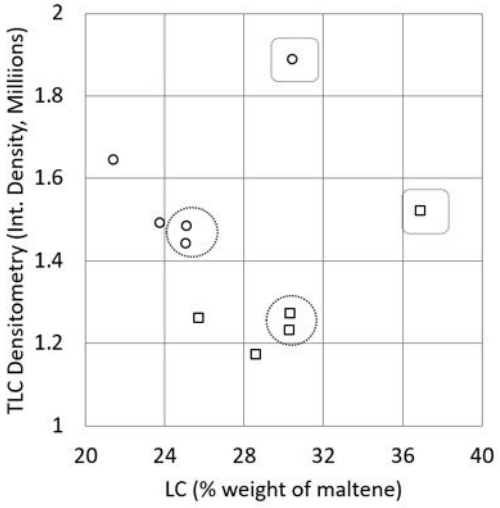

(b) Resin fraction of maltenes; Dotted boxes show 'Resin-spiked' bitumens .

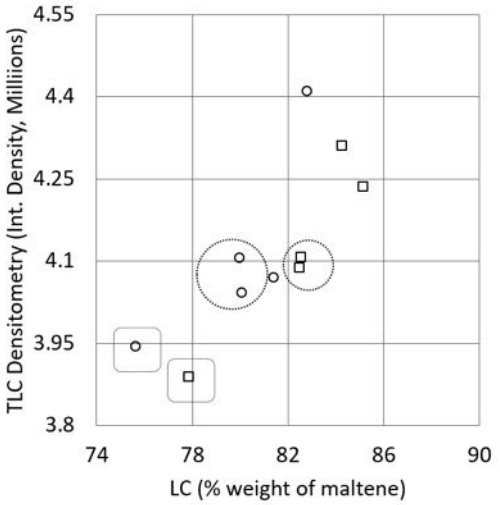

(c) Cumulative Aromatic and Resin fractions; Dotted boxes show 'Saturate-spiked' bitumens.

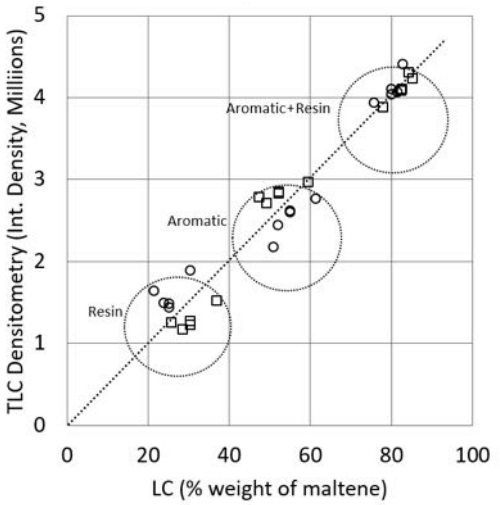

(d) Compilation of all data points as presented in (a), (b) and (c)

Figure 2.5: Comparison of maltene fractions obtained by TLC and LC (ASTM D4124); square markers represent bitumen 1 and its derivatives while circular markers indicate bitumen 2 and derivatives; dotted circles enclose bitumens with similar expected fraction and dotted squares enclose bitumens with spiked fraction according to ASTM D4124.

bitumen group. The aromatic-spiked bitumens (dotted boxes in Figure 2.5a) contain $\approx 7 \pm 0.5\%$ higher aromatic fraction compared to their respective base bitumens. Similarly, the resin-spiked bitumens (dotted boxes in Figure 2.5b) contain $\approx 6 \pm 0.5\%$ higher resins compared to their respective base bitumens. From Figure 2.5a and 2.5b, these differences can be clearly seen.

2. When aromatics and resins are individually considered as in Figure 2.5a and 2.5b, each of the base bitumens and their derivatives follows a slightly different trend compared to the other bitumen group. This is to be expected given the differences between the two methods in terms of the stationary phase, solvent, and the cutoff definition. Considering the continuous polarity distribution of molecules in the maltene, it is expected that mobile-phases with small differences in elution power will elute slightly different portions of maltene.

3. The first phase of proposed methods used the same solvent (n-heptane) as ASTM D4124 which separates transparent saturates from aromatics and resins; albeit using a different filtration medium and size. While saturates were not measured using densitometry, the total aromatic and resin content is inversely related to saturate content. From Figure 2.5c, it can be seen that saturate-spiked bitumens are placed at lowest part of the plot which agrees with the previous statement.

4. The asphaltene-spiked bitumens were fabricated to have essentially the same relative S-A-R proportions as the base bitumen after separation of asphaltene. In other words, the base bitumen and the bitumen spiked with asphaltenes should have the same relative concentration of S-A-R even though the relative maltene content in the overall bitumen would be different. In Figure 2.5a, 2.5b and 2.5c, it can be observed that the data points related to asphaltene-spiked and base bitumen (in the dotted circles) are in proximity to each other. This further corroborates the process.

2.8.2 SPE vs LC

Maltenes from ten bitumen samples were evaluated for their SAR fractions using SPE method. Figure 2.6 shows the comparison between the percentage of bitumen fractions measured using SPE with respect the percentage from liquid chromatography (ASTM D4124).

Analysis of Figure 2.6 provides several interesting observations as noted below:

1. SPE provided quantitative data for saturates, aromatics, and resins and was able to clearly differentiate between the saturate-, aromatic-, and resin-spiked fractions (dotted boxes in Figure 2.6a, 2.6b and 2.6c, respectively) from the other derivatives.

2. The two base bitumens and their derivatives show slightly different trend as seen in case of TLC. However, in the case of saturates, the data points from both sets of bitumens are closer to each other compared to aromatics or resins (Figure 2.6a).

3. As mentioned before, asphaltene-spiked bitumens and corresponding base bitumens are expected to have the same relative proportions of constituents in their maltene fractions. From SPE analysis, it is clear that the individual S-A-R fractions (circled with a dotted line) for the asphaltene and its respective base bitumen are close to each other.

2.8.3 TLC vs SPE

Figure 2.7 compares the results obtained from TLC and SPE to each other using the same data that were used to construct Figures 2.5 and 2.6.

An examination of data from Figure 2.7 yields the following notable observations:

1. In contrast to the comparisons made before (TLC vs. LC and SPE vs. LC), Figure 2.7 do not show separate trends for each of the two bitumens. Instead, both bitumens tend to follow a similar trend which leads to two additional conclusions. First, since TLC and SPE used the same solvents and stationary phase, it validates the previously stated conjecture that the different trends

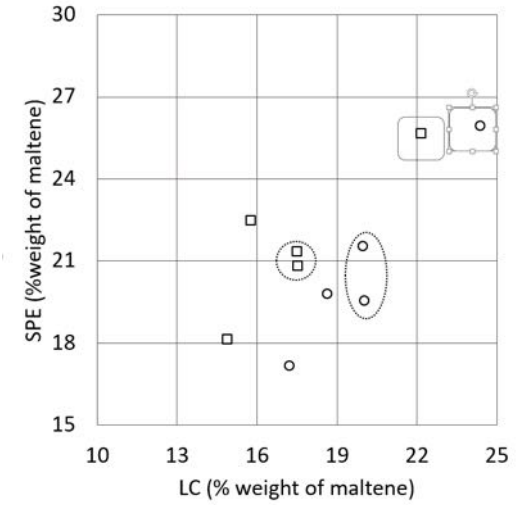

(a) Saturate fraction of maltenes; Dotted boxes show 'Saturate-spiked' bitumens.

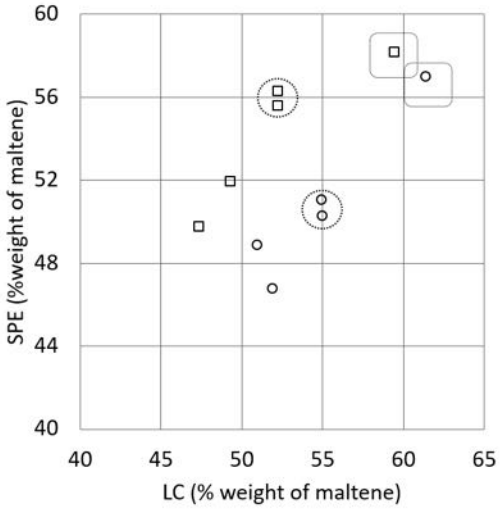

(b) Aromatic fraction of maltenes; 'Aromatic-spiked' bitumens are shown in dotted boxes.

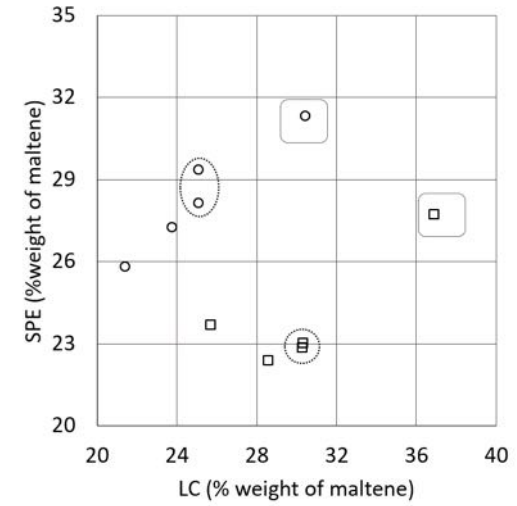

(c) Resin fraction of maltenes; Dotted boxes show 'Resin-spiked' bitumens .

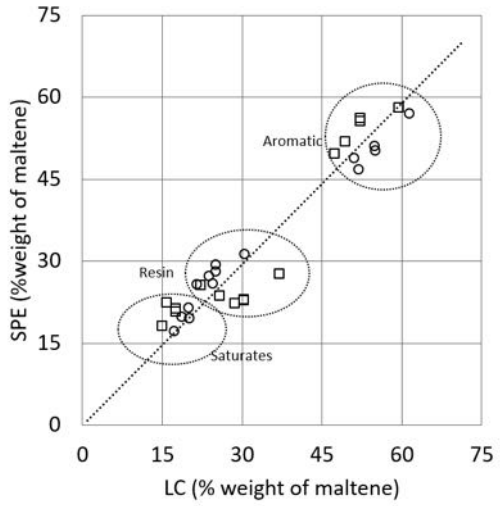

(d) Compilation of all data points as presented in (a), (b) and (c)

Figure 2.6: Comparison between maltene fractions obtained by SPE and LC (ASTM D4124); square markers represent bitumen 1 and its derivatives while circular markers indicate bitumen 2 and derivatives; dotted circles enclose bitumens with similar expected fraction and dotted squares enclose bitumens with spiked fraction according to ASTM D4124.

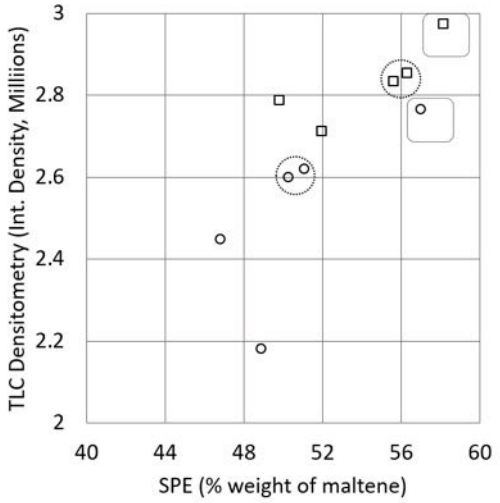

(a) Aromatic fraction of maltenes; 'Aromatic-spiked' bitumens are shown in dotted boxes.

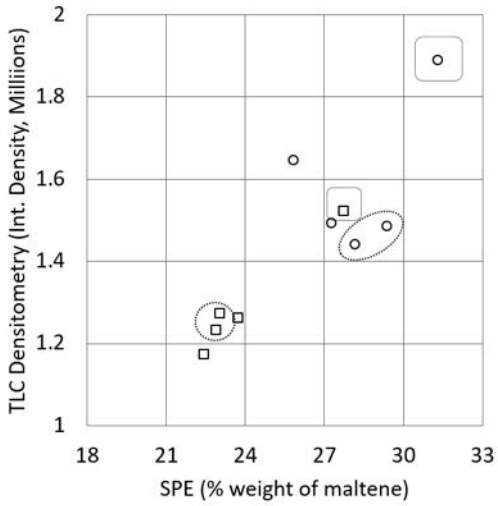

(b) Resin fraction of maltenes; Dotted boxes show 'Resin-spiked' bitumens .

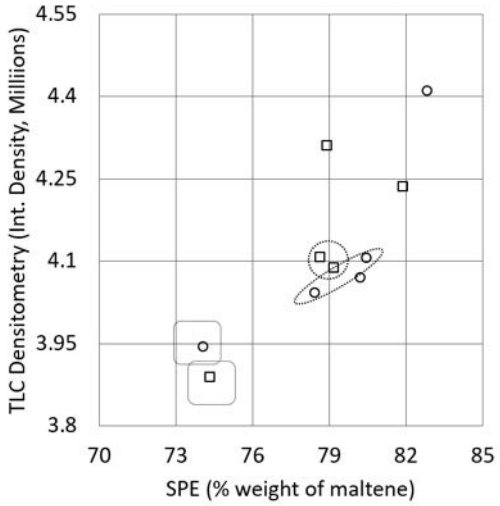

(c) Cumilative Aromatic and Resin fractions; Dotted boxes show 'Saturate-spiked' bitumens.

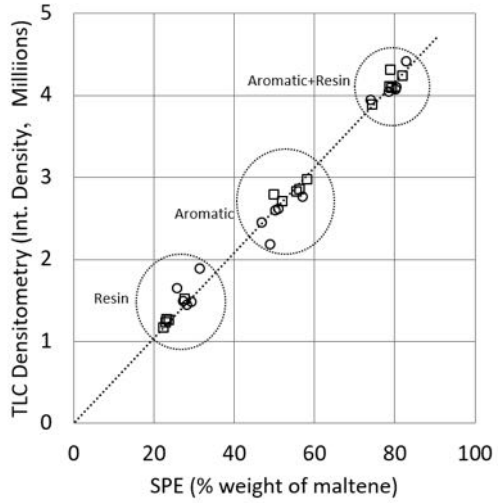

(d) Compilation of all data points as presented in (a), (b) and (c).

Figure 2.7: Comparison between maltene fractions obtained by using proposed methods involving TLC and SPE; square markers represent bitumen 1 and its derivatives while circular markers indicate bitumen 2 and derivatives; dotted circles enclose bitumens with similar expected fraction and dotted squares enclose bitumens with spiked fraction according to ASTM D4124.

for each of the two bitumens observed when comparing TLC vs. LC or SPE vs. LC (ASTM D4124) are due to the choice of solvent and stationary phase medium. Second, despite the fact that the TLC and SPE approaches are vastly different (TLC uses 10 μL sample, silica plate as the medium, solvent capillary rise for separation, and imaging densitometry for quantification; SPE uses about 50 mg sample, SPE silica cartridge as the medium, solvent injection for separation, and gravimetry for quantification), the correlation of results from these two methods demonstrates that the methods are clearly measuring similar fundamental characteristics.

2. Individual maltene fractions for the asphaltene-spiked and base bitumen show similar results, as expected, and are highlighted in encircled dotted lines of Figure 2.7a, 2.7b and 2.7c.

3. Since TLC method can not directly measure saturates, the total amount of aromatics and resins can be used as an indirect measure of saturates-content which is shown in Figure 2.7c. The data points corresponding to saturates-spiked bitumens (within dotted boxes) are placed low among the total aromatic and resin-content data points. This is expected, as they are negatively related to the saturates' content.

In summary, the comparison between TLC and SPE provides compelling evidence about the ability of these methods to distinguish between the polar fractions of different bitumens.

2.8.4 Repeatability of Measurements

Repeatability of the proposed method was observed and compared with suggested values from available standards. Table 2.5 presents these results for the SPE method. Results from TLC were not included in this table because the available standards are based on mass percentages of individual fractions. Since the TLC method developed in this study does not result in mass percentages but intensity on an arbitrary scale, an interconversion of scales is required to determine the equivalent variability that can be compared with ASTM D2007 or IP469. These detailed estimates will be considered in future studies.

For the gravimetric measurements with SPE, Table 2.5 presents the average difference from the mean in percentage points and similar measures as recommended in ASTM D2007 and IP469. Note that ASTM D4124 does not have recommendations for variability. The results from this table clearly show that for saturates, the variability from SPE was slightly higher compared to ASTM D2007 and IP469. This is very likely due to the smaller yield of the saturates from the liquid chromatography and can be easily improved by using larger sample sizes. On the other hand, the variability for aromatics and resins was similar to ASTM D2007 and certainly better than IP469 in all cases.

It should also be noted that there is no notable sample bias or trend in the test results when bitumen with different spiked fractions are compared. Although these results are from a single laboratory, the tests were conducted by two operators.

Table 2.5: Average of the difference in percentage points from the mean.

Bitumen		Saturates	Aromatics	Resins
SPE values for each of the ten bitumens				
Bitumen 1 (PG 64-22)	Base bitumen	1.2	1.5	0.6
	Saturate-spiked	0.7	0.4	0.3
	Aromatic-spiked	0.0	0.9	0.9
	Resin-spiked	1.4	1.1	0.3
	Asphaltene-spiked	2.4	2.4	0.7
Bitumen 2 (PG 67-22)	Base bitumen	1.8	0.1	1.7
	Saturate-spiked	2.0	0.6	1.3
	Aromatic-spiked	2.3	1.7	0.6
	Resin-spiked	2.5	1.9	0.6
	Asphaltene-spiked	0.1	0.4	0.5
SPE Average for all cases		1.4	1.3	0.7
ASTM D2007		1.0	1.1	0.6
IP469		0.9	2.5	3.0

2.9 Conclusion

The main goal of this study was to develop fast, inexpensive method(s) to determine the polarity-based distribution for bitumens that could be used on a routine

basis with high throughput. This would ultimately help create a sizable database of this property alongside typical engineering properties for bitumen from various sources. To this end, a method to separate and quantify asphaltenes and two different methods to separate and quantify various fractions from maltene were developed. In the proposed asphaltene separation method, commercially available syringe filters were used to separate asphaltenes from maltene solution in n-heptane. The dissolution of maltene in n-heptane was performed in airtight vials at room temperature and avoids the use of heating and reflux, which is required in many current standards. The proposed process provides high throughput (several samples can be evaluated simultaneously), and is inexpensive.

Two methods for maltene fractionation were also developed based on principles of chromatographic separation. The first method uses thin-layer chromatography plates which were spotted with maltene solutions and subsequently eluted using three solvents. The quantification is done using image analysis through fluorescent densitometry. This method requires minimal setup and offers fast analysis compared to current practices of SARA fractionation. The second method essentially utilizes standard pre-packed SPE cartridges as a miniature liquid chromatography column. Maltene separation was achieved using different solvents with the aid of a vacuum manifold and quantified gravimetrically.

A semi-quantitative comparison of results from these methods to the results from an existing standard shows that the proposed methods can be used to obtain polarity-based distributions for bitumen.

Authors believe that the sensitivity and repeatability of the proposed method combined with low capital cost, ease of training, and high throughput can facilitate the fingerprinting of bitumen using polarity-based distributions on a routine basis alongside the measurement of its engineering properties.

2.10 Acknowledgments

We acknowledge the support of National Science Foundation Grant CMMI-1053925 and Ms. Ishika B for her help with the review of this manuscript.

Chapter 3

Correlation of bitumen chemistry with rheology, aging and performance benchmarks

3.1 Overview

The chemical composition of a bitumen dictates its rheological properties as well its performance in an asphalt mixture. Any given bitumen comprises a wide variety of very complex hydrocarbons and its chemical composition is often characterized on the basis of elemental analysis, functional group analysis, ionic character, polar character, or molecular size distribution. Similarly, the mechanical properties of any given bitumen are typically characterized based on its time-temperature dependent rheological properties at different stress levels. This study characterizes the chemical makeup of a set of bitumens from several different producers based on their polarity and compares these characteristics to mechanical properties based on metrics associated with the Performance Grading (PG) of bitumen. Results show that high temperature stiffness is strongly dictated by the asphaltene content and the low temperature stiffness is strongly dictated by the aromatics and resin content. The useful temperature interval showed a good correlation with asphaltenes and resins. Bitumens that deviated from some of these correlations also showed uncharacteristic responses in some other mechanical or elemental property measurements. The relationship between time-dependent characteristics and polar fractions was not strong and requires further examination.

3.2 Introduction and Motivation

Bitumen is one of the most commonly used materials across the world for construction and maintenance of pavements. In its most rudimentary form, bitumen is a by-product obtained from the distillation of crude oil referred to as the bottom residue. The chemical composition of the bitumens from different sources varies widely even when the mechanical properties are similar. This is due to several different reasons. First, crude oil is a naturally occurring material and its chemical

composition varies with the geographic location of the source and in some cases even over time from the same source. This variability is further amplified in the bottom residue after high value products such as gasoline and diesel are distilled from the crude oil. Second, there are several different processes that are used to refine the crude oil to obtain different products. Therefore, the refining process itself will alter the chemical composition of the bottom residue. Third, bitumen obtained from refining crude oil is rarely ready for use in roadway construction. Bitumen obtained as the bottom residue of this refining process is often modified using additional processes (e.g. air blowing) and/or chemical or polymer modifiers. Lastly, there has been an increased emphasis on the use of eco-friendly materials for roadway construction. This has motivated the industry to evaluate the use of bio-based products and other industrial waste products as extenders for conventional bitumens. All of the aforementioned factors significantly influence the chemical composition of the bitumen that is ultimately incorporated in the asphalt mixture that is used for pavement construction or maintenance.

It is well recognized that the chemical composition of the bitumen dictates the overall durability of the asphalt mixture and consequently the service life of the pavement (e.g. a recent review by Daly (2017)). However, from an engineering perspective, only the mechanical properties of the bitumen are used for specifications and design. These mechanical properties are either empirical measures (e.g. penetration test, ring and ball softening point) or performance-based measures (e.g. the Performance Grading or PG system). The existing frameworks are not perfect and several studies have shown that bitumens with very similar grade can result in vastly different overall performance and in some cases premature failures attributed to the bitumen when used in the field. For example, Batista et al. (2017) compiled several studies by other authors who developed correlations of commonly used bitumen performance test results with actual field performances (permanent deformation). They noted that correlations measured in different studies were widely different (R^2 varied from 0.27 to 0.99). They also reported similar variability when different types of bitumen were used (e.g. polymer modified bitumen) even as a part of the same study. This implies that current test protocols may be inadequate to consistently predict field performance, specially when the bitumen is modified (Hajj and Bhasin 2017, Delgadillo et al. 2006, D'Angelo 2009).

The shortcomings of the existing frameworks is due to several reasons including but not limited to the fact that the mechanical properties measured and/or metrics derived from such measurements do not accurately and completely reflect the mechanisms that drive the distresses observed in the real-world conditions. Such mechanisms often include chemical changes within the bitumen and the physicochemical interactions between the bitumen and the mineral aggregate. An understanding of the relationship between the chemical makeup of the bitumen and its mechanical properties is imperative in order to (i) identify shortcomings and improve our current framework for specifying and selecting bitumens and (ii) to promote innovation and design of new types of bitumens, modifiers, additives, and extenders that can enhance the sustainability, durability, and service-life of asphalt pavements (e.g. rejuvenators to promote the use of reclaimed asphalt pavements and bio-based bitumen extenders).

3.3 Scope

Based on the motivation described in the previous section, the overall goal of this study was to examine the relationship between the chemical composition of bitumens and their rheological properties. Any given bitumen comprises a wide variety of very complex hydrocarbons that are often characterized on the basis of any one or more of the following attributes: elemental composition, concentration of different functional groups, ionic character, polar character, and molecular size distribution. Similarly, the mechanical properties of any given bitumen are typically characterized based on its time-temperature dependent rheological properties at different stress levels. In terms of the chemical composition, the scope of this study is limited to characterizing bitumens based on their polar character (colloquially known as SARA fractions which is an acronym for polar fractions referred to as Saturates, Aromatics, Resins, and Asphaltenes). The rationale for selecting polarity of molecules as a starting point for such a study was because polarity is intimately tied to the inter-molecular forces that define the stiffness and strength of a material, which are the basic properties of interest from an engineering standpoint. In terms of the mechanical properties, the scope of this study is limited to methods and metrics associated with the Performance Grading (PG) of bitumen.

Authors would like to emphasize that the limitations in the scope of this study are due to practical considerations and are not intended to preclude other metrics (both for chemical and mechanical properties) which are and should be a part of ongoing and future works.

In addition to examining the relationships between the chemical makeup and mechanical properties of bitumen, this study also demonstrates (i) the use of a recently developed low cost, high throughput, and repeatable procedure to separate bitumen based on its polar fractions for a large set of bitumens, and (ii) that the relationship between the chemical composition and mechanical properties of the bitumen can be used to identify bitumens with anomalous behaviors.

3.4 Background on chemical composition versus mechanical properties

This section reviews previous studies that have examined the relationship between chemical composition and mechanical properties of bitumen. Several researchers have recognized the importance of chemical makeup of bitumen and made significant effort to explore the relationship between bitumen chemistry and its physical properties. It should be noted that promising correlations between polar fractions and physical properties have been observed on multiple occasions, though many of these studies used very limited number of bitumens and different testing protocols (Redelius and Soenen 2015, Redelius 2004, Isacsson and Zeng 1997, Santagata et al. 2009, Sultana 2014, Weigel and Stephan 2018, Robertson et al. 2001).

Most previous studies in this area can be classified into two broad areas: (1) examining correlations between chemical makeup and high temperature properties such as viscosity or complex modulus at high temperatures, and (2) examining correlations between chemical makeup and low temperature properties such as stiffness.

3.4.1 Chemical composition and high temperature properties of commercial bitumens

One of the earliest studies in this area was a part of the Strategic Highway Research Program (SHRP) (Branthaver et al. 1993). As a part of the SHRP bitumen characterization and evaluation program, eight SHRP core bitumens were chemically fractionated using Ion Exchange Chromatography (IEC) and Size Exclusion Chromatography (SEC). Branthaver et al. (1993) used IEC fractionation to separate the SHRP core bitumens into into five fractions (neutrals, strong acid, weak acid, strong base, and weak base) or three fractions (neutral, amphoteric, acid and base). Amphoterics are those which have both acidic and basic components. Robertson et al. (2001), in their interpretive report on Branthaver et al. (1993), identified that amphoterics were the primary viscosity enhancing component in the bitumen. They also reported that that the presence of amphoterics resulted in a marked increase in viscosity as opposed to neutral and polar fractions (not including amphoterics).

Pauli and Branthaver (1998) used 16 SHRP bitumen to establish a model correlating relative viscosity, Heithaus parameters and asphaltene volume fraction. They noted that approximate relative viscosity correlates with iso-octane asphaltene volume fraction. However, using the same bitumen set, Redelius and Soenen (2015) noted that asphaltene content correlates well with relative viscosity (expressed as ratio of viscosities of bitumen and maltene). In addition, they concluded that viscosity and physical properties of bitumen are most reliant on London Dispersive interactions which can be estimated by molecular weight and aromatic pi-pi interaction (asphaltene has large polycyclic aromatics).

Weigel and Stephan (2018) conducted a study with 11 different bitumens (total 33 including samples subjected to short- and long-term aging). They used a slightly different method for SARA fractionation compared to ASTM D4124. They found that softening point correlated very well (R^2=0.886) with asphaltene content. They also found a good correlation between colloidal index (defined as the ratio of total asphaltene and saturate content with total aromatic and resin content) and aromatic to asphaltene ratio. Additionally, they observed that $\log|G^*|$ correlated with the above mentioned parameters in a similar way but the correlation was better at higher temperature. They observed that the concentration of saturates and

aromatics correlated with a decrease in viscosity (penetration or softening point), while the concentration of resins and asphaltenes resulted in an increase in these parameters. Similar effect was observed for complex modulus as well. Their work, despite the limited number of bitumen samples, provides more evidence on the strong interdependence of chemistry of bitumen and physical properties, particularly at high temperatures.

In a more recent study, Hajj et al. (2017) used poker chip test on eight commercial bitumen samples of two different PG Grades (PG64-22 and PG70-22) and compared strength and stiffness properties. This study was conducted at an intermediate temperature (18°C). Hajj et al. (2017) noted that while stiffness of bitumen corresponds to tensile strength in some cases, these two properties must be treated independent of each other.

3.4.2 Chemical composition and low temperature properties of commercial bitumens

Interestingly, very few works on low temperature properties and chemical make-up exist. Radenberg et al. (2014) explored the relationship of stiffness and m-value (rate of creep at 60 seconds obtained from a Bending Beam Rheometer) with individual chemical fraction as well as through multiple linear regression using 90 bitumen samples. They found correlation coefficient of multiple linear regression is 0.34 for low temperature (-16°C) stiffness and 0.43 for m-value. They also noted that correlation coefficients of individual SARA components were very low.

Isacsson and Zeng (1997) used five bitumen samples for chemical analysis by gel-permeation chromatography and thin layer chromatography and compared the metrics from these analyses to results from a low temperature fracture test (Thermal Stress Restrained Specimen Test, TSRST). They noted that there was a statistically significant relation between TSRST test data and asphaltene content. They also stated that the combined asphaltene and resin content also correlated well with TSRST data. The authors concluded that increased asphaltene resulted in an increased stiffness of the bitumen and thus resulted in higher (warmer) fracture temperatures.

Baumgardner (2012) analyzed bitumen from seven sources. He reported that parameters derived using the SARA fractions, namely Asphaltene to Resin ratio and Psh (a solubility factor), correlated well with the useful temperature interval (UTI). UTI is measured as the spread between highest and lowest temperature within which the bitumen is allowed to be used according to the Performance Grade specification. In this sense, UTI is not a low-temperature neither a high-temperature property. Rather, this parameter captures a temperature interval that is based on the utility of the bitumen across different aging conditions.

3.4.3 Chemical composition and rheological properties of laboratory synthesized bitumens

The aforementioned studies evaluated the properties of limited set of commercial bitumens. However, researchers have also used carefully synthesized bitumen to control and understand the relationship between bitumen polar fractions and its rheological properties and tensile strength. Sultana and Bhasin (2014) used a total of ten bitumens, comprising two source bitumens and four laboratory-synthesized bitumens produced by 'doping' the source or original bitumen with each of four SARA fractions. They measured the complex modulus of these specimens (using a frequency sweep test) and tensile strength (using a poker chip test). It was apparent that doping with asphaltene increased the complex modulus of the bitumen while doping with aromatic or saturates reduced the modulus. They also noted that the influence of this increase in modulus was more substantial at higher temperatures (or lower testing frequency). Another important finding was that the tensile strength of the bitumen also followed a trend similar to the complex modulus, i.e., an increase in the polar fraction of the bitumen resulted in an increase in its tensile strength. The apparent correlation between stiffness and strength contrasts with the results from a later study by Hajj et al. (2017). However, it should be noted that Hajj et al. (2017) compared eight bitumens from different sources (with different chemical compositions) while Sultana (2014) compared different concentrations of specific polar fractions using the same parent bitumen.

In another study, Eberhardsteiner et al. (2015) used a set of carefully modified bitumens to evaluate the relationship between the chemical composition and rhe-

ological properties of the bitumen. They added different dosages of asphaltene to the maltene from the same source. They measured creep-recovery using a dynamic shear rheometer. Consistent with the previous study, they noted that increasing asphaltene content resulted in a reduction of creep compliance (increased stiffness). They also noted that addition of asphaltene to maltene resulted in an abrupt increase of stiffness, even at a small dosage which indicates initiation of a structural change in bitumen. The authors found that non-recoverable compliance decreases with increasing asphaltene content.

Although in the works cited above, the researchers explored only a limited number of bitumens combined with synthetic derivatives of such bitumen, the findings provide meaningful insights into establishing the relationship between the chemical composition of the bitumens and its mechanical properties.

3.4.4 Chemical composition and rheological properties of large and diverse set of commercial bitumens

The use of carefully controlled and laboratory synthesized bitumens allow researchers to closely examine the relationship between bitumen chemistry, rheology, and strength. However, it is equally important to extend this understanding to real world bitumens. Several studies cited in the previous sections address this by comparing properties of commercial bitumens to different performance metrics. However, many of these studies included only a limited number of bitumen sources. One of the goals of this study was to examine this relationship using a large set of commercial bitumens. Two similar and recent studies that evaluated a large set of commercial bitumens and are in some respects similar to this current study are summarized below (Stangl 2010, Radenberg et al. 2014) .

Stangl (2010) analyzed 14 different bitumens with different modifications and each of them had three aging variants (unaged, short-term and long-term). The bitumens came from four different crude sources and presented a range of rheological and chemical properties. Also, one bitumen was polymer modified while others were unmodified. Stangl (2010) found a good relationship between asphaltene content and aging ratio based on the complex modulus but this relationship was poor when only complex modulus or viscosity was considered directly in lieu

of the aging ratio. More importantly, he noted that direct correlations between chemical properties and complex moduli were strong when the bitumens were obtained from the same source but these correlations were weak when bitumen from different sources were pooled together. However, Stangl (2010) did not conduct multivariate analysis to explain mechanical parameters using SARA fraction and/or their derivatives.

In another large volume study, Radenberg et al. (2014) analyzed 90 different bitumens from eight refineries in Germany. SARA separations were conducted using a process similar to ASTM D4124 (2009), along with physical property tests such as needle penetration test, ring and ball test, Fraass breaking point, complex shear modulus, phase angle, and bending beam rheometer tests. Radenberg et al. (2014) reported that asphaltene content related positively with equiviscous temperature (temperature at which complex shear modulus is 15 kPa) and negatively with phase angle at 50°C with coefficient of correlation of 0.59 and 0.65, respectively. They found that other fractions (SAR) did not correlate well with these physical properties and that there was much larger variation in chemical makeup compared to the physical properties. They also reported that the correlation between asphaltene content and complex shear modulus was better at high temperatures and that this correlation was not as good at temperatures below 30°C. Both Radenberg et al. (2014) and Weigel and Stephan (2018) concluded that the SARA fraction is not a sole and comprehensive measure of all bitumen properties.

Glaser et al. (2016) selected 8 unmodified bitumen for their study. SAR-AD procedure, developed at Western Research Institute, was utilized for chemical fractionation. The chemical fractionation data was fitted with rheological parameters over a range of temperature which showed positive correlation with cyclohexane asphaltene and saturates but negative relationship with naphthene saturates. They also noted that amount of mobile fraction dictates low temperature behavior whereas multiple fractions act in tandem at high temperatures.

In summary, several studies have shown that chemical properties are a useful tool to better understand the physical properties and more importantly the rheological properties of bitumens. Several of these studies have utilized either a limited number of commercial or laboratory synthesized bitumens to reinforce the above concept. Two recent studies have attempted to generalize this understand-

ing to a larger set of commercial bitumens sourced from regions in and around Germany (Radenberg et al. 2014, Weigel and Stephan 2018). One of the goals of this present study is also to examine the relationship between bitumen chemistry and mechanical properties using a large set of commercial bitumens from the southern region of the United States. As demonstrated later in this paper, some of the findings from this study and previous studies point to certain common findings despite differences in geographical sampling of materials and methods.

3.5 Materials

A total of 34 unaged bitumen samples with different Performance Grades were collected from 12 producers (labeled A to L in succeeding discussion) from the South Central region of the United States. Among these bitumens, 11 were graded by the manufacturer as PG 64-22, two as 64-28, seven as 70-22 and 76-22 each, four as 58-28 and one each as 58-22, 70-28, 76-28. Figure 4.1 presents the sources and corresponding grades sampled from these sources. The bitumen samples were short-term and long-term aged using the Rolling thin film oven (RTFO) and the pressure aging vessel (PAV) respectively. In summary, each of the aforementioned bitumens was evaluated for its SARA fraction in three different aging conditions while five bitumen samples were not fractionated due to practical limitations (three short-term and two long-term aged bitumen).

It must be noted that the bitumen specimens were sampled on an 'as-is' basis from commercial bitumen suppliers in the South Central region of the United States. No information was provided by the producers regarding the use of any performance modifiers or extenders. However, based on the grades of the bitumen, it is very likely that some of these bitumens incorporate modifiers. The bitumens evaluated in this study represent diverse sources, production processes, and potential modifiers (albeit from a limited geographic region) instead of a carefully curated or synthesized set of samples produced in the laboratory as in the case of other studies by the authors and some other researchers (Sultana 2014, Sultana and Bhasin 2014, Sultana et al. 2014, Weigel and Stephan 2018, Eberhardsteiner et al. 2015).

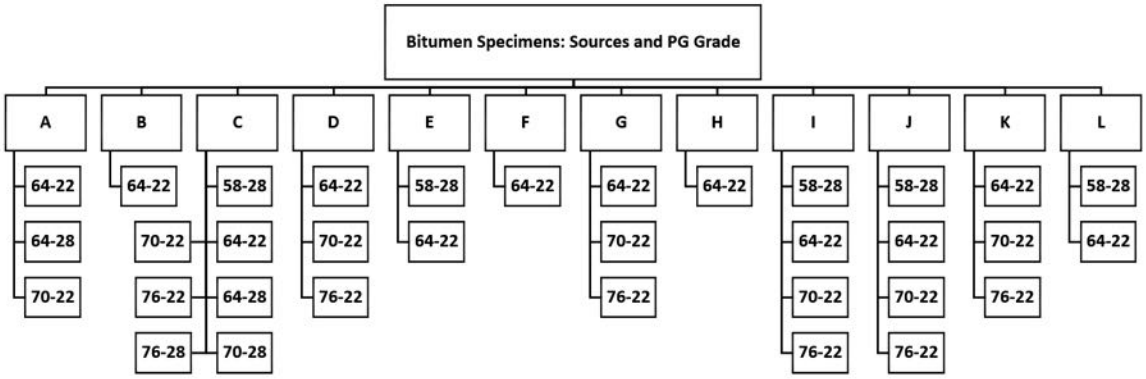

Figure 3.1: Bitumen sources and their products (identified by PG grade) used for this study

3.6 Chemical makeup (SARA fractionation)

In a preceding study, the authors developed a method to conduct SARA fractionation (Sakib and Bhasin 2018). One of the major goals of that study was to develop a method for SARA fractionation that required low capital cost, was repeatable, could be performed in typical asphalt testing laboratories, and could be used to deliver high throughput. This method is referred to as 'TexSARA' to avoid confusion and distinguish it from other methods used to measure SARA fractions. The method is briefly summarized below.

A small amount of bitumen (0.3-0.4 gram) is measured and dissolved in 1:100 (g:mL) n-heptane while being stirred at room temperature for 24 hours. The solution is filtered to remove precipitated asphaltene. Disposable syringe filters acts as filter medium and when they are mounted on a vacuum manifold, vacuum drives the solution through the filter. Unlike commonly used Buchner funnel/fritted glass filter combo, these inexpensive filters are disposable and offer finer filtration (PTFE 0.2 μm filters).

Maltene recovered this way is measured by drying and then about 50 mg maltene is introduced to a chromatography column. To reduce expense, time, and to increase repeatability, pre-packaged commercially available silica-filled Solid Phase Extraction (SPE) cartridges are used as a miniature chromatographic column in lieu of the long glass columns. These SPE cartridges are essentially regular sized syringes filled with 50 g silica. As SPE cartridges are disposable and require

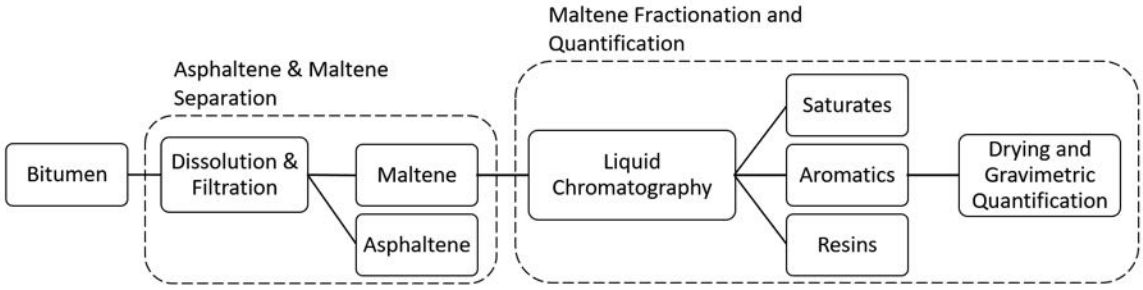

Figure 3.2: Proposed process of TexSARA fractionation (Sakib and Bhasin 2018)

small amount of the sample and solvent, the process is much faster than existing methods such as ASTM D-4124. After introduction of maltene, solvents are sequentially passed through the chromatography column to fractionate maltene. Table 3.1 contains the solvents in their sequence of introduction to SPE cartridge and quantity along with corresponding eluted fraction. A more detailed description can be found in Sakib and Bhasin (2018).

Table 3.1: Solvent Schedule of S-A-R separation using SPE cartridge.

Elutant Solvent	mL	Collected Fraction
n-Heptane	20	Pre-wash
maltene solution + n-Heptane	15 + 10	Saturates
80% Toluene - 20% n-Heptane	25	Aromatics
90% DCM - 10% Methanol	40	Resins

3.7 Mechanical properties

3.7.1 Aging

Bitumen samples were obtained in unaged condition. Prescribed amount of bitumen was processed to produce samples of short-term and long-term aged bitumen. A rolling thin film oven (RTFO) was used to short-term age the bitumen samples to correspond with aging that takes place during mixture production and field placement. A portion of the short-term aged bitumen was then used with the

Figure 3.3: TexSARA setup using SPE cartridges and vacuum manifold (Sakib and Bhasin 2018)

Pressure Aging Vessel (PAV) to long-term age the bitumen samples. Long-term aging is intended to represent the condition of exposed bitumen in pavements after a few years in use.

3.7.2 High temperature properties

The following methods and metrics were used to characterize the high temperature properties of the bitumens.

Test methods

The properties of the bitumens were measured using two different test procedures: complex modulus and creep-recovery. Complex modulus, $|G^*|$ is a measure of the shear modulus of bitumen at a given temperature when subjected to a sinusoidal loading at a specific frequency. An 1-mm thick bitumen specimen was sandwiched between two 25-mm diameter metal plates of a dynamic shear rheometer (DSR). The specimen was subjected to a shear strain following a sinusoidal wave form with an amplitude of 10% and frequency of 1.59 Hz. All bitumens were evaluated at their rated high temperature grade as well as at six degrees Celsius above and below their rated grade. These measurements were conducted on the unaged and short-term aged bitumen samples which is a required step to determine their PG.

Research over the past decade has indicated that high temperature PG based on complex modulus may not be a good indicator of rutting resistance, particularly for modified bitumens (Delgadillo et al. 2006, D'Angelo 2009). Consequently, the traditional method to determine the high temperature grade is being replaced by the 'PG-plus' approach that entails the use of creep-recovery tests at high temperatures to determine the high temperature grade. With an aim to capture creep-recovery characteristics, the multiple stress creep recovery test (MSCR) was also performed using a DSR. For this test, the bitumen samples were subjected to 20 cycles of creep loading (10 cycles at 0.1 kPa followed by 10 cycles at 3.2 kPa, for 1 second) with each creep loading followed by recovery period (9 second). The test was used to estimate the non-recoverable compliance and elastic recovery of the bitumens (ASTM D7405). The short-term aged samples were used for this test.

Metrics

The following metrics were obtained for further analysis from the complex modulus and creep-recovery tests.

(H1) $|G^*|$ at 64°C (where, $|G^*|$ is the complex modulus).

(H2) $|G^*|/\sin\delta$ at 64°C (where, δ is the phase angle).

(H3) The continuous grade of the bitumens based on their unaged condition, i.e. the temperature at which $|G^*|/\sin\delta = 1$ kPa; in the context of this research the continuous grade must be interpreted not as an indicator of rutting, rather as an equi-stiffness temperature for the purposes of comparison.

(H4) The continuous grade of the bitumens based on their short-term condition, i.e. the temperature at which $|G^*|/\sin\delta = 2.2$ kPa; interpretation is the same as above.

(H5) The logarithm of non-recoverable compliance, $\log J_{nr}$, measured at 64°C and at a stress level of 3.2 kPa from the creep-recovery test.

(H6) Elastic recovery, ER, measured at 64°C and at a stress level of 3.2 kPa from the creep-recovery test.

(H7) Continuous grade from the creep-recovery test defined as the temperature at which $J_{nr} = 4.5$ kPa^{-1}; as before, this should be interpreted as the temperature at which all bitumens showed similar compliance and not necessarily as a rutting indicator.

3.7.3 Low temperature properties

Methods

Low temperature stiffness and rate of relaxation of a bitumen are particularly important in the context of the asphalt mixtures resistance to thermal cracking. In simplest terms, the thermal stress accumulation as the temperature drops is directly related to the stiffness of the bitumen and the rate at which this stress dissipates is reflected in the rate of relaxation of the stress at low temperatures. In this

study, a Bending Beam Rheometer (BBR) was used to measure low temperature stiffness of bitumen following ASTM D6648. In summary, a 6" long, 1/2" deep and 1/4" thick long-term aged bitumen beam specimen was mounted on two supports 4" apart and loaded for 4 minutes with 1 N load at the center of the beam after appropriate thermal conditioning. The deformation was measured over time to compute the stiffness at any given point in time and rate of change of stiffness. All long-term aged bitumens were evaluated using the BBR for three different temperatures.

Metrics

The following metrics were obtained for further analysis from the above tests.

(L1) Creep stiffness, S, measured at 60 seconds and -12°C (this is based on the parameter used in the current PG specification).

(L2) Creep stiffness, S, measured at 5 seconds and -12°C (this is similar to the above parameter, except that it reflects bitumen stiffness with a smaller influence of time-dependent deformation).

(L3) The continuous low temperature grade based on stiffness defined as the temperature at which S-value is 300 MPa (this is obtained by interpolating test data from different temperatures).

(L4) Slope of the stiffness vs. time curve, $m - value$, measured at 60 seconds and -12°C.

(L5) The continuous low temperature grade based on rate of deformation or m-value defined as the temperature at which $m - value$ is 0.3 (this was obtained by interpolating test data from different temperatures).

(L6) Difference in low temperature grade, ΔT_c, computed as the difference between low temperature grades based on stiffness criterion and m-value criterion (a magnitude of ΔT_c that is greater than 6°C has been regarded as symptomatic of undesirable modifiers).

(L7) Useful temperature interval or UTI, defined as the spread between high temperature grade and low temperature grade; six variations of this parameters were evaluated based on the high temperature grade using either one of the three high temperature parameters (unaged $G^*/\sin\delta$, short-term aged $G^*/\sin\delta$, and short-term aged J_{nr}) and low temperature grade using either one of the two parameters (stiffness and m-value).

Note that UTI is strictly speaking not a low temperature property. UTI was included in this study based on the findings from Baumgardner (2012) that indicated that chemistry of bitumen dictates UTI such that higher asphaltene to resin ratio results higher UTI and vice versa.

3.7.4 Tensile Strength of Bitumen

Method

The tensile strength of a bitumen is an important parameter that is directly related to its ability to resist cracking in an asphalt mixture. However, this parameter is not typically measured on a routine basis to specify or screen asphalt bitumens. Establishing a method to incorporate the tensile strength of bitumen in a screening and specification framework is an important goal of several research studies. One method to measure the tensile strength of the bitumen in a confined state of stress that is similar to what the bitumen experiences in an asphalt mixture is to use the poker chip test.

The poker chip tests involves subjecting a thin circular film of an asphalt bitumen confined between metal plates to direct tension. In previous studies, the authors have developed and evaluated the use of the poker chip test to distinguish between flow and fracture in the bitumen and also to demonstrate the broad range of tensile strengths exhibited by bitumens with the same PG (Motamed et al. 2014, Sultana et al. 2014, Hajj et al. 2017).

Tensile strength (from poker chip test) of bitumen samples used in this study were compiled from Hure (2017). The test was conducted on an Instron E1000 universal testing machine with 14.6 mm diameter plates and 0.300 mm film thickness using short term aged specimen. Figure 3.4 shows the testing equipment and bitumen specimen mounted on steel substrate.

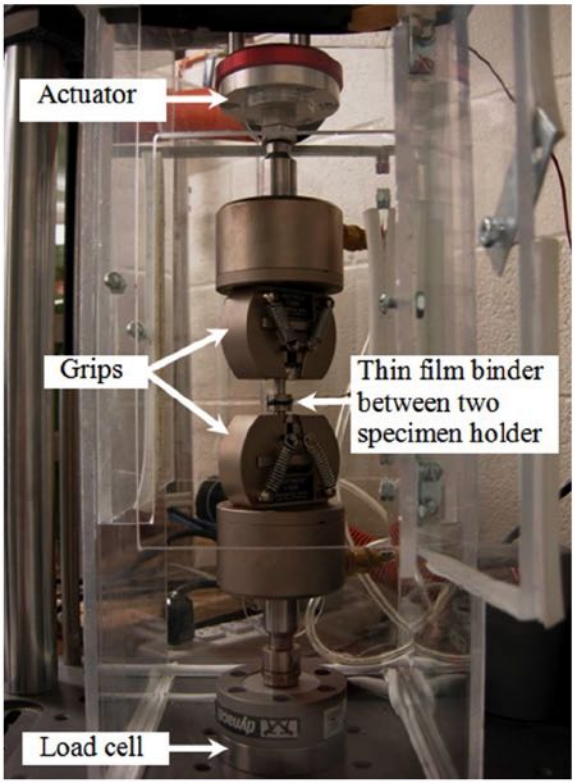

Figure 3.4: Poker chip text configuration (Hure 2017)

Metrics

The tensile strength of bitumen, σ_{max} in MPa, when subjected to a monotonically increasing load at 1 N/sec at 18°C was used as a metric for further analysis.

3.7.5 Other properties

Analysis for metal content

The unaged bitumens were also evaluated for the metal content using X-ray florescence (XRF). A hand-held Bruker Tracer XRF spectrometer was used for the XRF analysis. The XRF spectra was semi-quantitatively analyzed to identify metals that were present in relatively high abundance compared to most samples in the group. According to Arnold and Shastry (2015), some of these metals are symptomatic of certain types of additives that might have been used to modify the bitumen (e.g. Polyphosphoric acid, recycled engine oil bottoms, crumb rubber). In the context of

this study, bitumens that showed unusually high concentration of these metal(s), were identified as 'outliers'.

Spot test

Spot test was performed using a method similar to Tex-501-C and AASHTO T-102(09) but with Toluene as solvent. In summary, a small amount of a bitumen sample was dissolved in toluene and a drop of the solution was used to make a 'spot' on a Whatman no.50 filter paper which was scanned and analyzed using an image processing software Image J. Spot test is an indicator of bitumen incompatibility. Such incompatible bitumen samples usually create heterogeneous black rings or dark spots on the filter paper in place of a ideal homogeneous circle. If a clear separation was noted in the test, that bitumen was flagged and used in further analysis.

3.8 Data Analysis

This study generated significant amount of information on the chemical characteristics and mechanical properties of a large set of bitumens. Significant portion of the mechanical test data was obtained from Hure (2017) who used the same set of bitumens, as a part of the same project. Considering the three aging conditions for the 34 bitumens, the chemical analysis resulted in a database of 102 bitumens (with five exceptions as noted earlier). As a first step to better understand the relationship between the chemical properties of the bitumen (specifically the concentration of the TexSARA fractions) and mechanical properties a regression analysis was conducted between the metrics for chemical properties and mechanical properties. For the chemical properties, apart from the concentrations of each of the TexSARA fractions, i.e. saturates, aromatics, resins and asphaltenes, other metrics such as colloidal index and different ratios of fractions were also considered in this preliminary analysis. These derived parameters were based on previous research from other researchers (Guzman et al. 2017, Sepulveda et al. 2017, Weigel and Stephan 2018, Stangl 2010, Baumgardner 2012). Some of these parameters are used for identifying instability issues with crude oil. This preliminary analysis was conducted using bivariate linear regression of mechanical properties with

TexSARA fractions and their derivatives and for each pair, correlation coefficient, R^2 was measured.

The metrics identified in the previous section were based on high and low temperature rheological properties of the bitumen (with the exception of UTI, which is based on both) and its tensile strength at an intermediate temperature. Another broad way to categorize these properties is based on what these metrics represent in terms of the physical properties as listed below.

1. Parameters such as $|G^*|$, $|G^*|/\sin\delta$, and S-value can be regarded as a measure of the inherent stiffness that is obtained at shorter loading times (authors recognize that these are not strictly a measure of the time-independent elastic component of the bitumens but are being used as an approximation given the scope of the study).

2. The parameter, σ_{max}, represents the tensile strength of the bitumen (at a high rate of loading).

3. Parameters such as m-value and elastic recovery can be regarded as metrics that represent the time-dependent nature of the bitumens.

4. Parameters such as ΔT_c and UTI do not necessarily fall in one of the above categories but represent some combination of the above parameters.

Table 3.2 enumerates the value of coefficient of determination, R^2, from each pair of correlation. Highest R^2 value for each parameter is underlined. A preliminary examination of the data in Table 3.2 demonstrates that stiffness parameters that are less influenced by loading time (or frequency) generally show a better correlation with some of the metrics based on the TexSARA fractions particularly with the asphaltene content. The two metrics, m-value and ER that are more strongly dictated by the time-dependent response of the bitumen show a relatively weaker correlation with the metrics based on the TexSARA fractions. Based on this preliminary analysis, some of the metrics from each of the four broad categories were selected for further analysis.

Table 3.2: Correlation coefficients for measured physical properties and chemical fractions (highest value is underlined)

Parameters	S	Ar	R	A	S+A	R+Ar	R/A	S/A	Ar/A	Ar/(S+A)	S/(Ar*A)	CII	A/(A+R)
G^* at 64°C (Unaged & RTFO)	0.08	0.02	0.01	<u>0.39</u>	0.06	0.06	0.13	0.25	0.20	0.05	0.21	0.06	0.14
$G^*/\sin\delta$ at 64°C (Unaged & RTFO)	0.06	0.03	0.02	<u>0.50</u>	0.12	0.12	0.17	0.26	0.26	0.10	0.20	0.12	0.19
High true grade (Unaged $G^*/\sin\delta$)	0.02	0.00	0.02	<u>0.22</u>	0.06	0.06	0.10	0.11	0.09	0.03	0.09	0.06	0.10
High true grade (RTFO $G^*/\sin\delta$)	0.11	0.01	0.04	<u>0.54</u>	0.08	0.08	0.22	0.30	0.29	0.06	0.29	0.07	0.22
$\log J_{nr}$ at 64°C & 3.2 kPa (RTFO)	0.01	0.02	0.02	<u>0.23</u>	0.08	0.09	0.11	0.07	0.15	0.08	0.06	0.08	0.10
Elastic Recovery at 64°C & 3.2 kPa (RTFO)	0.01	0.11	0.00	0.22	0.07	0.07	0.04	0.08	<u>0.23</u>	0.14	0.04	0.07	0.03
High true Grade (RTFO log Jnr)	0.00	0.03	0.05	<u>0.31</u>	0.17	0.17	0.16	0.08	0.22	0.14	0.06	0.17	0.17
Stiffness at -12°C & 60s (PAV aged)	0.31	0.25	0.00	0.01	0.21	0.21	0.00	0.25	0.08	0.38	<u>0.38</u>	0.21	0.00
Stiffness at -12°C & 5s (PAV aged)	0.37	0.30	0.01	0.08	0.15	0.15	0.03	0.37	0.04	0.35	<u>0.52</u>	0.16	0.02
Low true grade (PAV aged S-value)	0.34	0.28	0.01	0.05	0.16	0.16	0.02	0.31	0.06	0.36	<u>0.47</u>	0.18	0.01
m-value at -12°C & 60sec (PAV aged)	0.00	0.08	0.02	0.03	0.00	0.00	0.00	0.02	<u>0.10</u>	0.06	0.00	0.00	0.00
Low true grade (PAV aged m-value)	0.00	0.04	0.00	0.06	0.02	0.02	0.00	0.02	<u>0.10</u>	0.05	0.00	0.02	0.00
ΔT_c (PAV aged Δ of S-value and m-value)	0.36	0.09	0.00	0.20	0.06	0.06	0.03	0.45	0.01	0.13	<u>0.50</u>	0.07	0.02
UTI (RTFO $G^*/\sin\delta$ - m-value)	0.10	0.06	0.01	<u>0.62</u>	0.11	0.12	0.18	0.34	0.47	0.15	0.26	0.11	0.19
Tensile strength, σ_{max} at 18°C (RTFO aged)	0.11	0.04	0.02	0.15	0.00	0.00	0.09	0.16	0.04	0.01	<u>0.20</u>	0.0	0.09

3.8.1 Evaluation of parameters reflecting stiffness at short loading times

Of all the metrics discussed in the previous section, two parameters that reflect the stiffness of the bitumen in frequency or time domain at short loading times, $|G^*|$ measured using the DSR at 64°C and stiffness or S measured using the BBR at -12°C, were selected for further analysis. A multivariate non-linear model was used to examine the relationship between the aforementioned parameters and the parameters derived from TexSARA fractions using the Origin software and the following model:

$$y = \sum a_i x_i^{b_i} + c \tag{3.1}$$

In equation 3.1, x_i is the concentration of the polar fractions or a derivative of these fractions such as the colloidal index, and y is the measured mechanical property.

Complex moduli or $|G^*|$ measured at 64°C for all the unaged and short-term aged bitumens were fitted using the model described in equation 3.1 where the independent variable(s) varied from one or more TexSARA fractions or their derivatives. Equation 3.2 shows the best relationship among all options.

$$|G^*|_{64°C} = 0.172 \times Asphaltene^{3.155} \tag{3.2}$$

Including other TexSARA fractions (saturates, aromatics, resins, and/or derivatives) did not influence the relationship. In summary, the asphaltene content is the most significant factor (among the TexSARA fractions) that explains the complex shear moduli of the bitumens at high temperatures. Figure 3.5 compares the measured versus predicted value of $|G^*|$.

One of the goals of this study was not merely to examine the correlation between the physical properties of the bitumens and TexSARA fractions (or its derivatives) but also to use this information to more carefully examine anomalous bitumens. Six bitumens highlighted in Figure 3.5 that appeared to be farther away from the line of equality were further examined.

The short term aged I70-22 bitumen appears on the right of the fitted line. This bitumen showed anomalous behavior in some others tests as well. Specifically XRF results indicated presence of zinc and iron in this bitumen and the spot test

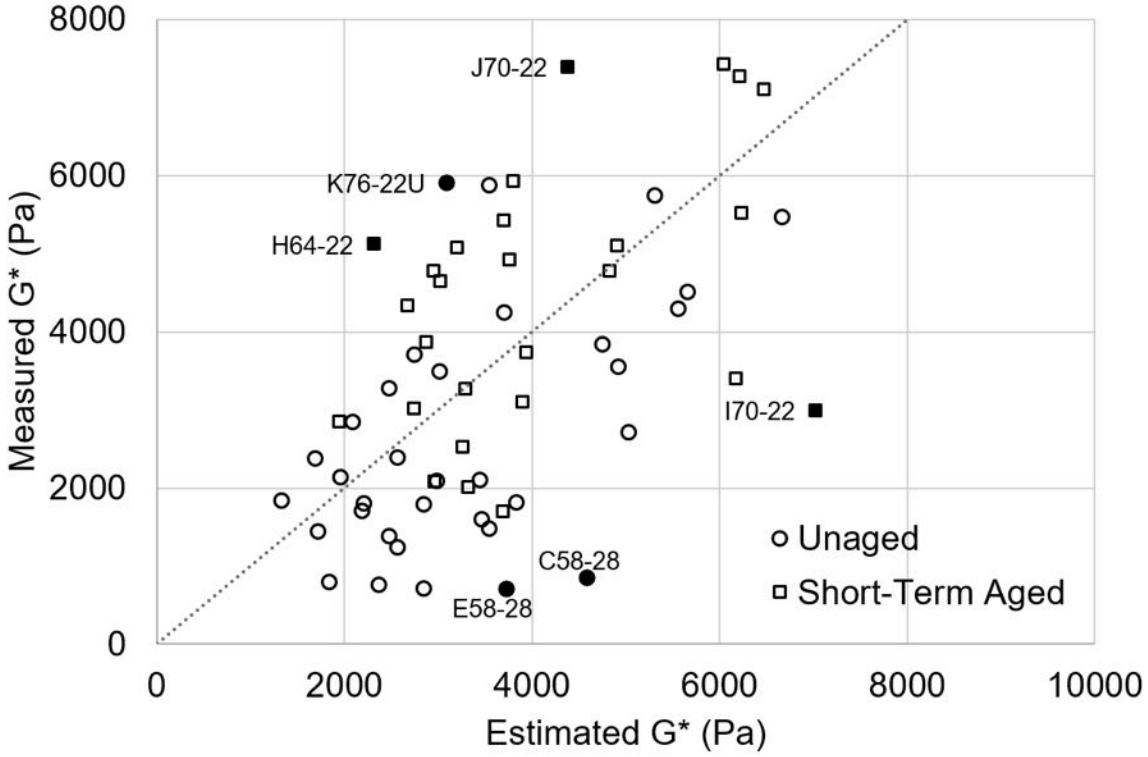

Figure 3.5: Correlation between measured $G*$ and TexSARA predicted value

showed separation. In addition, the continuous high temperature grade based on the value of J_{nr} was more than 12°C higher than the continuous grade based on the $|G^*|/\sin\delta$ parameter. The three bitumens on the left side of the line of equality represent short term aged J70-22, K76-22 and H64-22. These three bitumens also showed a very high value of ΔT_c (greater than 6°C). Two bitumens on the bottom right of the line of equality represent unaged E58-28, and C58-28. Based on the tests conducted in this study, these two bitumens did not show any anomalous results.

In summary, at least four of the six bitumens that appeared to deviate substantially from the line of equality showed anomalous behavior based on metrics that are not typically included in the PG specification.

Similar to $|G^*|$ at high temperatures, the S value can be regarded as a measure of stiffness in time domain at low temperatures. The model shown in equation 3.1 was used to fit S values from the BBR test to the TexSARA fractions and its derivatives. Equation 3.3 shows the best relationship among several different models that

were evaluated.

$$S = -7.71 \times Aromatic + 8.81 \times Resin \tag{3.3}$$

Unlike equation 3.2, the low temperature stiffness is more strongly dictated by the aromatic and resin fractions. It must also be noted that including other fractions (saturates or asphaltenes) or derivatives of TexSARA fractions did not improve the relationship. This is an interesting observation because typically asphaltene is considered as the 'stiffness-building fraction' as observed in the previous discussion on G^*. However, some authors noted that this is true only at high temperatures (Radenberg et al. 2014, Weigel and Stephan 2018), which is also consistent with the findings from this study.

Figure 3.6 compares the measured S value to the predicted values using equation 3.3. As before, a few bitumens tend to appear away from the line of equality. The A64-28 bitumen shows much higher stiffness than expected. Based on XRF analysis, this bitumen had significantly higher iron and zinc which is an indicator of recycled engine oil or crumb rubber modification. It should be noted that the bitumen I70-22, which also showed high iron and zinc did not appear to deviate from the line of equality in this case, whereas it did so when comparing $|G^*|$. Two bitumens C58-28 and C64-22 also appear to deviate from the line of equality but did not show any anomalous response for the properties measured in this study.

Finally, a similar analysis was conducted using stiffness values at 5 seconds instead of 60 seconds. Results from this analysis were similar to the analysis based on S measured at 60 seconds.

3.8.2 Evaluation of tensile strength of the bitumen

Tensile strength of bitumen measured using poker chip setup were compared with TexSARA fraction data using equation 3.1. As before, Origin statistical analysis software was used to find the best correlation between poker chip tensile strengths and TexSARA fractions and/or its derivatives using model 3.1. The following equation 3.4 was found to have the best relationship among the various

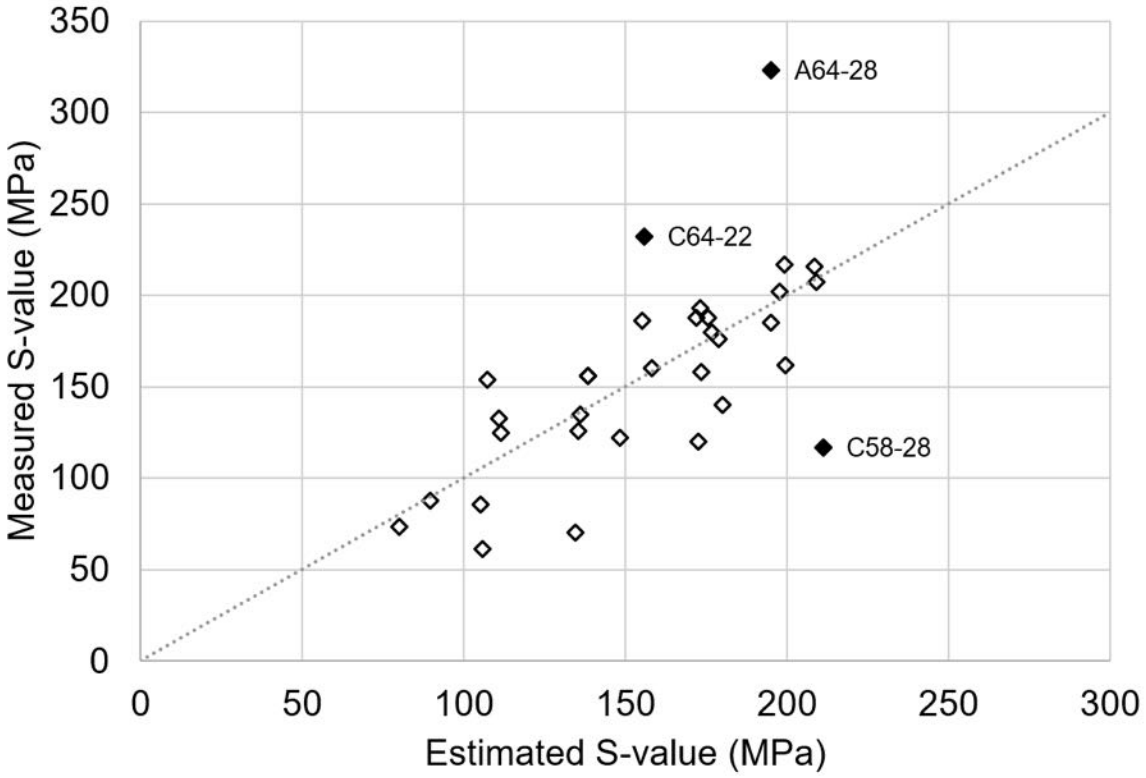

Figure 3.6: Correlation between measured BBR stiffness value (MPa) and TexSARA predicted value

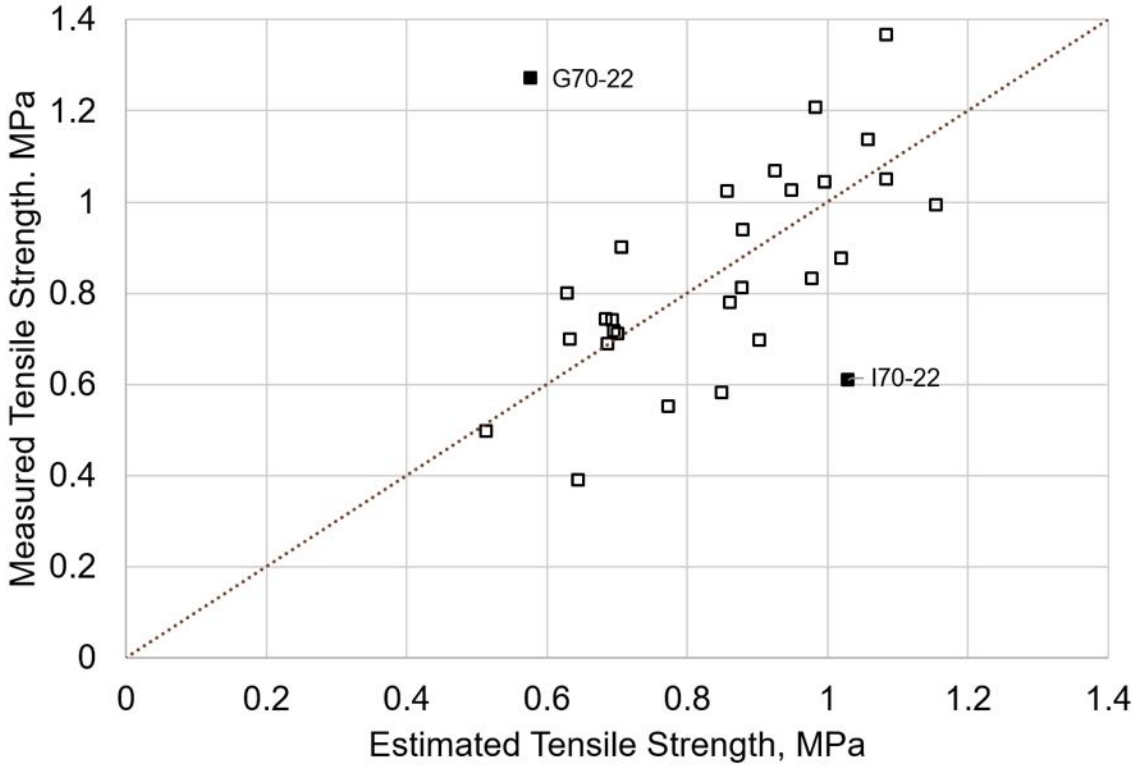

Figure 3.7: Correlation between measured tensile strength using the poker chip test and chemical fractions' estimated value

options that were evaluated.

$$\sigma_{Max}(MPa) = -0.0184 \times Saturate + 0.0276 \times Aromatic + 0.0504 \times Asphaltene - 1.0975 \tag{3.4}$$

Equation 3.4 indicates a positive relationship between tensile strength and asphaltene as well as aromatics and a negative relationship with saturates. This is expected because the bitumen is expected to derive its tensile strength from polar interactions between molecules. Figure 3.7 illustrates two bitumens that depart from the line of equality I70-22 and G70-22. These two bitumens provide interesting insight into the chemical makeup versus performance relationship. I70-22 bitumen was previously flagged as anomalous by other parameters such as high temperature grade, spot test, J_{nr} as well as high metal content in XRF. In addition, the other anomalous bitumen, G70-22 was also flagged as an outlier when comparing TexSARA with with J_{nr} (not included in this paper) and for having a high

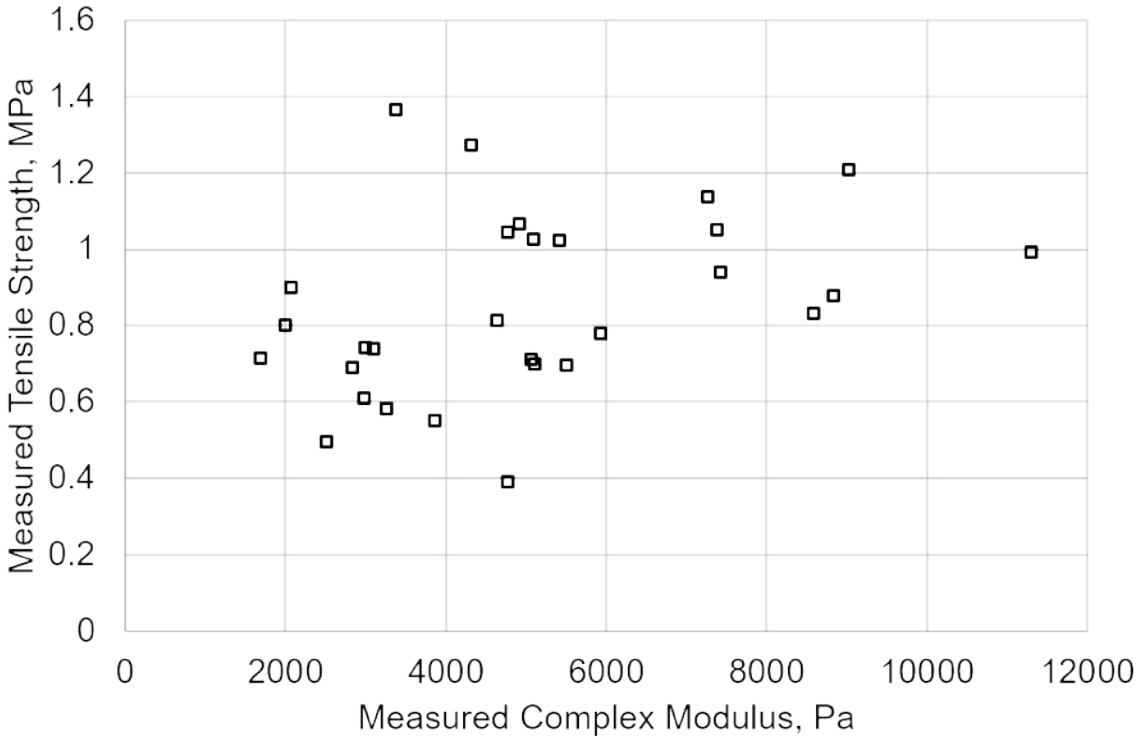

Figure 3.8: Tensile strength by poker chip test vs. complex shear modulus of bitumen

ΔT_c.

In the context of tensile strength of the bitumen, it is also important to highlight that for the sampled bitumens, the stiffness (represented as complex modulus at 64°C) and tensile strength showed no correlation as shown in Figure 3.8. Specifically, this variability is much higher for softer bitumens than stiffer bitumens ($|G^*| > 6000$ MPa). This observation is in agreement with Hajj et al. (2017) who noted that stiffness and tensile strength are not necessarily correlated, and the latter must be independently evaluated for bitumens.

3.8.3 Evaluation of parameters reflecting time dependent behavior

The parameters ER measured using the DSR at high temperatures and m-value measured using the BBR at low temperature are metrics that are relatively more

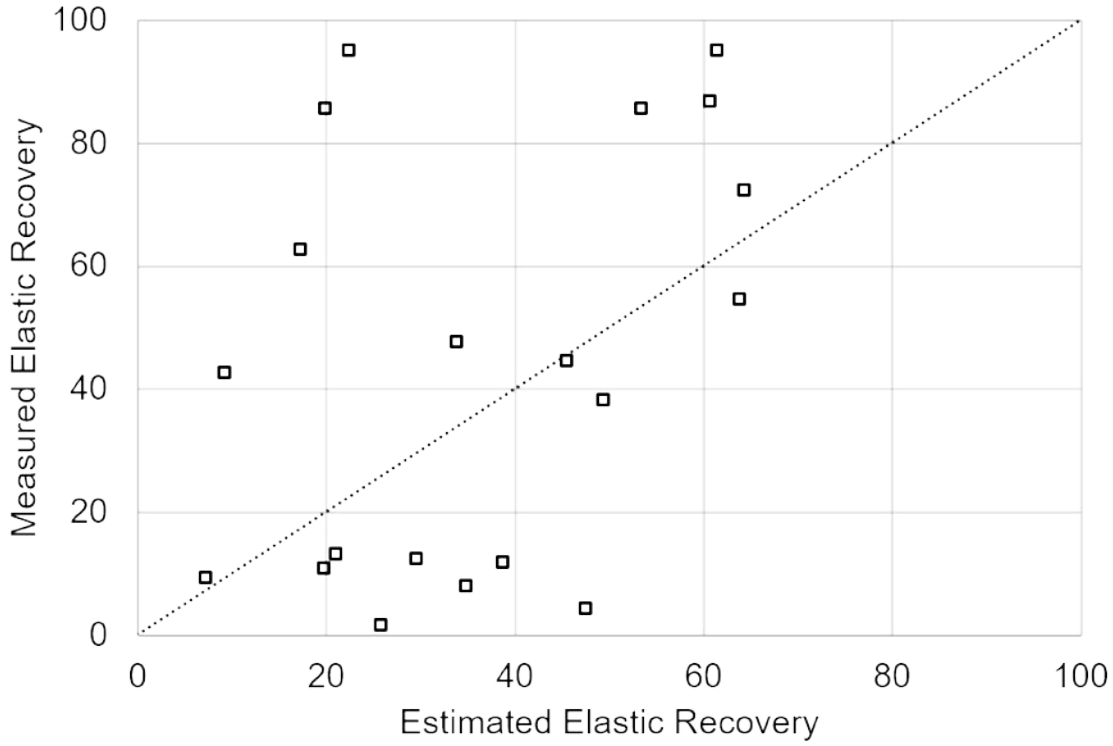

Figure 3.9: Correlation between measured DSR elastic recovery and TexSARA predicted value

strongly dominated by the time-dependent behavior of the bitumen. These parameters and their correlation with metrics based on the TexSARA fractions are further examined in this section. As before, equation 3.1 was used to compare these parameters individually with the TexSARA fractions and its derivatives as the independent variables. For each of the two parameters, ER, and m-value, the correlation between the parameter and TexSARA fractions was very poor. Figures 3.9 and 3.10 compare the measured values for the two parameters to the predicted values based on the best model that could be obtained. Results from these figures show that the TexSARA fractions (or any of its derivatives) do not adequately explain these parameters related to the time-dependent properties.

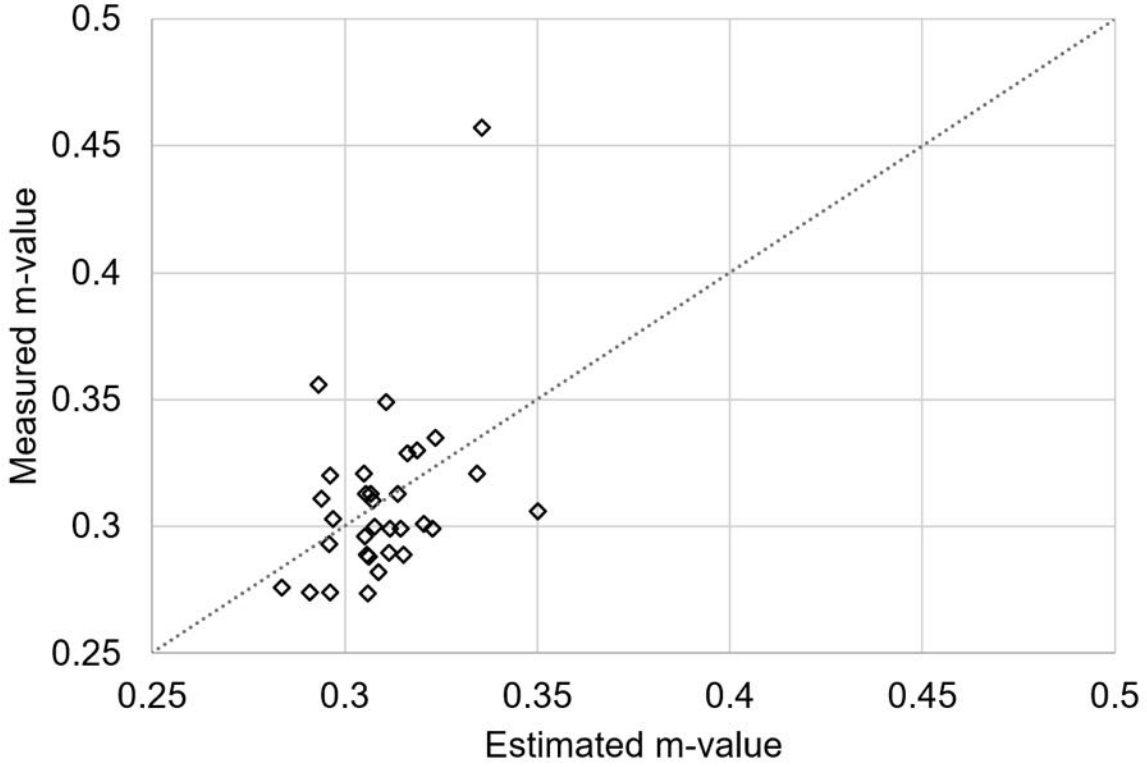

Figure 3.10: Correlation between measured BBR m-value (MPa) at -12°C and TexSARA predicted value

3.8.4 Evaluation of parameters reflecting temperature at similar stiffness

Previous studies have compared SARA fractions to equi-viscous temperatures for various bitumens. In the context of rheological measurements, the parameter that would be similar to equi-viscous temperature is the continuous high- or low-temperature grade. The continuous high-temperature grade is defined as the temperature at which the value of $|G^*|/\sin\delta = 1$ kPa for the unaged bitumen or the temperature at which the value of $|G^*|/\sin\delta = 2.2$ kPa for the short-term aged bitumen, whichever is lower. In fact, the definition for unaged bitumen can also be extended to the short-term aged bitumen and vice-versa when the purpose is to merely examine the equivalent temperature at a specific value of complex modulus. Similarly, the continuous low-temperature grade is defined as 10°C below the higher of the temperature at which the value of $S = 300$ MPa or m-value $= 0.3$. Therefore, it was possible to use four different scenarios to compare with the TexSARA fractions. Of these, the correlations with TexSARA fractions using the continuous high temperature grade based on short-term aged $|G^*|/\sin\delta$ and the continuous low temperature grade based on long-term aged S value were much better than the correlations using temperatures corresponding to unaged $|G^*|/\sin\delta$ or m-value. This is consistent with the results observed and discussed in the previous sections.

3.8.5 Useful Temperature Interval (UTI)

The useful temperature interval or UTI indicates the range of temperature for which any given bitumen meets PG requirements. In other words, UTI is essentially the difference or spread between the high and low temperature grade. Increasing the UTI for any given bitumen is one the reasons for bitumen modification. Thus, despite being a derived parameter, UTI provides useful information pertaining to its performance. Also note that based on the above definition, UTI reflects the behavior of the bitumen across three different aging conditions and different types of tests on either end of temperature range. Baumgardner (2012) noted that UTI has strong correlation with asphaltene to asphaltene+resin ratio (A/A+R). Therefore, it was of interest to use the data from this study to examine

such correlations.

As discussed in the previous section, the high temperature grade is lower of the continuous grade based on criteria for unaged and short-term aged samples evaluated using the DSR. Similarly, the low temperature grade is higher of the continuous grade based on criteria for stiffness and m-value of long-term aged sample evaluated using the BBR. If each criterion at high- and low-temperature were considered separately as an independent parameter, there can be as many as four different definitions of UTI. Since these UTI include parameters for both unaged, short-term aged, and long-term aged bitumens, the UTI could be compared to TexSARA fractions (or their derivatives) corresponding to any of these three aging conditions, resulting in 12 different possible comparison sets. Of these possible sets, the strongest correlations exist between UTI computed as the difference between continuous high temperature grade based on short-term aged criterion and continuous low temperature grade based on long-term aged m-value and TexSARA fraction measurements for short-term aged bitumen. Equation 3.5 shows the results for this model and Figure 3.11 compares the measured UTI values to the predicted values.

$$UTI = 36.21 + 1.98 \times asphaltene_{RT} + 0.045 \times resin_{RT} \tag{3.5}$$

Figure 3.11 also shows bitumen G76-22 that departs substantially from the line of equality. Interestingly, G76-22 also showed a very high value of continuous grade based on J_{nr} (more than 12°C than the grade based on $|G^*|/\sin\delta$) and also showed a very high value for ΔT_c (greater than 6°C).

3.9 Conclusions and Discussion

This study utilized a novel SARA separation technique that enabled the authors to explore a large number of bitumens from different sources. The TexSARA fractions were then compared to a number of different metrics based on the rheological properties of the selected bitumens. The following are some of the conclusions that can be drawn from this exercise:

1. Metrics that reflect the stiffness of the bitumen and are less influenced by the time-dependent nature of the bitumen show a better correlation with

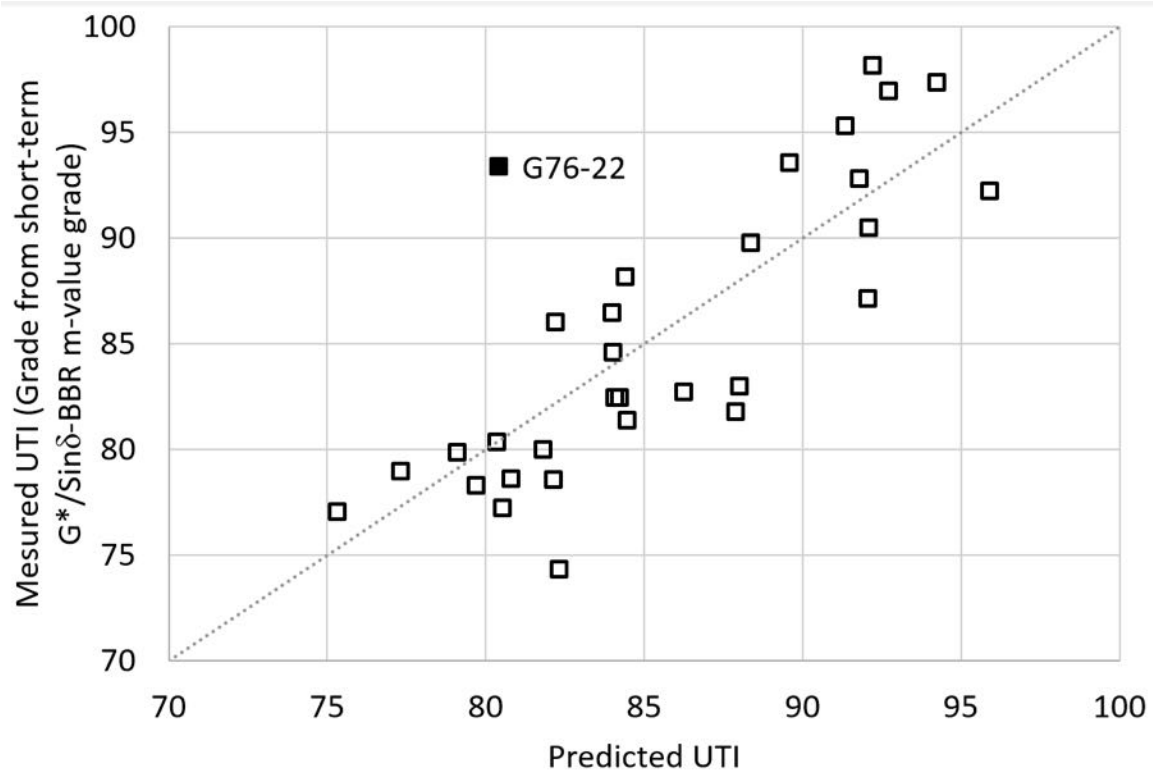

Figure 3.11: Correlation between UTI (Short-term aged complex shear modulus based true grade and BBR m-value-based true grade) and TexSARA predicted value

TexSARA fractions. Specifically, $|G^*|$ measured using a DSR at high temperatures showed a strong relationship with the asphaltene fraction and S or stiffness at 60- or 5-seconds measure using a BBR at low temperatures showed a strong relationship with aromatics (inverse relationship) and resins (direct relationship).

2. Tensile strength of bitumen (measured using the method described in this paper) shows a good correlation with TexSARA fractions, similar to other less-time-dependent parameters. Specifically, the tensile strength was directly related with the concentration of aromatics and resins, and inversely related with the concentration of saturates.

3. Metrics that are more strongly influenced by the time-dependent behavior of the bitumen had a relatively weaker correlation with TexSARA fractions. Specifically, elastic recovery based on the 9-second recovery in creep-recovery test using the DSR at high temperatures and m-value based on the slope at 60-seconds measured using the BBR low temperatures, did not show a strong correlation with TexSARA fractions or its derivatives. It is possible that the latter could be an artifact of the lack of diversity in m-values because most bitumens in this region are designed to marginally meet the m-value criterion at low temperatures. It is also possible that factors such as time-dependent deformation are driven by factors other than molecular polarity (e.g. molecular entanglement). These factors should be explored further.

4. Some traditionally used factors, such as Gaestel Index, did not show particularly good correlation with the rheological properties measured in this study.

5. In some cases properties of the bitumen predicted using the TexSARA based model was substantially different from the measured property compared to other bitumen in the group. In such cases, such anomalous bitumens also showed uncharacteristic response in certain other tests and parameters (e.g. high metal content using XRF, spot test, or ΔT_c. This approach provides a useful tool to further analyze such exceptions and better understand the factors that can be manipulated to control the behavior of the bitumen. Authors would like to caution that the inverse is not always true, i.e. bitumens with

uncharacteristic response in certain mechanical tests may not always have stand out in TexSARA based prediction models. Therefore, such analysis must not be construed as a screening tool rather as an opportunity to better examine and understand the behavior of such bitumens that can ultimately facilitate the design of additives and modifiers.

The authors would like to note that due to limitations in the scope of this work the chemical characteristics of the bitumens were restricted to SARA fractions and the mechanical characteristics were restricted to metrics associated with PG of bitumens. Results from this study strongly indicate that future work should focus on a more comprehensive rheological characterization of the bitumens focusing on the elastic and viscoelastic components separately (e.g. G' and G'' obtained through frequency sweep measurements). The findings from this study also suggest that future work should examine factors other than polarity based fractionation that appear to more strongly influence the time-dependent behavior of the bitumens. Finally, the authors would like to emphasize that the data collected from this study can be further analyzed using more rigorous statistical tools in future work.

3.10 Acknowledgments

We acknowledge the support of National Science Foundation Grant CMMI-1053925 and Texas Department of Transportation for supporting parts of this study. We also acknowledge the support of Rachel Hure, Rogelio Rodriguez, Ramez Hajj, Solomon Nyanhongo, Peter Hartley and Ayah Alomari, for their help with testing.

Chapter 4

Effect of bitumen chemistry on surface microstructure

4.1 Overview

Bitumen composition shows significant variability due to the variation in source and refining process. While bitumen is one of the most important construction materials, bitumen chemistry and its effect on bitumen performance is less understood than most other engineering materials. The evidence of bitumen surface microstructure, commonly observed using atomic force microscope (AFM) highlights that bitumen is not an homogeneous mixture and therefore its microstructure must be considered as an intermediate step in the process of understanding the relationship between bitumen chemistry and its engineering properties. There is no clear consensus in the literature on the chemical species and mechanisms that drive the formation of the bitumen microstructure. Due to practical constraints of using AFM, most previous studies were limited to examining only a few samples which may not be adequate to draw robust and global conclusions. This study employs two new techniques for chemical fractions and microscopy, to analyze a total of 64 bitumens. Results show that bitumens of different grades from the same source exhibit similar microstructures, which is true even after short-term aging. Chemical composition based on polarity distributions alone is not adequate to explain the surface microstructure for all bitumens regardless of the source. Bitumens with unusual looking surfaces, such as no bee structures and/or heterogeneous surface, were also found to have irregular elemental or rheological test results.

4.2 Introduction and Motivation

Bitumen is the binding agent used to produce asphalt mixtures used in the maintenance and construction of flexible pavements around the world. Bitumen is commonly produced by processing the residua from crude oil distillation. Owing to the variability in the chemical composition of the crude oil, the chemistry and physical characteristics of bitumen vary widely. In fact, the variability in bitumen is more amplified than in the crude oil as higher value products, with better

consistency in chemical makeup, are extracted from the crude oil during refining. In addition, producers and contractors use different type of modifiers and extenders in bitumen to reduce cost and impart certain desirable characteristics valued by contractors and procuring agencies. As a result, bitumen from different sources with very different chemical makeups may have similar mechanical properties under a certain set of testing conditions. In practice, this suggests that similar bitumen that satisfy certain specification-designated benchmarks may vary in their composition and consequently result in unexpected performance in the field. This is also partly due to the fact that such specifications are not perfect and do not accurately represent all of the mechanisms that drive failure observed in the real world field conditions. For example, Batista et al. (2017) compiled several studies and noted that commonly used permanent deformation criteria do not show good correlation with actual field performance, particularly when including modified bitumen. Similar observations have been made by Delgadillo et al. (2006) and D'Angelo (2009) among others.

A combination of the imperfections in the current specifications to accurately reflect field performance along with the high degree of variability in the chemical composition of the bitumens reduces the reliability with which a specific bitumen can be used in the field. These factors also inhibit innovation to engineer more sustainable and durable bitumens, and modifiers/additives for bitumens. This has become particularly more pertinent in recent times as the industry is constantly driven to innovate and develop modifiers that enhance bitumen durability and promote use of practices such as high recycled content mixes and bio-based extenders. Considering the above scenario, it is critical to develop a fundamental understanding of the relationship between the chemical makeup of bitumens and its resulting mechanical performance and durability. Several studies in the past decade have established that the bitumen is not a homogeneous material and exhibits a distinct microstructure both in its bulk and surface (Loeber et al. 1996, Ramm et al. 2016, Nahar 2016). These studies have also demonstrated that the chemical composition of the bitumen influences its microstructure, which in turn influences its rheological properties and resistance to failure (Sultana and Bhasin 2014, Jahangir et al. 2015, Hofko et al. 2016). For example, studies have demonstrated that there are microstructural features in the bitumen bulk using dark-field microscopy and

these structures are dependent on the thermal history of the bitumen (Ramm et al. 2016, 2018). These studies have also established that bitumen rheology (or the variation of rheology as a function of its thermal history) strongly correlated with the variation in the bulk microstructural features. Consequently, the overarching goal of better understanding the relationship between the chemical makeup of the bitumen and its mechanical properties cannot be achieved without understanding the intermediate link between these two aspects, i.e. the microstructure of the bitumen.

Previous studies that investigated the relationship between the chemical composition and microstructure formation in bitumen used a very limited number and variety of bitumens (Sultana et al. 2014, Nahar 2016, Hofko et al. 2016) . An important reason for this limited sample size is because it is extremely resource intensive to characterize the chemical makeup of the bitumen (e.g. based on polar fractions using tests such as ASTM D4124) as well as its microstructure using microscopic techniques (e.g. using atomic force microscopy). Two recent studies have addressed these gaps. Sakib and Bhasin (2018) developed a method to evaluate the chemical makeup of bitumens based on its polar fractions, commonly referred to as the SARA fractions (acronym for Saturates, Aromatics, Resins and Asphaltenes). The proposed method, hereafter identified as 'TexSARA' to avoid confusion, reduces the activity time required for fractionation per bitumen to about 30 to 40 minutes which is much less than most other methods and requires low capital cost. The procedure can be performed using commercially available cost-effective disposable components, which improves repeatability and increases throughput. Similarly, Ramm et al. (2016) also presented a simplified technique for rapid and direct optical observation of surface microstructure, commonly known as 'bee' structures in lieu of the AFM. While effect of 'bee' structures on bitumen rheology is not established, surface 'bee' microstructure hold significant potential as an analytical tool as underlying chemistry was shown to affect its size and distribution (Nahar 2016). Overcoming the resource barrier for both chemical (SARA) fractionation and observation of surface microstructure allowed the authors to examine a large variety of asphalt bitumens and draw conclusions that may be more broadly applicable.

4.3 Scope

The main objective of this study was to examine the influence of bitumen source and chemical composition on the surface microstructures using a diverse set of 33 different bitumens. In order to characterize the chemical composition, this study utilized a newly developed chromatographic fractionation method that significantly reduces the time and resources required to obtain the polar fractions of any given bitumen without compromising the repeatability of the method (Sakib and Bhasin 2018). In order to examine the surface microstructures, the authors utilized an optical microscopy technique, proposed by Ramm et al. (2016) in lieu of the atomic force microscopy (AFM) that is commonly cited in the literature. Similar to the chemical fractionation technique, the use of optical microscopy allowed the researchers to examine a large set of bitumens in a very resource efficient manner. Metrics from the optical microscopy were then obtained using image analysis techniques, which were further used for quantitative comparison with the chemical characteristics.

4.4 Background

4.4.1 Chemical composition

The chemical composition of any given bitumen can be characterized based on one or more attributes such as elemental composition, ionic character, molecular weight distribution, polarity distribution, and functional group types. Characterizing the chemical makeup of bitumen based on the polar characteristics of its constituent molecules is a common approach that is used to better understand the relationship between the chemical composition of the bitumen and its engineering properties. This is typically achieved by fractionating the bitumen into four fractions based on their relative polarities using liquid chromatography. These four fractions in the order of increasing polarity are referred to as saturates (S), aromatics (Ar), resins (R) and asphaltenes (A) or their acronym SARA for short.

It is important to emphasize a couple of different aspects related to these SARA fractions. Similar to any other type of chromatography, the eluted fraction of liquid chromatography (that is used to separate different fractions) is dependent of

the solvent (elutant) used and the chromatography medium (usually silica or alumina). While there are few standards (ASTM D4124 2009, ASTM D2007 2016, ASTM D6560 2012, ASTM D3279 1997) available, different researchers have explored different types of solvent and elution media for developing meaningful fractionation technique depending on the ultimate objective. It must be recognized that these four fractions are not discrete but represent four simplified and discrete classes of what is likely a continuous distribution of polarities within the bitumen. Consequently, as Redelius (2004) noted, choosing a somewhat different solvent will cut a slightly different slice in the polarity continuum of the bitumen. Interestingly, most of the authors used 'SARA' to designate polar fractions in any given bitumen, although these fractions are highly method dependent. In this study, the authors use the terms saturates, aromatics, resins, and asphaltenes to denote the four chemical fractions as well. However, to acknowledge that these fractions are method dependent and not universal, the set of four fractions used in this study is identified according to the method of separation, 'TexSARA'.

4.4.2 Bitumen microstructure

The heterogeneity in bitumen and its microstructure have received a lot of attention over the last two decades starting with observation of surface microstructure using an AFM (Loeber et al. 1996, Pauli et al. 2001, Schmets et al. 2010). The observed microstructural features were referred to as 'bee structures' (Loeber et al. 1996). Note that in general bitumen is a challenging material to image under a microscope due to several reasons such as its color, adhesion, challenges in sample preparation, and fluorescence among others. Claudy et al. (1992) were one of the earliest user of optical microscopy technique to observe bitumen microstructure. However, due to the challenges stated above, researchers commonly use AFM to observe surface microstructure.

'Bee' structures have been the subject of several research studies that have tried to explain the origin of these structures, the relationship with bitumen chemistry, rheology, thermal history, aging, and specimen conditioning. The focus of this study was on the relationship between the formation of such bee structures with the chemical composition of the bitumen. The following discussion examines the literature from this perspective. However, it must recognized that although the

discussion and the remainder of this paper is focused on the connection between the chemical composition and microstructure, the ultimate and eventual goal of this exercise it to be able to understand the inter-relationship between chemical composition - microstructure - rheology / durability of the bitumen.

Pauli et al. (2001) observed surface microstructure of eight bitumens from SHRP inventory using AFM and reported that the asphaltene content was related to the presence of bee structure. Masson et al. (2006) identified four phases in microstructure based on their examination of 12 SHRP bitumen and proposed that each of these phases were tied to certain bitumen fractions. For example, 'catana' phase (this would be similar to the inclusions if the surface were being treated as a composite) was related to the asphaltene content which is encapsulated with 'peri' phase consisting of resins and aromatics (this would be analogous to an interfacial zone between the matrix and inclusion in a composite) which are enclaves in 'sal' phase made with saturates (this would be analogous to the matrix in a composite). However, several researchers subsequently noted that areas with and without bee structures were similar in many aspects and the phases mentioned above may not be separate chemical entities or fractions.

Masson et al. (2006) also showed that chemical fractions do not correlate well with area fractions of bitumen seen in AFM. They stated that current model may be inadequate to explain the bee structure phenomena. However, area fractions of 'catana phase' indicated good correlation with vanadium and nickel content.

Pauli et al. (2011) reported that bee structures were related to wax or aliphatic chains. Schmets et al. (2010), along with Das et al. (2013), also reported that these microstructures were associated with the wax content in the bitumen. Lyne et al. (2013) analyzed seven bitumen of which five had significant wax content. They proposed that there is a layer at the bitumen surface ('laminate') that comprises lighter wax fractions and the wrinkles on that surface are seen as bee structures. Soenen et al. (2014) conducted a round robin test using four bitumens that incorporated different types of wax (including one control bitumen with no wax). They also concluded that positive relationship exist between bitumen bee structures and wax content. Using optical microscopy, Ramm et al. (2016) also noted that when microstructures of a straight run bitumen (no modifiers) were compared to the same bitumen modified using 1% w/w wax, the wax-modified bitumen showed

much higher number and larger sized bee structures.

Allen et al. (2012) reported that the 'bee' structures had different mechanical properties (stiffness) compared to other locations on the bitumen surface. However, these differences were significantly smaller in magnitude compared to the differences commonly observed between saturates, aromatics, resins and asphaltenes, which was in contradiction to the model proposed by Masson et al. (2006).

In another study, Allen et al. (2014) reported that the saturates fraction facilitated the formation of bee structures in the unaged condition. They also reconciled their observations with previous studies proposing that while wax is considered by many as the primary influencer of bee structures, waxes can also be regarded as a subset of the saturates fraction.

Nahar (2016) examined heat cast specimens for eleven different bitumen sources using the AFM. She also examined the maltene fractions of the bitumens after removing the asphaltenes using the AFM. She hypothesized that asphaltene content was correlated with the formation of bee-structures along with wax content because the maltenes (bitumen without asphaltene) did not show any microstructure formation. Also, area fraction of the bees were found to be related with total amount of trace metals (V, Ni, Fe), with similar observation made by Masson et al. (2006) (both of these studies used SHRP bitumens). Similarly, Hofko et al. (2016) varied the asphaltene content of a single bitumen sample from 0% to 30% and scanned six variations of such synthesized bitumen samples. They noted that bee structures were absent in the pure maltene state and they also independently and simultaneously hypothesized the relationship between asphaltene content and the formation of these structures. They also noted that high asphaltene content (>30%) resulted in very pronounced morphological features. Finally, in a theoretical study, Bhasin and Ganesan (2015) conducted a preliminary analysis using phase field models to demonstrate that it is possible that these structures do not correspond to a specific fraction or component within the bitumen but may be agglomerates that have relatively higher or lower concentrations of certain fractions.

It is very important to recognize that if a certain bitumen component or fraction facilitates the formation of larger microstructures, it does not necessarily imply that the resulting microstructures compositionally correspond to that specific fraction. In some cases, this distinction is often not highlighted in the literature.

In summary, the above review highlights that there is no clear consensus to explain the chemical origins of the microstructure observed on the surface using atomic force microscopy (AFM). It must also be pointed out that although AFM is a versatile tool with excellent magnification and resolution for topographical features as well as ability to examine surface roughness, its potential is significantly limited due to several factors. These include the extensive time required for the sample preparation and scanning, limitations in the temperature range within which the specimen surfaces can be scanned, and limitations in the region or area that can be scanned. As a result, the studies cited above were limited with a maximum of 12 bitumen samples with most of the studies using less than eight samples. Understandably, analysis of such limited samples restricts our understanding of bitumen microstructures and its relation with chemistry of bitumen. Further, Menapace et al. (2016) also demonstrated that the method of sample preparation (solvent cast versus heat cast) and the duration between sample preparation and scanning can alter the observed microstructure. These factors were not standardized or controlled across the different studies cited above.

Ramm et al. (2016) used optical microscopy to observe surface and bulk microstructure. In this case, the authors did not need any specialized sample preparation and could use traditional heating and sampling methods used for bitumen in a laboratory. In addition, this method can be used to scan the surface and bulk of the bitumen in a wide range of temperatures. The imaging can be done in a matter of seconds and does not require any consumables. For this study, we used this optical microscopy technique to scan a large number of samples without any potential artifacts that may be due to specimen preparation procedures. Finally, the authors would like to note that previous studies have shown that size and distribution of the microstructure in the bulk is different. These microstructural features (bulk and surface) were influenced by the chemical additive, time and thermal history of the specimen (Ramm et al. 2016, 2018). For the purposes of this study, the surface microstructure was quantified using image analysis and compared to the chemical composition of the selected bitumens.

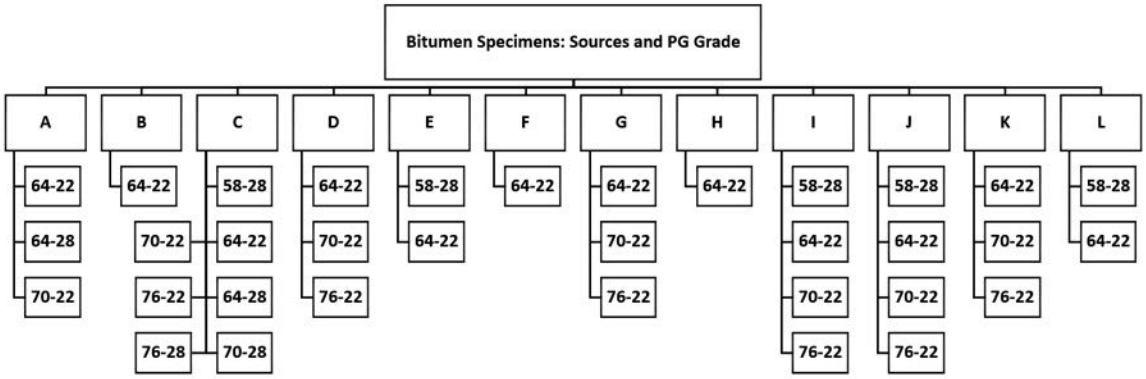

Figure 4.1: Bitumen sources and their products (identified by PG grade) used for this study

4.5 Materials

A total of 33 unaged bitumen samples were acquired from 12 producers from south-central USA (labeled A to L in Figure 4.1). High Temperature performance grade of these bitumens (according to the producers) varied from 58°C to 76°C whereas low temperature grades were either -22°C or -28°C. The bitumens were short-term aged using rolling thin film oven. 31 short term aged bitumens were used for this study. Therefore, a total of 64 bitumens was analyzed for their chemical characteristics using TexSARA fractionation as a metric and for the surface microstructure using analysis of images acquired using surface microscopy.

The bitumen samples acquired for this study were commercially available and no information was provided to the researchers on modifiers or extenders that may have been used to produce the bitumen. The inventory of samples evaluated in this study represent diverse origin, processes, and modifiers albeit from a limited geographic region within the United States.

4.6 Method for SARA fractionation

In a recent study, the authors reported a method to conduct SARA fractionation (TexSARA) that is relatively much faster, repeatable, and less resource intensive than existing methods(Sakib and Bhasin 2018).

For fractionation of bitumen using TexSARA, a small amount of bitumen (0.3-

0.4 gram) was measured and dissolved in 1:100 (g:mL) n-heptane while being stirred at room temperature for 24 hours. The solution was then filtered to remove the precipitated asphaltene. Disposable syringe filters were used as a filtering medium by mounting them on a vacuum manifold and using the vacuum to drive the solution through the filter. Unlike commonly used Buchner funnel/fritted glass filters, these inexpensive filters are disposable and allow finer filtration (PTFE 0.2 μm filters).

Maltene recovered this way was measured by drying and then about 50 mg maltene in solution form was introduced into the chromatography column. To reduce expense, time requirement, and to increase repeatability, commercially available silica-filled Solid Phase Extraction (SPE) cartridges were used instead of the long glass chromatography columns. These cartridges are essentially regular sized syringes filled with 50 g silica. As SPE cartridges are disposable and require small amount of solvents (the dosage of maltene is also small), the process is much faster than existing methods such as ASTM D-4124. After introduction of maltene, solvents are sequentially passed through the chromatography column to fractionate maltene. Table 4.1 contains the solvents in their sequence of introduction to SPE cartridge and quantity along with corresponding eluted fraction. Figure 4.2 and 4.3 show the process of TexSARA separation and the setup, respectively. A more detailed description can be found in Sakib and Bhasin (2018).

Table 4.1: Solvent Schedule of S-A-R separation using SPE cartridge (Sakib and Bhasin 2018).

Elutant Solvent	mL	Collected Fraction
n-Heptane	20	Pre-wash
maltene solution + n-Heptane	15 + 10	Saturates
80% Toluene - 20% n-Heptane	25	Aromatics
90% DCM - 10% Methanol	40	Resins

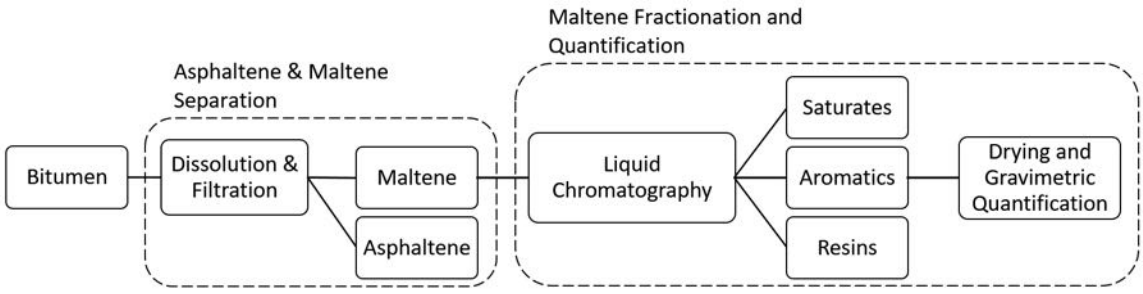

Figure 4.2: Proposed process of TexSARA fractionation (Sakib and Bhasin 2018)

Figure 4.3: TexSARA setup using SPE cartridges and vacuum manifold (Sakib and Bhasin 2018)

4.7 Method to Evaluate Microstructure

As discussed in the previous sections, the authors used optical microscopy to evaluate surface microstructures. An AmScope 14MP CMOS camera was mounted on the Letiz Ergolux reflection microscope for image capture. Light source was 20W halogen lamp with optical filter selected wavelength centered around 500 nm (with 100nm Full width at half maximum). Two different objectives with 20x and 100x magnification enabled us to capture $455\mu m \times 350\mu m$ area and $65\mu m \times 50\mu m$ area, respectively. Figure 4.4 illustrates the setup and bitumen samples in silicone mold that were being analyzed.

For test specimen preparation, bitumens were heated so that it is sufficiently fluid to be poured into silicone mold at temperature around 140°C. The mold (with bitumen) was cooled slowly over a hot plate to qualitatively represent gradual cooling of bituminous mixture in a realistic mixing scenario. It was also observed that rapid cooling or quenching suppresses molecular mobility and therefore leaves the bitumen in an amorphous state. Nahar (2016) and Claudy et al. (1992) noted that initial heating temperature and cooling rate affects the microstructure significantly. In fact, Claudy et al. (1992) noted that higher wax content bitumens show greater cooling rate sensitivity with respect to microstructure formation.

Time required for imaging a specimen is minimal. The equipment is easy to focus and high quality images can be obtained for multiple locations of the sample at different magnifications. Real-time observation and ability to examine the surface at different resolutions helps identify any irregularities on the specimen and address such issues accordingly (e.g. an artifact of specimen fabrication). Images obtained from the microscopy were processed in ImageJ software for quantitative analysis. Figure 4.5 presents two representative images of the same bitumen one taken by AFM and other taken by optical microscopy. It is apparent that while the optical microscopy can not provide phase information and surface profile, it compensated by scanning much larger area in order of magnitude less time.

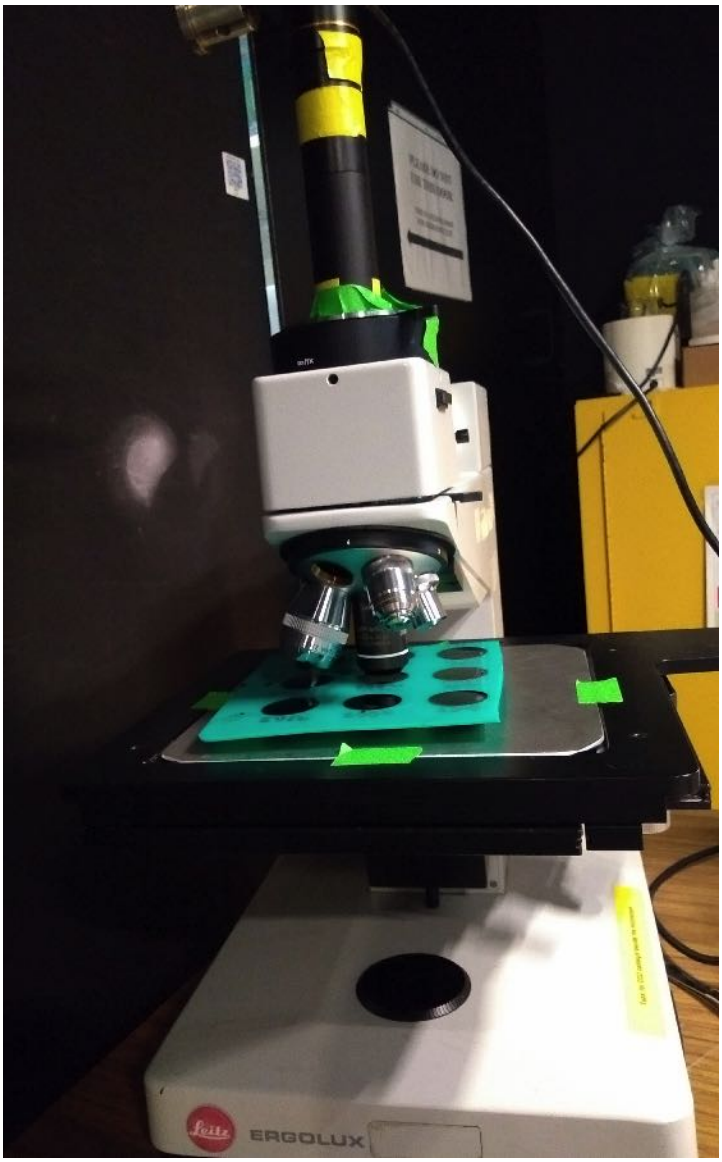

Figure 4.4: Optical microscopy setup with bitumen sample on mold and 100× objective on a sample

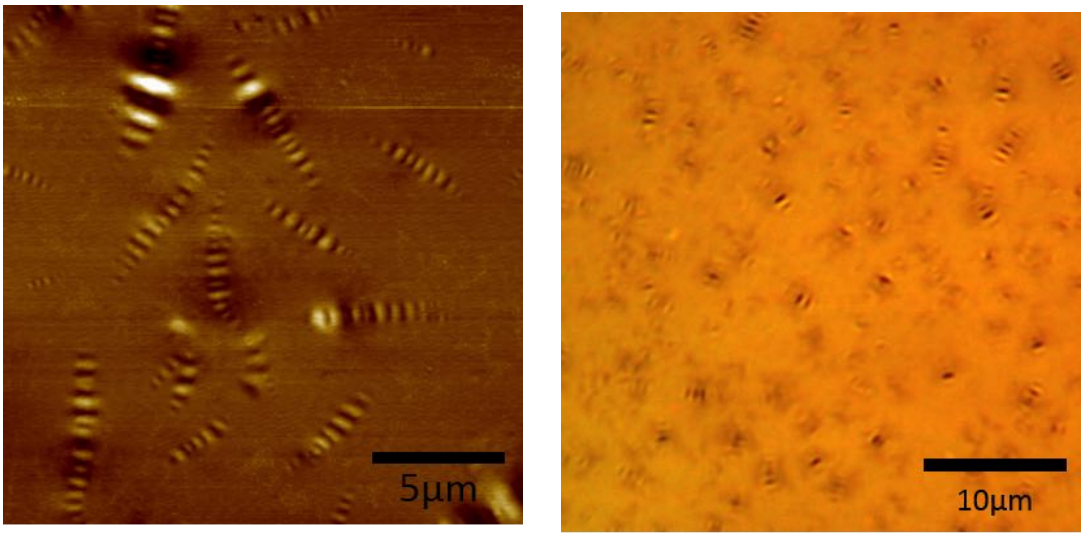

(a) AFM image (b) Optical Microscopy

Figure 4.5: Bee structures seen using AFM and Optical Microscopy (Ramm et al. 2016)

4.8 Correlation of bitumen surface microstructure and chemistry

Figures 4.6 to 4.39 present microstructure images of the bitumens sequentially arranged according to their sources first, then in the order of increasing high temperature grade. Images of each bitumen sample at 20× and 100× magnification are shown side by side.

4.8.1 Qualitative examination of the microstructure

Few observations can be readily drawn based on a qualitative assessment of the figures. First, the features of the bitumen microstructure remained similar after short-term aging for most samples although the density of these features typically decreased in most cases (exceptions are C70-28 and H64-22). In this context, the term density refers to the number of discrete structures in a given area. In other words, the number of discrete structures were generally lower in the short-term aged bitumen specimen compared to the unaged specimen. The change before and after short-term aging may be due to change in the chemistry of the bitumen, i.e. due to the loss of volatiles and oxidative aging. This change can also be at-

tributed to an increased viscosity of the bitumen that in turn reduces the mobility of the molecules to reorganize and restructure. These two are not independent because the latter (changes in viscosity) is also driven by the former (changes in the chemical composition).

Second, bitumens from the same producer tend to have a similar microstructure even when they are of different grades. This is likely because a given producer may be using the same crude stock to produce different grades of bitumens. In some cases, the density and the size of discrete structures changes to some extent in the bitumens from the same source but the characteristic features or shape of these discrete structures does not change substantially. For example, I64-22, I70-22, I76-22 are from the same source 'I' and demonstrate very similar shape characteristics for the discrete features as seen in Figure 4.28 to 4.30.

There are few exceptions to the above where bitumens from the same source with different PG show different bee structure pattern. Further investigation of these bitumens using XRF revealed that although these bitumens were from the same producer, they were either produced using a different crude stock and/or subjected to a significant modification(s) that changed their characteristics. For example, Bitumen J58-28 (Figure 4.31) shows different microstructure compared to other three types of bitumen acquired from 'J'-source (Figure 4.32 to 4.34). This bitumen (J58-28) had a relatively much higher concentration of iron, calcium, and zinc as measured using an XRF compared to the other three bitumens from the same source. The metal concentration also suggests that this specific bitumen was modified using modifier(s) rich in metal content, potentially with the goal of lowering the high temperature grade. This hypothesis is further accentuated by the fact that the saturate content of J58-28 was about 25% whereas the other three bitumens had 15-20% saturates. The other similar exception was C64-22 (Figure 4.11, which was very different compared to other bitumen grades from the producer 'C' (Figure 4.10 to 4.15). Interestingly, in this case while C64-22 shows typical features similar to other bitumens from other producers, the remaining bitumens from producer 'C' do not show typical and discrete 'bee' like microstructure. Also, these bitumens (from producer 'C' with the exception of C64-22 adn C58-28) showed a very high continuous temperature grade based on creep-recovery criteria. However, C64-22, which shows typical 'bee' structures and from the same producer,

did not show any unusual behavior in terms of its rheological characteristics.

Third, some of the unaged and short-term aged bitumens showed heterogeneity in their microstructure at larger length scales (i.e. when observed using 20× objective with image footprint that was more than 300 μm). It should be noted that after heating, each bitumen sample was manually stirred using a spatula before pouring into the mold. There were two different types of large scale heterogeneity that were observed: (i) discrete disc like features that are typically 1-3 μm or less in diameter but in some cases may be as large as about 10 μm that are visible only using the lower magnification on a larger sized image, and (ii) large scale streaks or patterns in the distribution or density of the microstructural entities. The disc like features do not appear to be an artifact of specimen preparation. Instead these features appear to be spatially uniformly distributed when observed using the 20× magnification and can be regarded as a multi-scale microstructure and not large scale heterogeneity. For example, the bitumen samples J58-28, I58-28, and L58-28 showed this pattern (Figures 4.31, 4.27 and 4.38, respectively) . Interestingly, all of these bitumens had a high temperature grade of 58°C. The bitumen L58-28 was found to contain higher concentrations of iron, zinc and calcium, compared to other bitumens from the same source, which suggests that some form of metal-rich softening agent may have been included. Bitumens J58-28 and I58-28 had more than 25% of saturates which is very high compared to the other bitumens from the same producers (<20%). However, the saturates content for L58-28 was not high. Therefore, the saturate content may not be the only factor that can explain this multi-scale microstructure.

The second type of heterogeneity is in the form of 'streaks' observed at a larger length scale. Examples of such streaks can be seen in 20× images of J70-22 as well as short-term aged L64-22, C70-28 and F64-22 (Figures 4.33, 4.39, 4.14 and 4.22, respectively) . These larger scale heterogeneities are apparently an artifact from sample preparation. However, these observations are still informative because they point out that manual mixing and pouring of a bitumen sample may not always result in a homogeneous sample drawn out from typical laboratory containers.

Another irregularity that draws attention is D76-22 (Figure 4.19). The sample shows clear streaking/separation of black substance. The bitumen was found to

have high asphaltene content, which may have caused the dark area. However, it is not clear from the images whether the dark area is very dense bee-structures or any aggregation of dark particles. Another interesting observation is that bitumens from source C were shown to have sting-like inclusions which did not look like 'bee-structure' on otherwise a very flat surface. Bitumen from source G is interesting as there seems to be two different types of microstructures present on the surface. There are few very large and irregular structures interspersed among much smaller bee-structures.

4.8.2 Quantitative examination of the microstructure

The images (from 20$\times$ magnification) were analyzed to obtain quantitative metrics using an open source image processing software, ImageJ. At least two images were acquired for each sample, which were analyzed independently and the parameters obtained using imageJ were averaged. Two parameters were derived from image analysis, namely, average microstructure count and average area covered by microstructure on the surface. In some cases there were some "string" like features that could not be completely resolved in the images (for example, C64-28) and were inevitably included in the computation of the aforementioned parameters.

The direct comparison for these parameters with TexSARA fractions (considering all sources and the two aging conditions) did not yield a satisfactory relationship. The best correlation that could be obtained was for microstructure count with asphaltene content (R^2 of 0.14) . It appears that there is not a strong direct global correlation that relates specific TexSARA fractions to the surface size and/or density of microstructures without considering some other factors that can be used to distinguish between different crude stocks. This observation is somewhat contradictory to some other observations made in other previous research studies. It is likely that there was a sampling bias in some of the previous research studies since these studies incorporated only a very limited number of bitumens (and its derivatives) that were likely from the same producer or region.

To further explore whether bitumens from the same producers showed similar microstructure, bivariate comparisons were made using microstructure count and area with parameters based on TexSARA fractions but this time limiting such rela-

tionships to bitumens from the same source. Producers that had provided three or more different grades of bitumens were considered for this analysis. This was to ensure that there were at least six data points (including short-term aged) for such a comparison. Table 4.2 presents the R^2 values of the relevant correlations. The values of R^2 were much better for this particular exercise, yielding bivariate R^2 as high as 0.96 while some other relationships had R^2 values in the range of 0.6 to 0.7.

For better understanding of the interrelation of the fractions, multivariate linear regression was performed comparing parameters based on the microstructure to the concentration of the TexSARA fractions using the model shown in equation 4.1. The last column of Table 4.2 presents R^2 values obtained from these analyses. The fitting parameters, such as c and m_i varied substantially from one source to another.

$$\%\text{area or count} = \sum m_S Saturates + m_{Ar} Aromatics_i + m_A Asphaltenes_i + c \quad (4.1)$$

Based on a bivariate regression, the S+A content was found to exhibit a good relationship with bee structure count for three sources while the parameter S/A had better correlation with the bee count for two sources. This was consistent with the results from the multivariate regression that showed that the coefficients for saturates and asphaltenes were usually higher than that of aromatics (except bitumens from source 'C' and 'G').

Two other factors must be noted from these results. First, the TexSARA fractions of the bitumens from source 'C' did not show good correlation with microstructure parameters. This was to be expected because as seen from Figures 4.10 to 4.16 all bitumens (except Figure 4.17) showed a more dispersed and interconnected structure as opposed to discrete inclusions that are visible in other bitumens. Second, results from the multivariate linear regression were generally better but authors also recognize that this could be artificially inflated because the sample size for such regression with multiple parameters was also small (six) for four of the bitumens.

In summary, while reasonable relationships between TexSARA fractions and bee structure properties were established for some of the bitumens when such bitumens were obtained from the same source, such correlations could not be globally applied without considering other potential factors that different crude sources. In

Table 4.2: Correlation matrix of bee structure parameters and TexSARA fractions

Source Name	Number of Samples	Bee Parameters	S	Ar	R	A	S+A	S/A	CI*	MLR*
C	14	Bee Count	0.02	0.01	0.01	0.00	0.00	0.00	0.00	0.07
		Area Fraction	0.03	0.02	0.02	0.18	0.08	0.15	0.08	0.28
D	6	Bee Count	0.16	0.93	0.47	0.88	0.95	0.27	0.94	0.99
		Area Fraction	0.13	0.73	0.42	0.67	0.74	0.19	0.74	0.79
G	6	Bee Count	0.40	0.07	0.23	0.10	0.24	0.45	0.22	0.48
		Area Fraction	0.26	0.00	0.66	0.20	0.10	0.42	0.08	0.8
I	8	Bee Count	0.20	0.38	0.01	0.03	0.56	0.07	0.54	0.59
		Area Fraction	0.13	0.27	0.03	0.06	0.48	0.04	0.43	0.68
J	6	Bee Count	0.43	0.00	0.24	0.16	0.33	0.37	0.34	0.55
		Area Fraction	0.43	0.00	0.24	0.12	0.39	0.39	0.38	0.58
K	6	Bee Count	0.31	0.16	0.45	0.05	0.17	0.73	0.17	0.98
		Area Fraction	0.12	0.14	0.23	0.00	0.04	0.41	0.05	0.87

*CI: Colloidal Index; MLR: Multiple Linear Regression

addition, while single variable and multivariate linear regressions show that the microstructure is influenced by both Saturates and Asphaltenes, the nature of this relationship was also different for bitumens from different sources.

4.9 Conclusion

This study explored the relationship between bitumen surface microstructure and TexSARA fractions. Considering the interest in the research community on observation and interpretation of 'bee' microstructure and lack of consensus about origin and/or influencer of bee structure formation, understanding the phenomena with a set of chemically diverse bitumens is important. This study utilized 33 unaged and 31 short-term aged bitumens from 12 different sources in order to have a more robust basis to explore the relationship between microstructure and chemical makeup.

The observations that were made in this study are noted below:

1. Bitumens with different grades from the same producer were found to have microstructures with similar features. This is very likely because produc-

ers typically use the same crude stock to produce multiple grade. The Saturates and Asphaltenes appear to influence the bee structure count and/or area fraction for bitumens from the same source. However, this relationship is different for bitumens from different producers.

2. Bitumen microstructure remains similar after short-term aging although in most cases the spatial density of the entities or bee structures decreases.

3. Some of the softer bitumens showed scale-heterogeneity (PG58 bitumens from producers 'I', 'J' and 'L'). In this case the microstructural entities were more rounded in shape and had a much larger variation in size. This is in contrast with other bitumens that showed more oblong shaped or 'bee' shaped entities that were similar in size. These bitumens also demonstrated much higher metal concentrations compared to other bitumens.

4. Lower magnification images showed that the bitumen microstructures had very significant spatial heterogeneity (e.g. Figures 4.19(a-b), 4.22(c), 4.33(c) and 4.39(c)). It appears that this was an artifact of specimen preparation that appeared even after heating, manual stirring of the bitumen sample and gradual cooling over a hot plate, which is a process typically used for preparing other samples for mechanical tests. This heterogeneity that was inadvertently captured during the study highlights two important conclusions. First, the microstructure is clearly sensitive to the thermal variations within the sample and thermal history as demonstrated in previous studies. Second, selection of a small microscopic region without recognizing such variations may lead to misleading conclusions.

4.10 Acknowledgments

We acknowledge the support of National Science Foundation Grant CMMI-1053925 and Texas Department of Transportation for funding parts of this study. We also acknowledge the support from Dr. Mike Downer and Adam Ramm for providing access and help with microscopy.

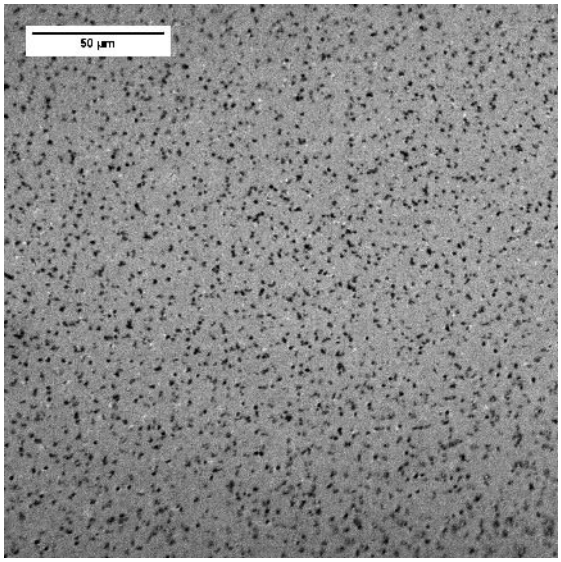

(a) A64-28 20× unaged

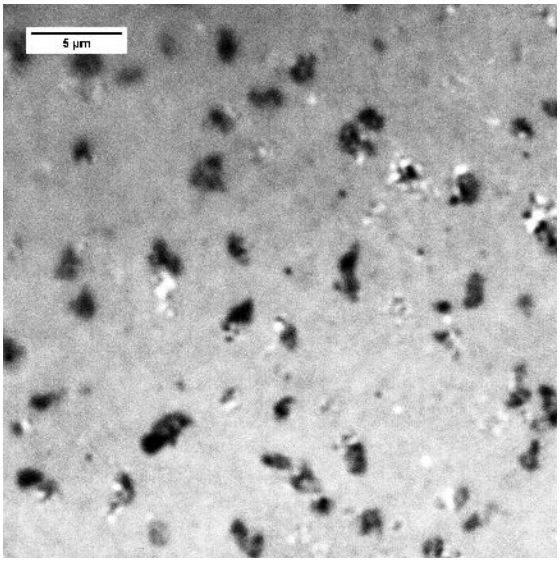

(b) A64-28 100× unaged

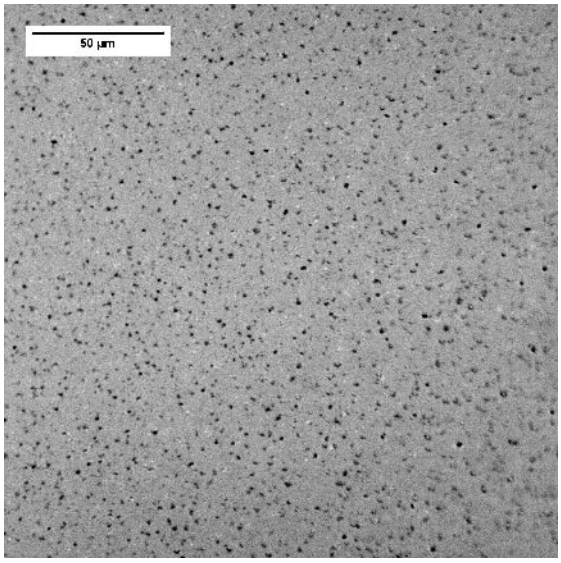

(c) A64-28 20× short-term aged

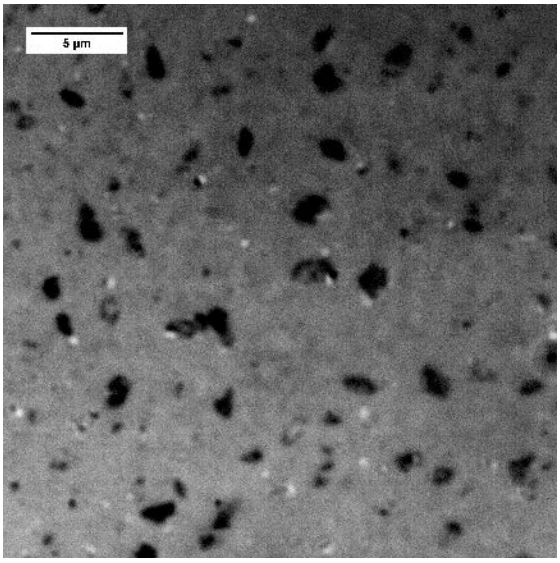

(d) A64-28 100× short-term aged

Figure 4.6: 20× and 100× Microstructure images of A64-28 in two aging conditions

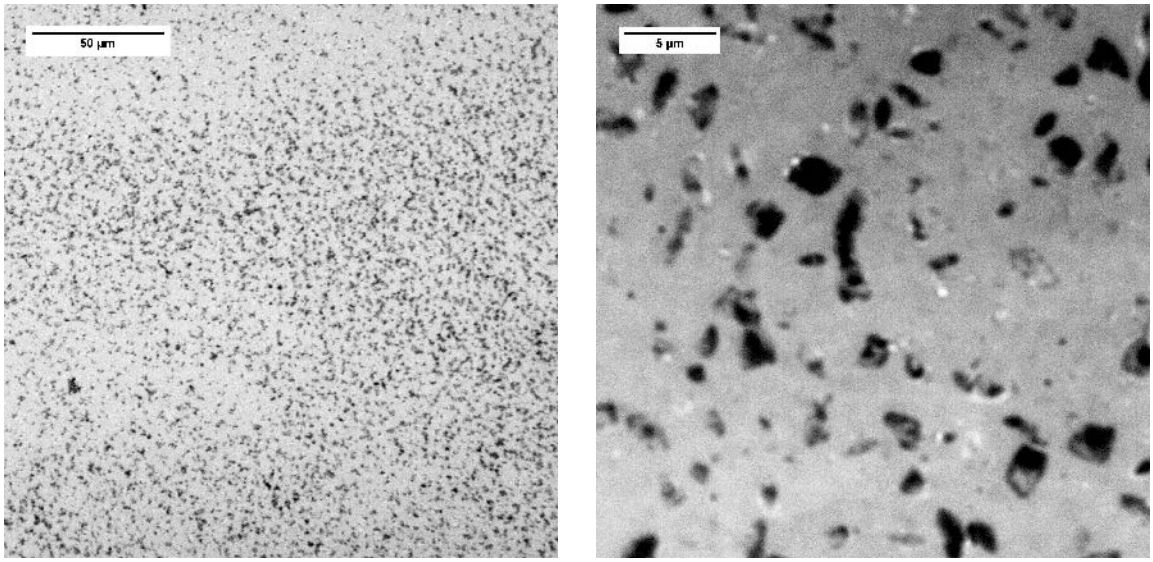

(a) A64-22 20× short-term aged

(b) A64-22 100× short-term aged

Figure 4.7: 20× and 100× Microstructure images of A64-22 in short-term aging condition (unaged specimen was not available)

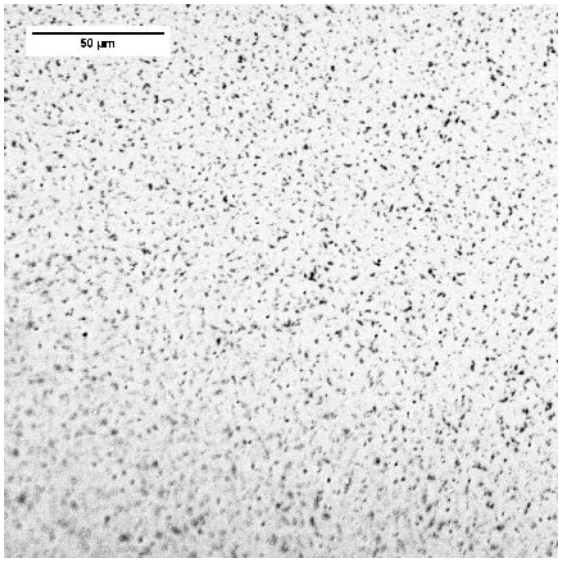

(a) A70-22 20× unaged

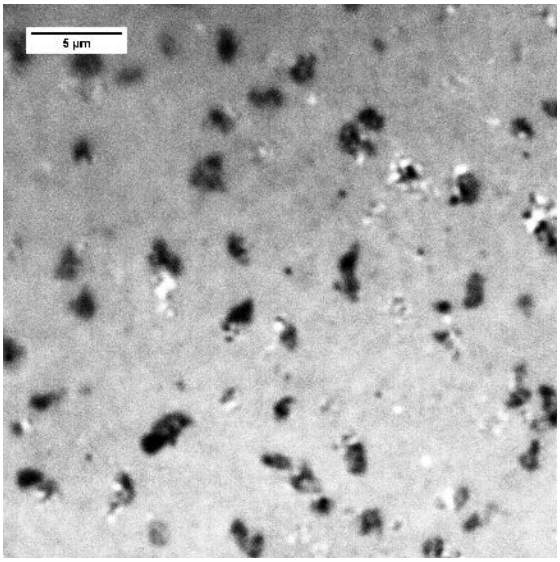

(b) A70-22 100× unaged

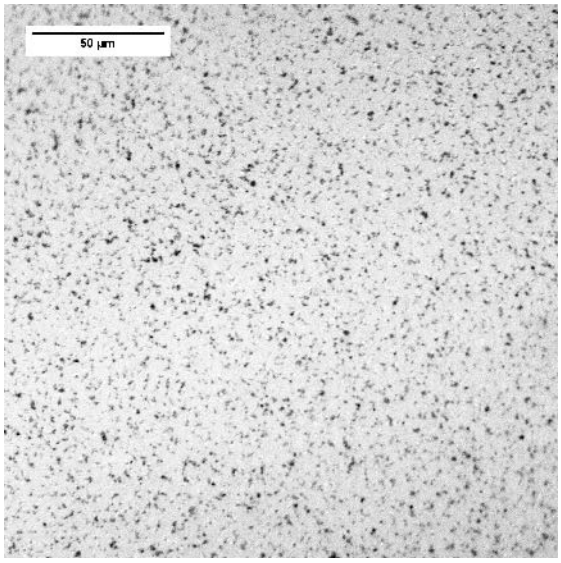

(c) A70-22 20× short-term aged

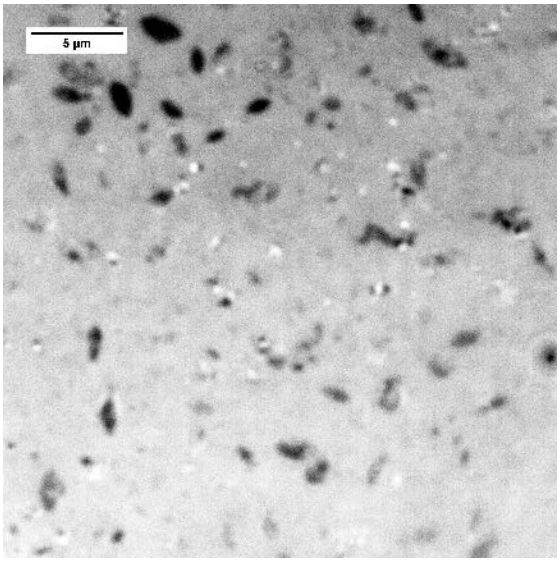

(d) A70-22 100× short-term aged

Figure 4.8: 20× and 100× Microstructure images of A70-22 in two aging conditions

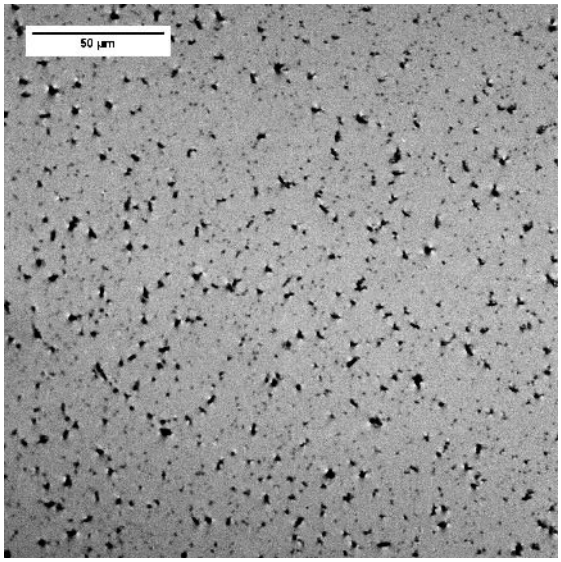

(a) B64-22 20× unaged

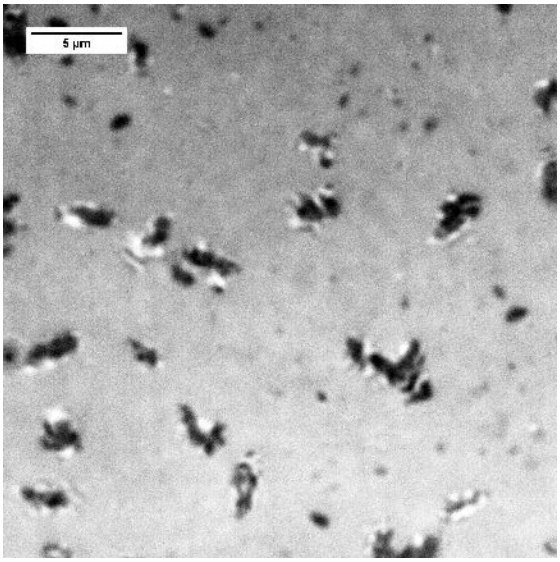

(b) B64-22 100× unaged

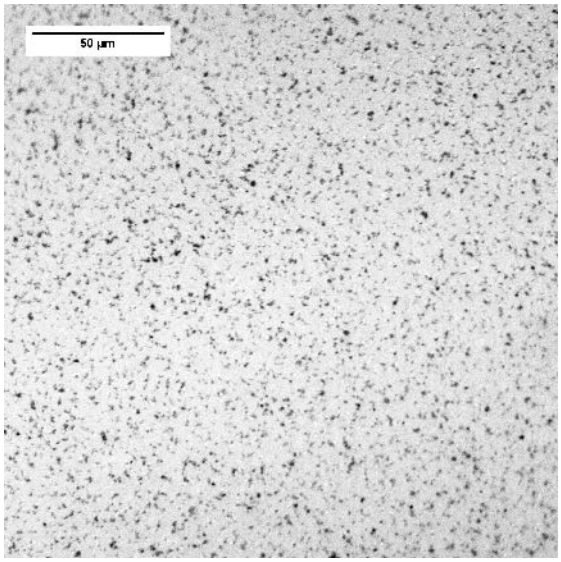

(c) B64-22 20× short-term aged

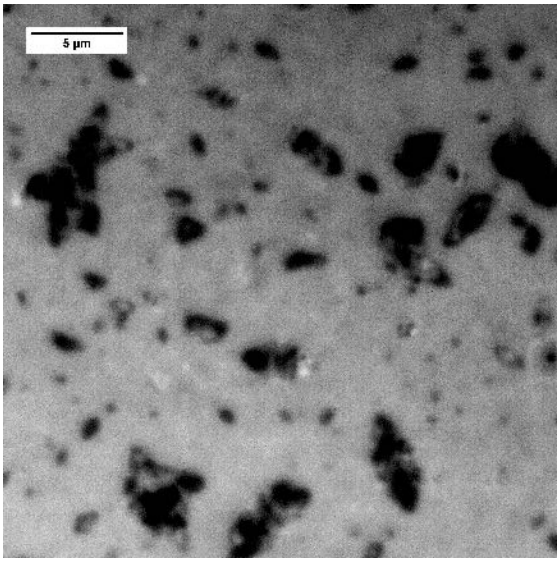

(d) B64-22 100× short-term aged

Figure 4.9: 20× and 100× Microstructure images of B64-22 in two aging conditions

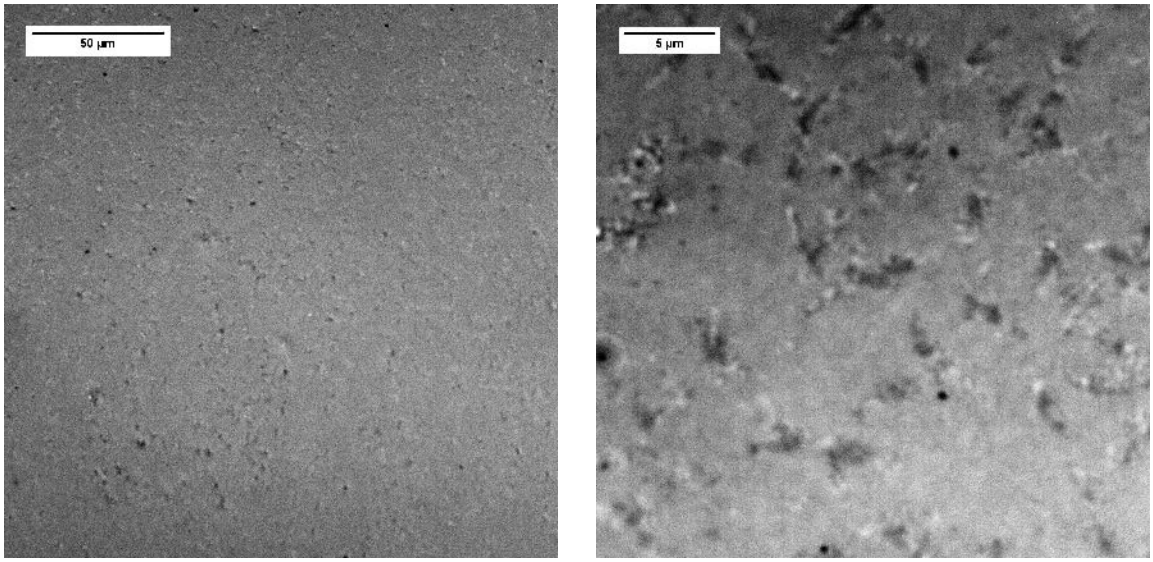

(a) C58-28 20× unaged (b) C58-28 100× unaged

Figure 4.10: 20× and 100× Microstructure images of C58-28 in unaged conditions (short term aged sample not available)

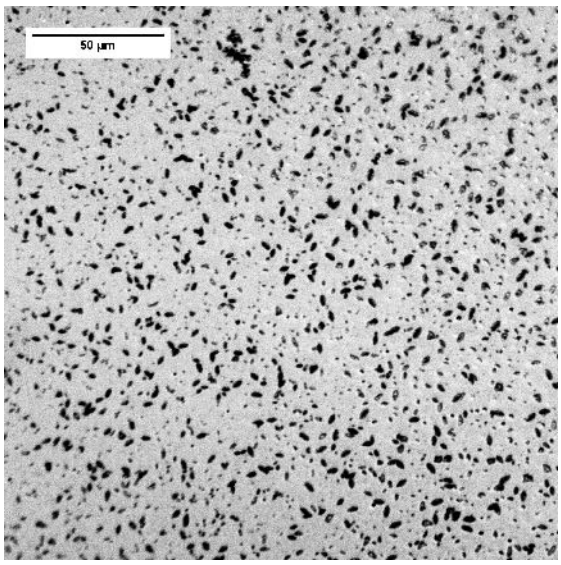

(a) C64-22 20× unaged

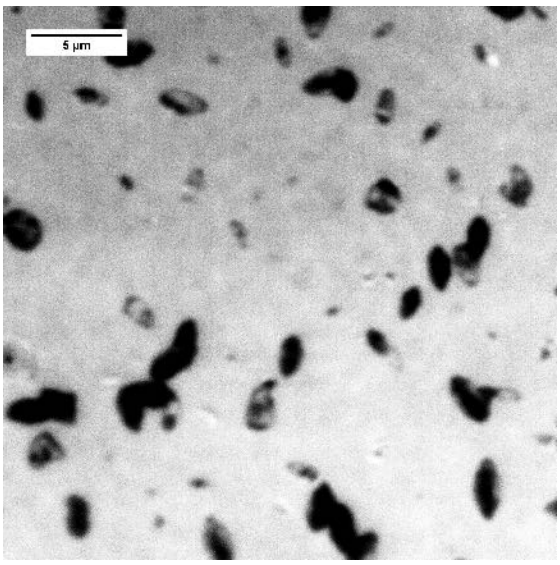

(b) C64-22 100× unaged

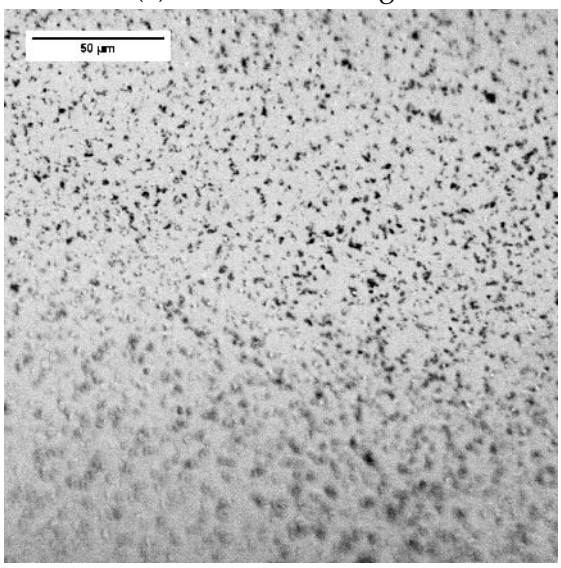

(c) C64-22 20× short-term aged

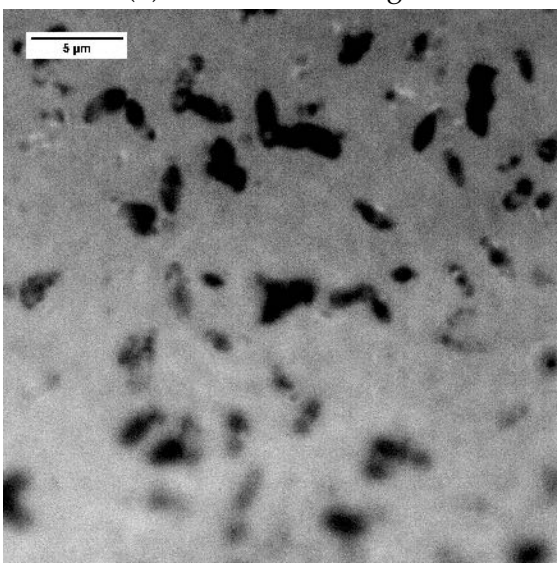

(d) C64-22 100× short-term aged

Figure 4.11: 20× and 100× Microstructure images of C64-22 in two aging conditions

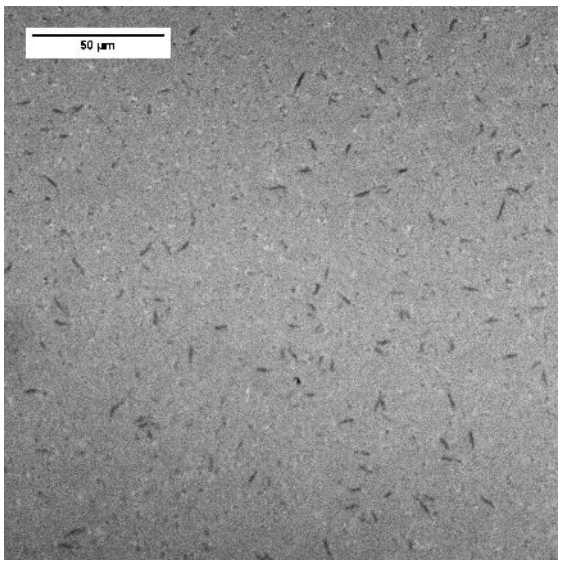

(a) C64-28 20× unaged

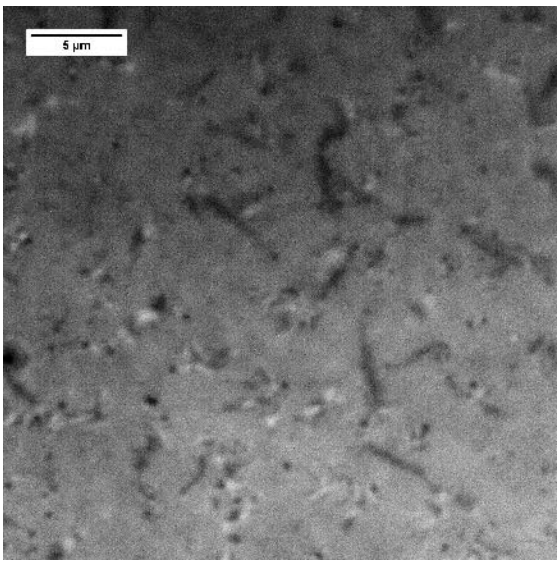

(b) C64-28 100× unaged

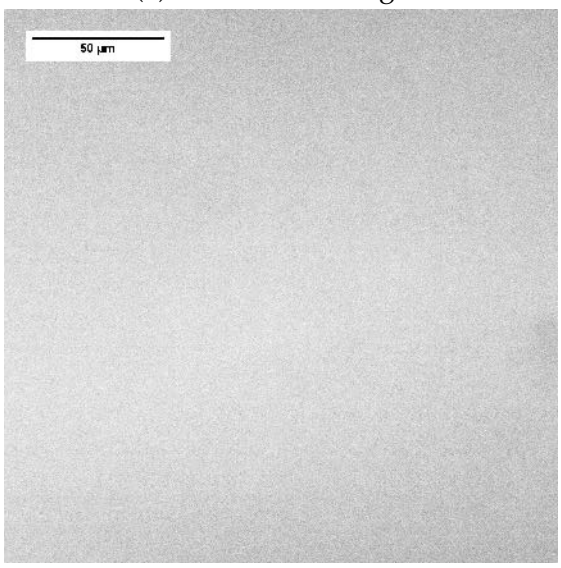

(c) C64-28 20× short-term aged

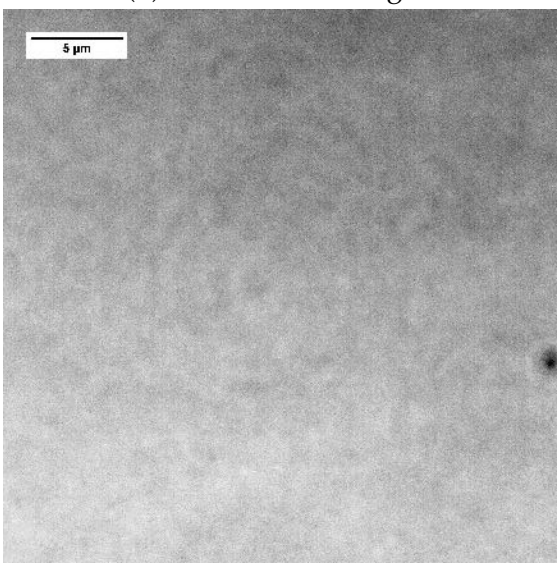

(d) C64-28 100× short-term aged

Figure 4.12: 20× and 100× Microstructure images of C64-28 in two aging conditions

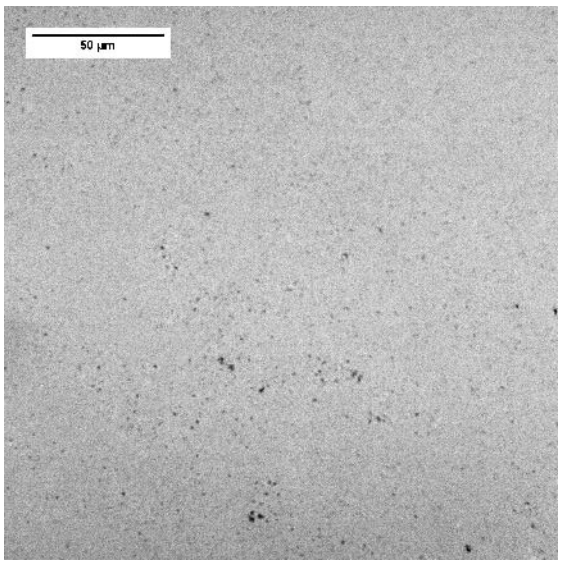

(a) C70-22 20× unaged

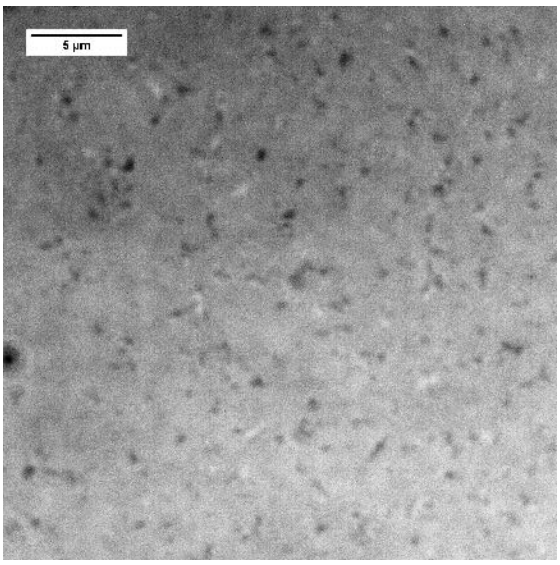

(b) C70-22 100× unaged

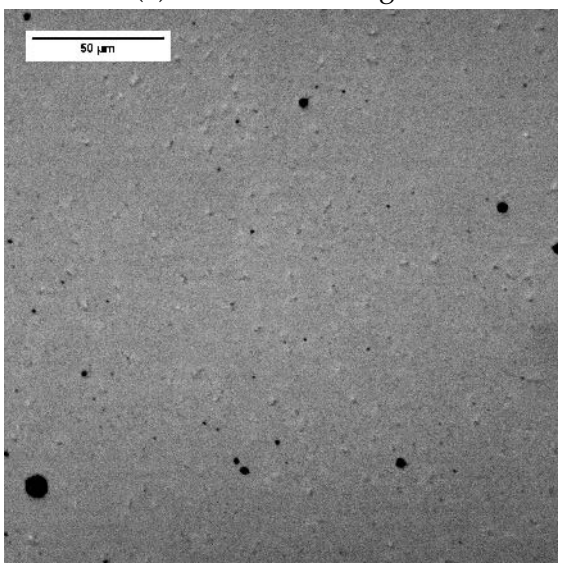

(c) C70-22 20× short-term aged

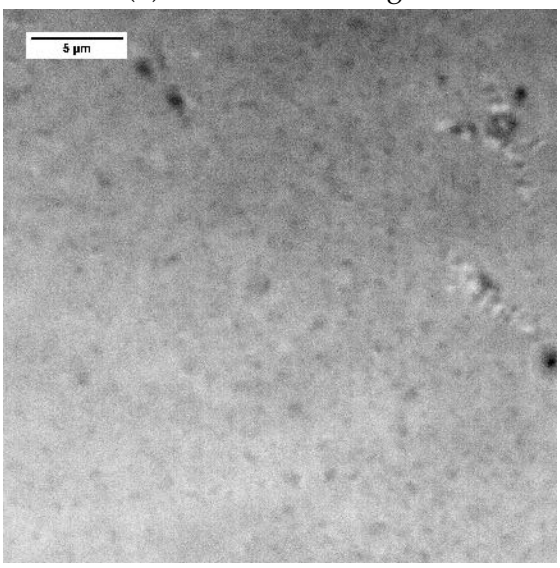

(d) C70-22 100× short-term aged

Figure 4.13: 20× and 100× Microstructure images of C70-22 in two aging conditions

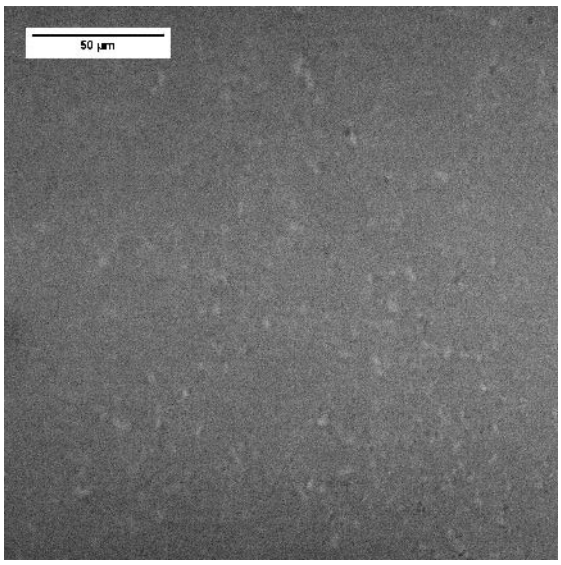

(a) C70-28 20× unaged

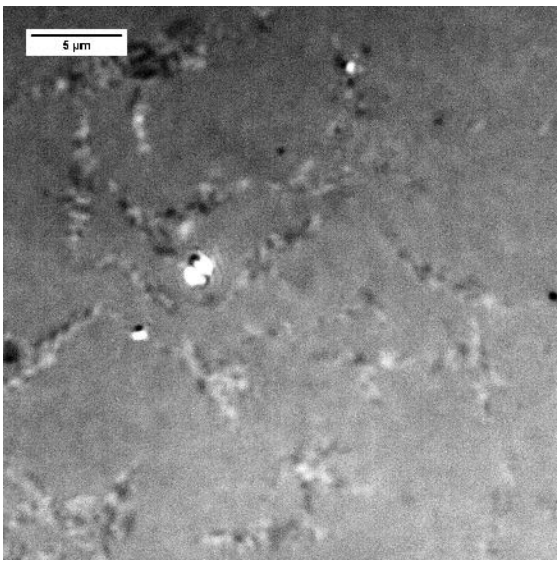

(b) C70-28 100× unaged

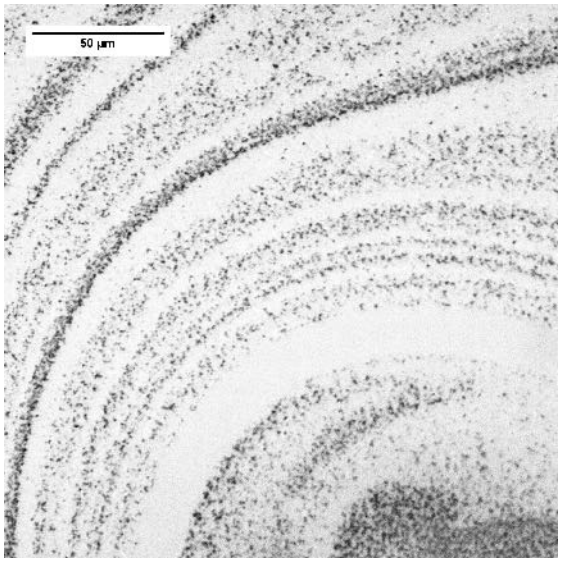

(c) C70-28 20× short-term aged

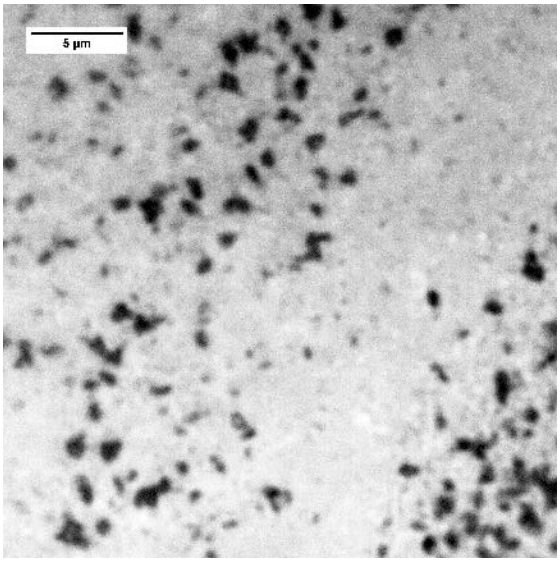

(d) C70-28 100× short-term aged

Figure 4.14: 20× and 100× Microstructure images of C70-28 in two aging conditions

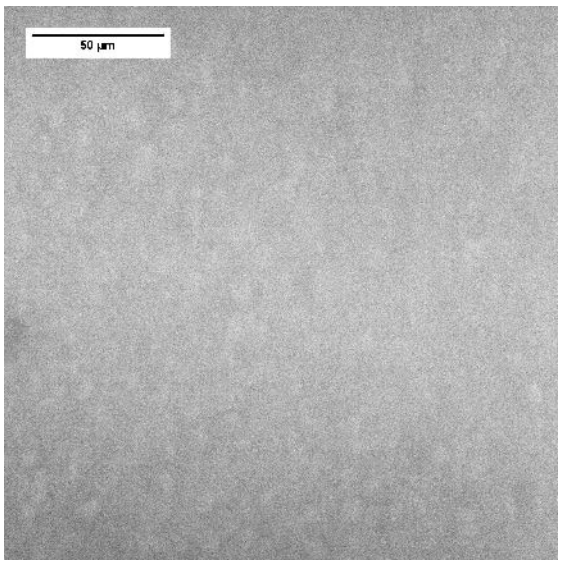

(a) C76-22 20× unaged

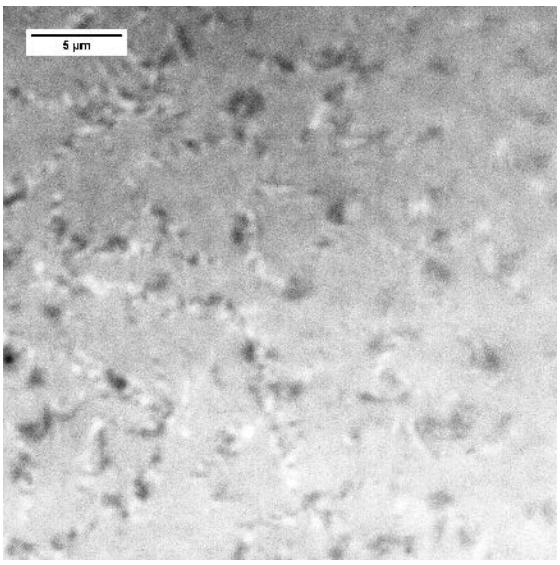

(b) C76-22 100× unaged

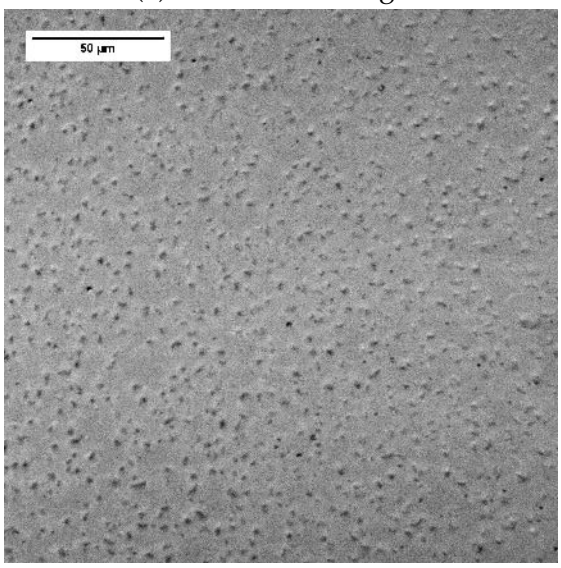

(c) C76-22 20× short-term aged

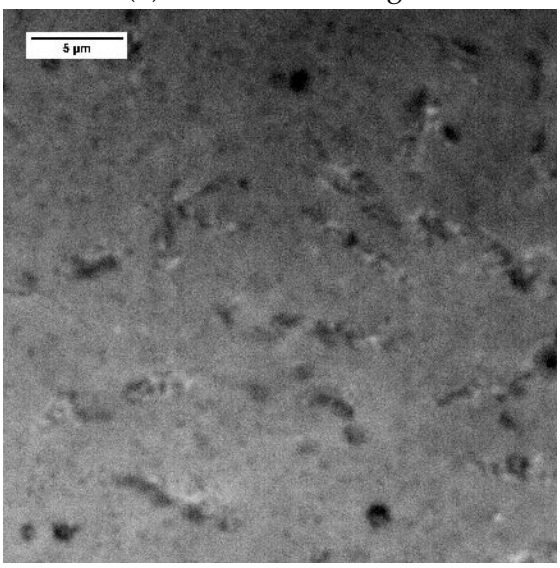

(d) C76-22 100× short-term aged

Figure 4.15: 20× and 100× Microstructure images of C76-22 in two aging conditions

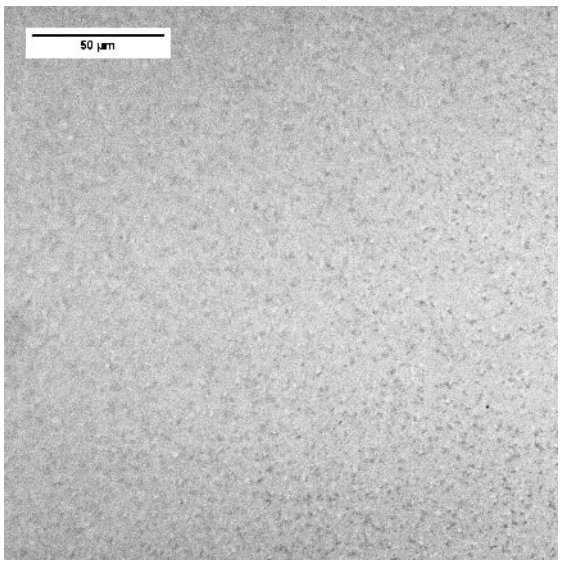

(a) C76-28 20× unaged

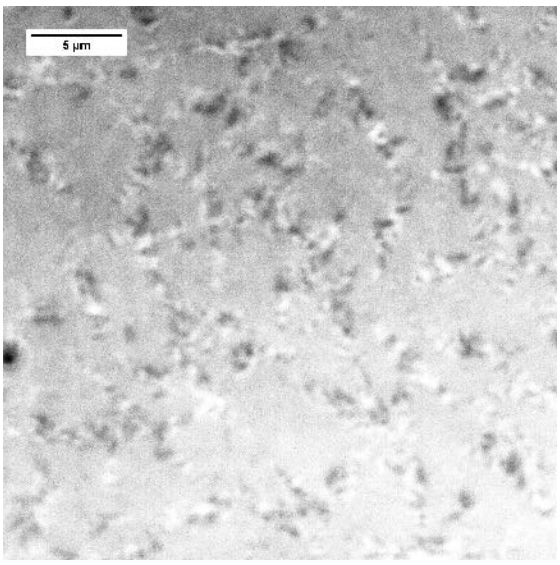

(b) C76-28 100× unaged

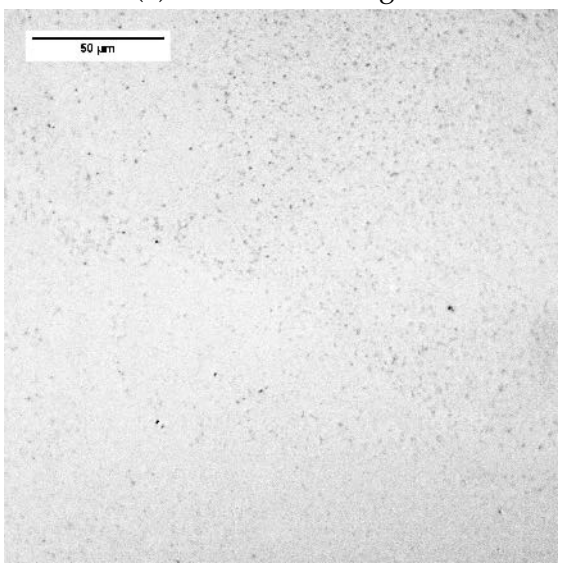

(c) C76-28 20× short-term aged

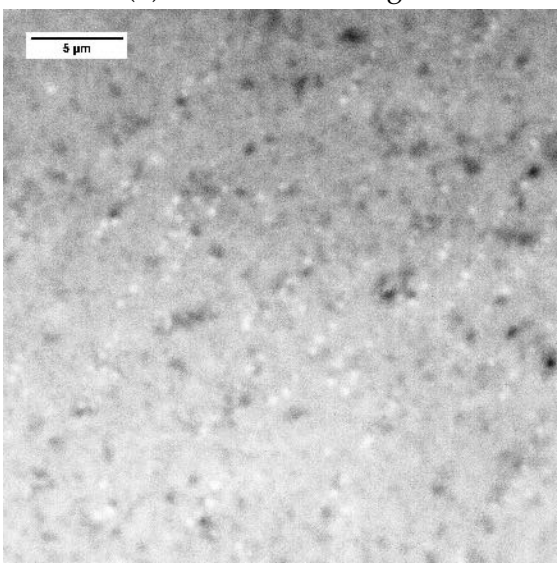

(d) C76-28 100× short-term aged

Figure 4.16: 20× and 100× Microstructure images of C76-28 in two aging conditions

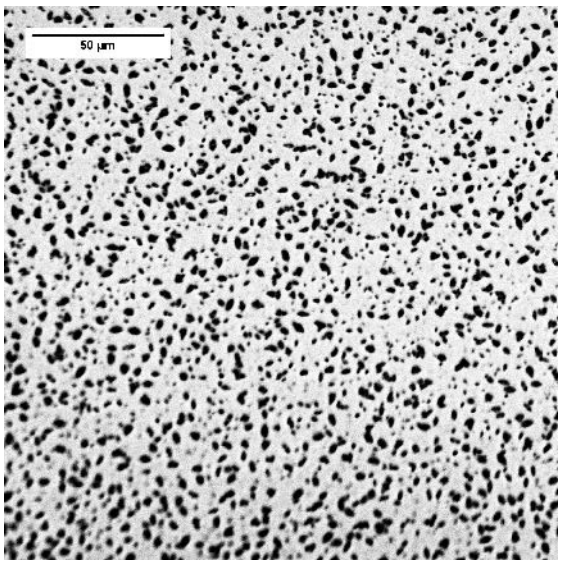

(a) D64-22 20× unaged

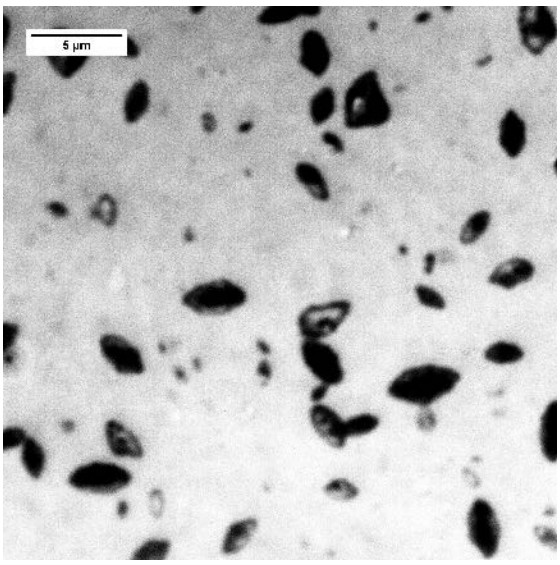

(b) D64-22 100× unaged

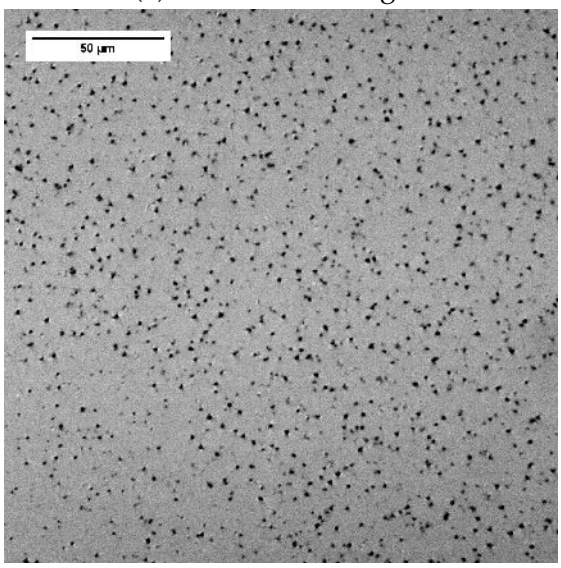

(c) D64-22 20× short-term aged

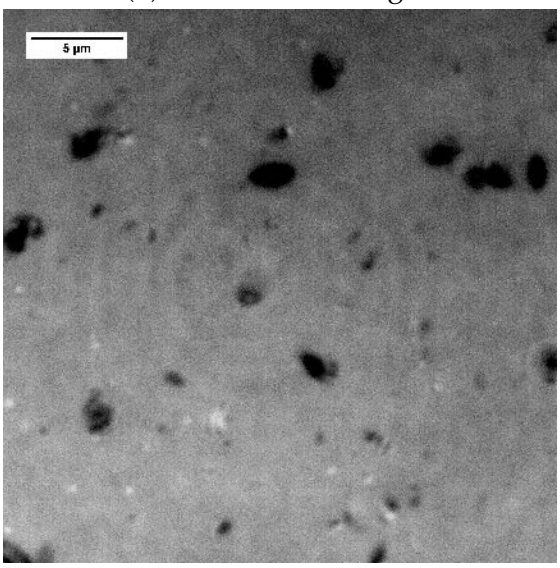

(d) D64-22 100× short-term aged

Figure 4.17: 20× and 100× Microstructure images of D64-22 in two aging conditions

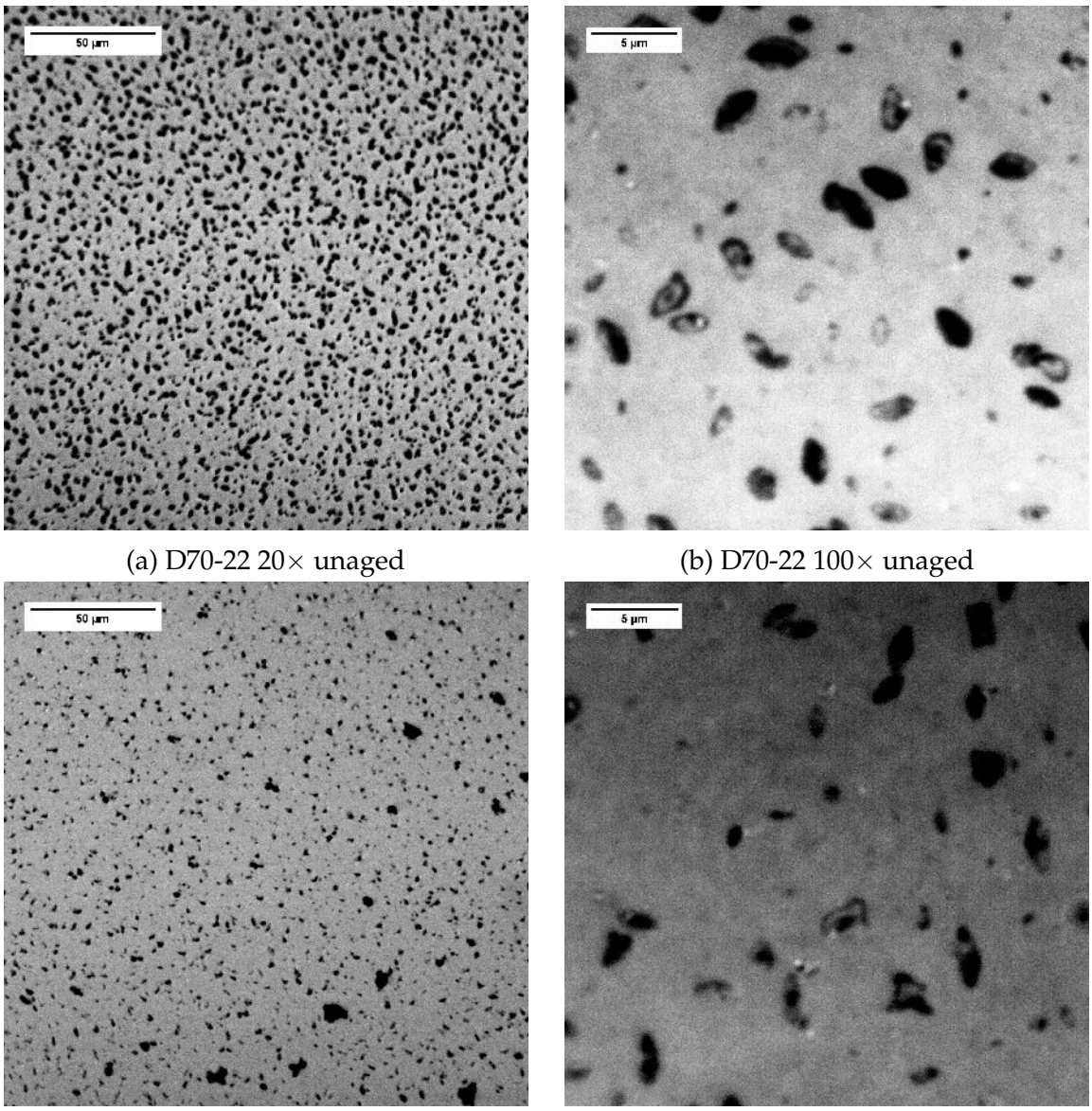

(a) D70-22 20× unaged

(b) D70-22 100× unaged

(c) D70-22 20× short-term aged

(d) D70-22 100× short-term aged

Figure 4.18: 20× and 100× Microstructure images of D70-22 in two aging conditions

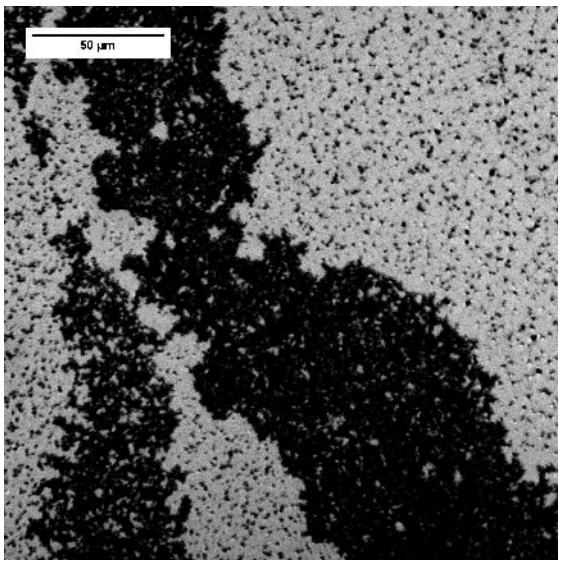

(a) D76-22 20× unaged

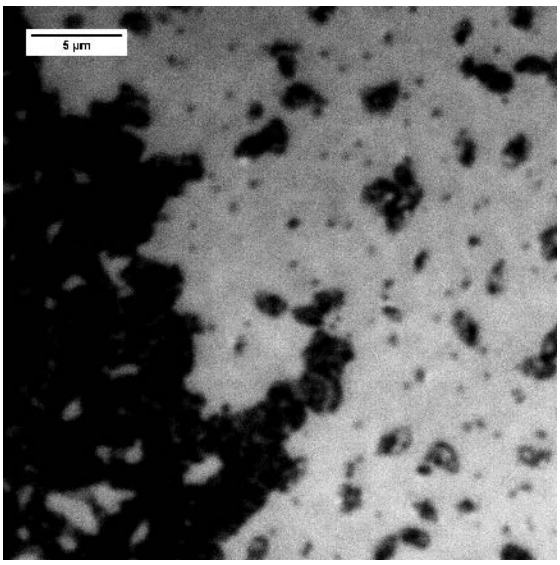

(b) D76-22 100× unaged

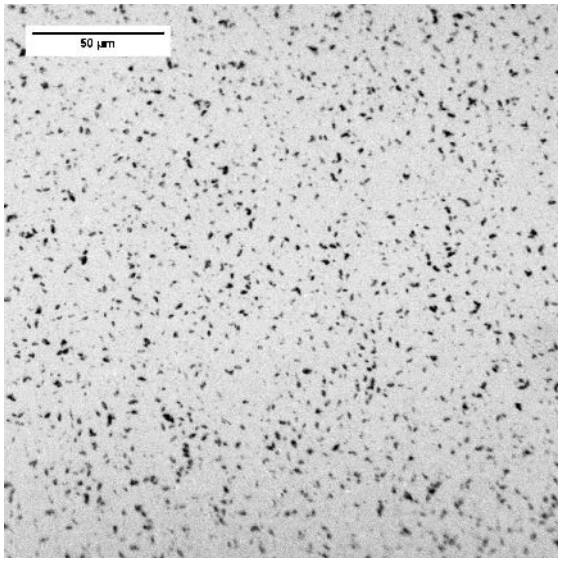

(c) D76-22 20× short-term aged

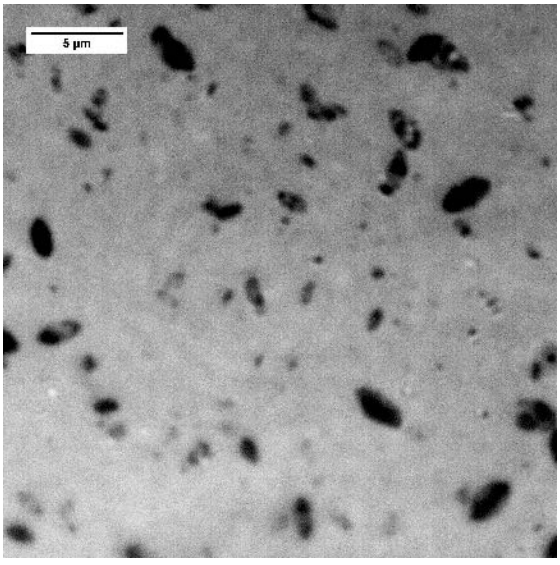

(d) D76-22 100× short-term aged

Figure 4.19: 20× and 100× Microstructure images of D76-22 in two aging conditions

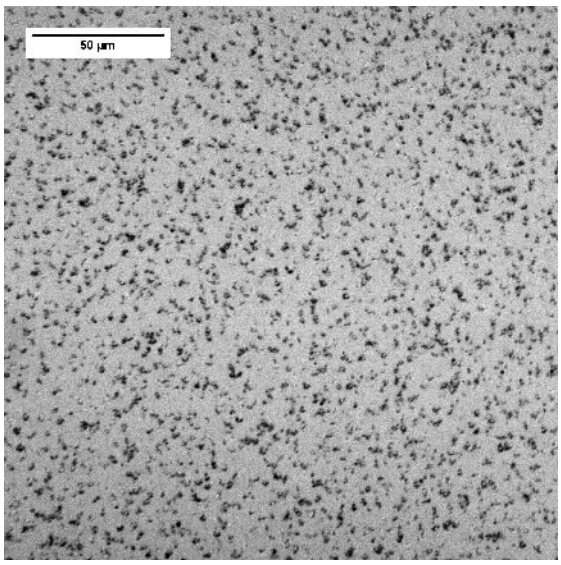

(a) E58-28 20× unaged

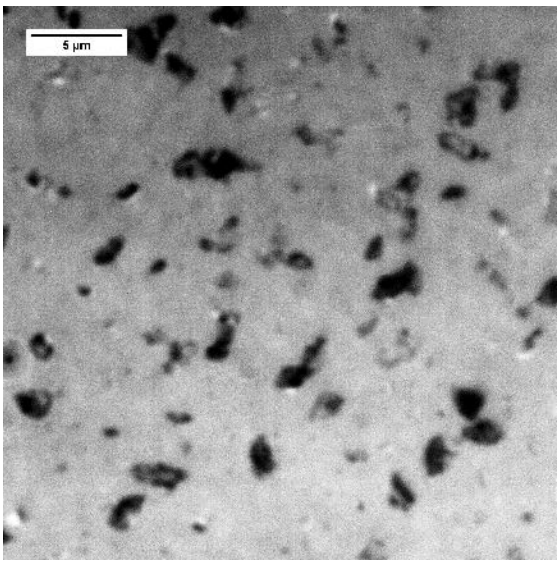

(b) E58-28 100× unaged

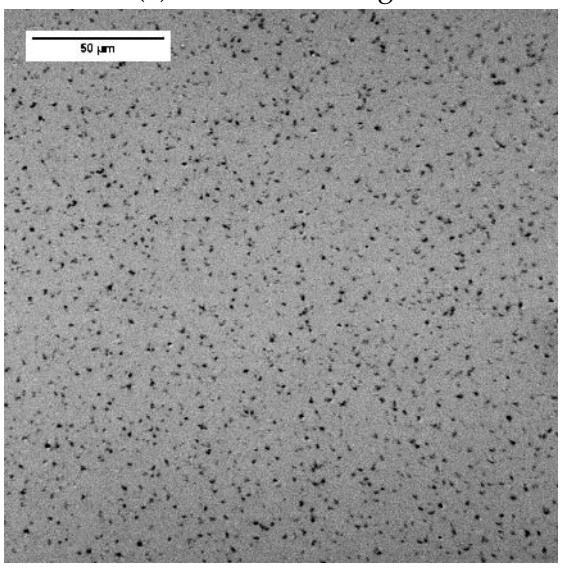

(c) E58-28 20× short-term aged

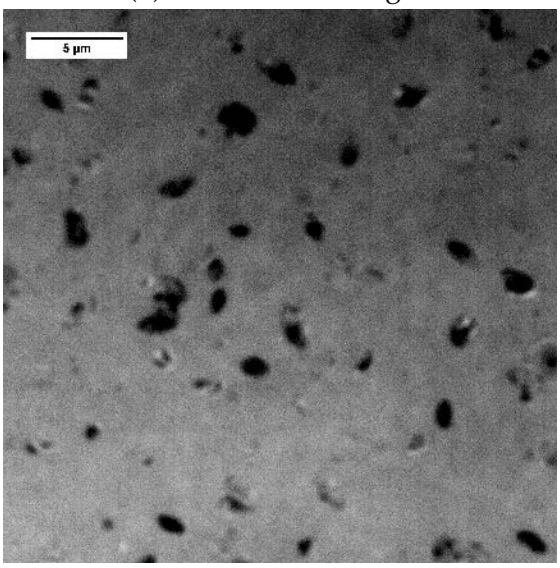

(d) E58-28 100× short-term aged

Figure 4.20: 20× and 100× Microstructure images of E58-28 in two aging conditions

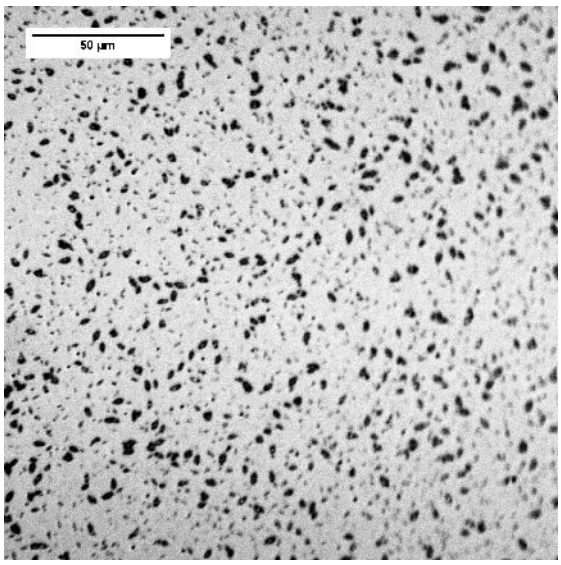

(a) E64-22 20× unaged

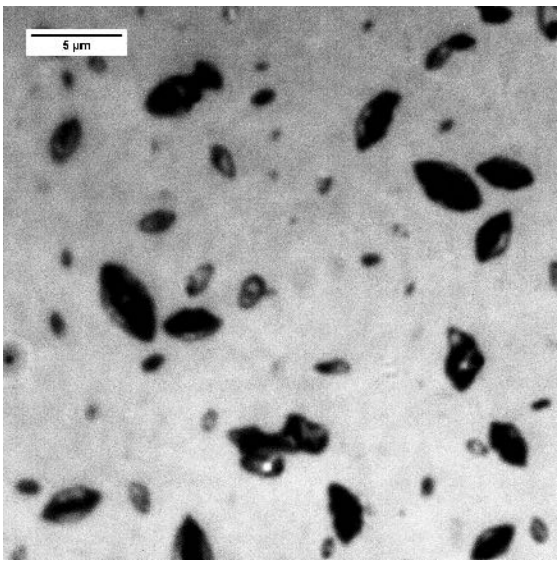

(b) E64-22 100× unaged

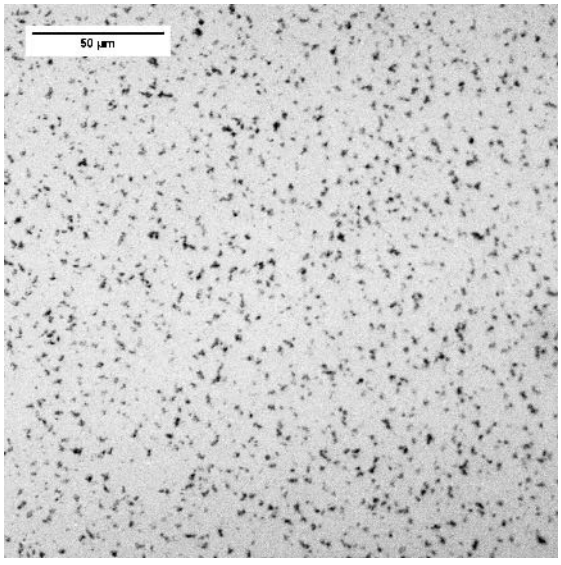

(c) E64-22 20× short-term aged

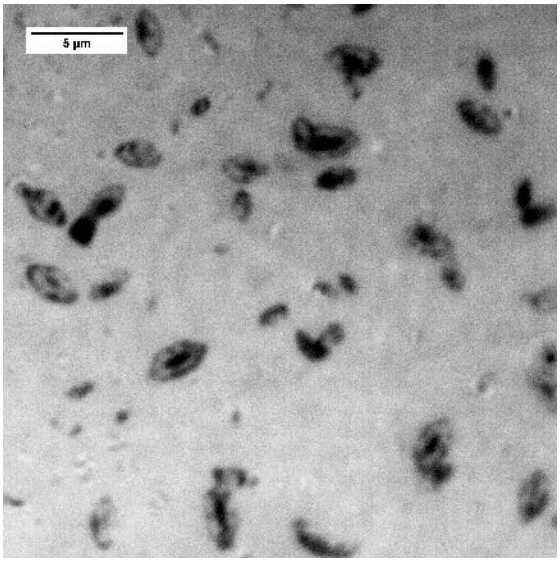

(d) E64-22 100× short-term aged

Figure 4.21: 20× and 100× Microstructure images of E64-22 in two aging conditions

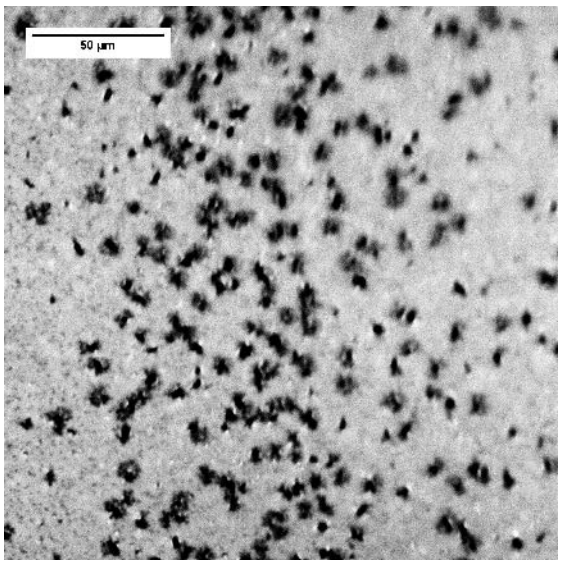

(a) F64-22 20× unaged

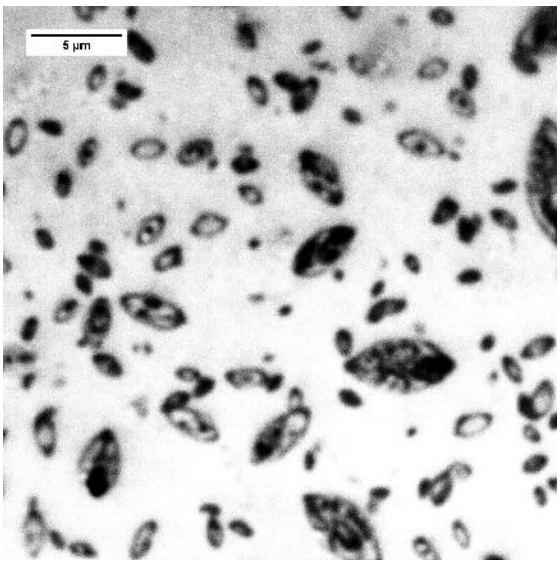

(b) F64-22 100× unaged

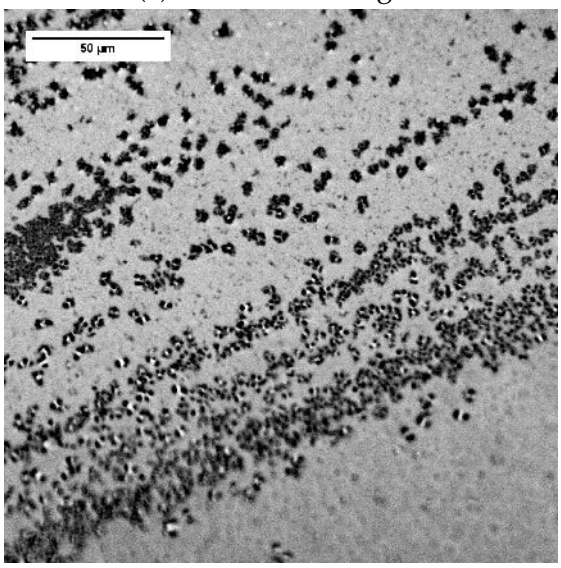

(c) F64-22 20× short-term aged

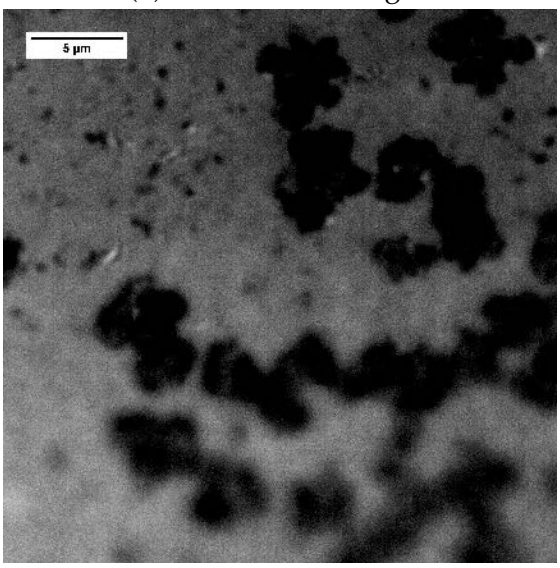

(d) F64-22 100× short-term aged

Figure 4.22: 20× and 100× Microstructure images of F64-22 in two aging conditions

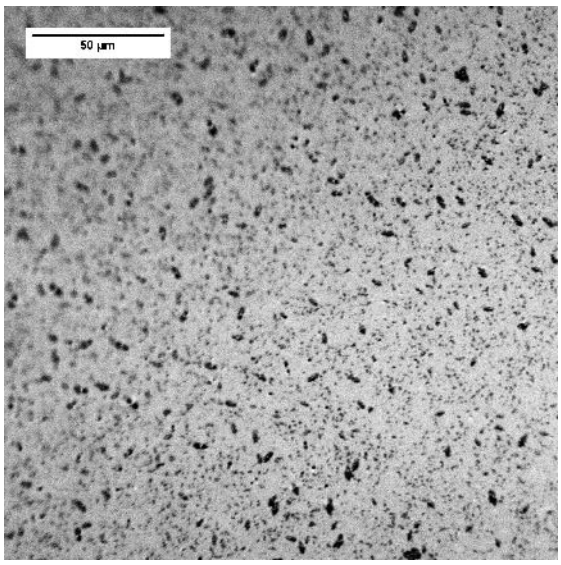

(a) G64-22 20× unaged

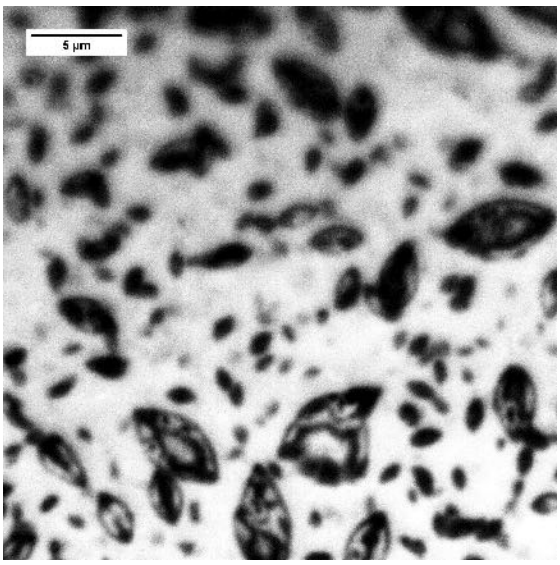

(b) G64-22 100× unaged

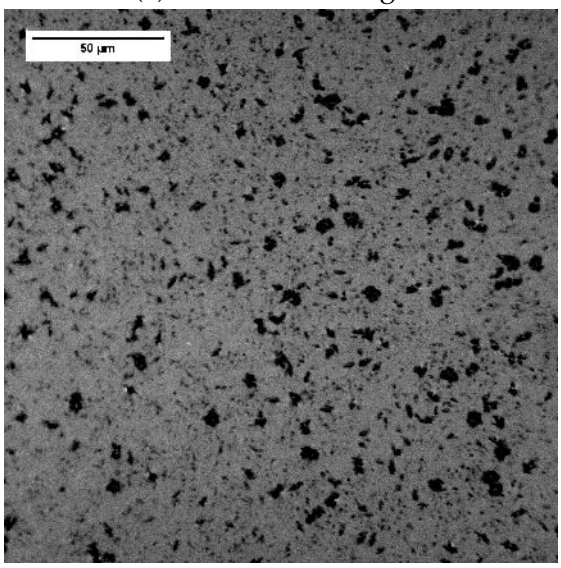

(c) G64-22 20× short-term aged

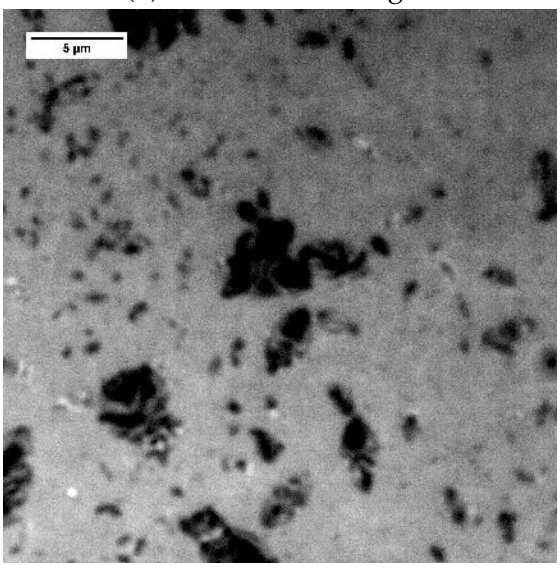

(d) G64-22 100× short-term aged

Figure 4.23: 20× and 100× Microstructure images of G64-22 in two aging conditions

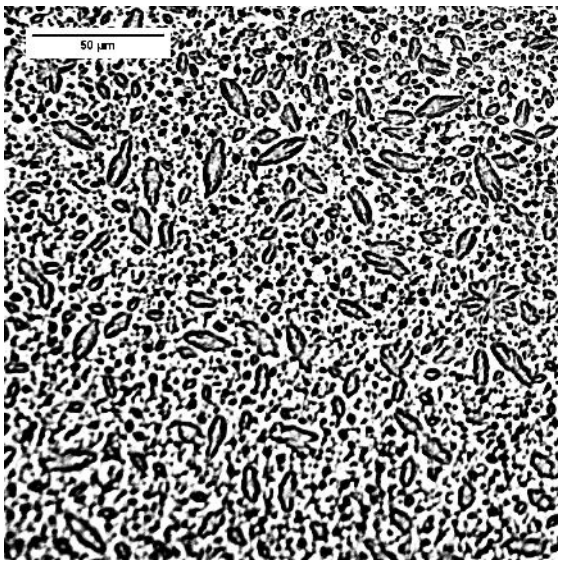

(a) G70-22 20× unaged

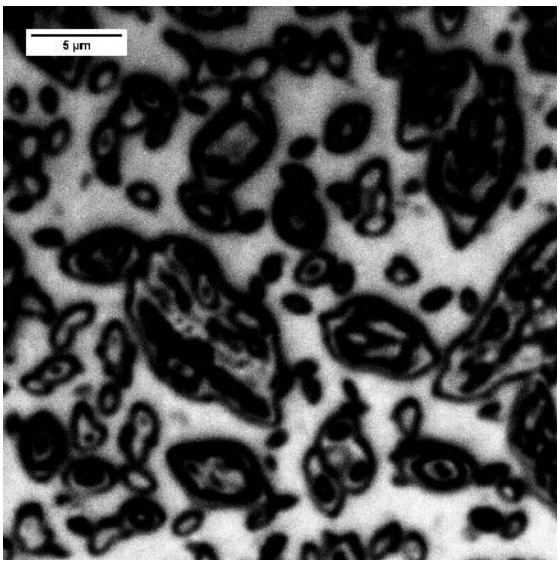

(b) G70-22 100× unaged

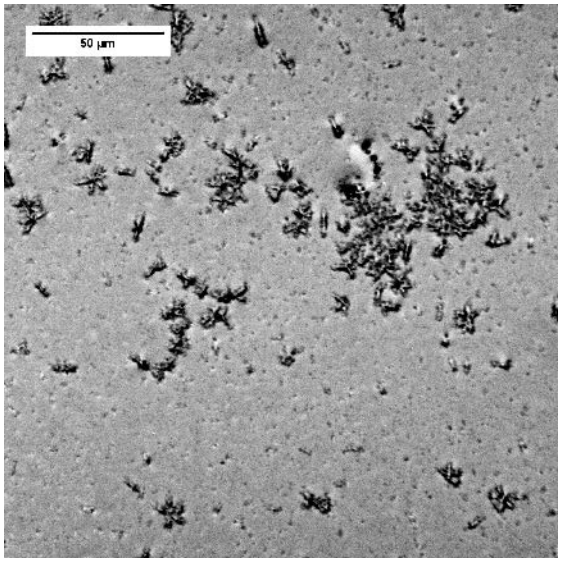

(c) G70-22 20× short-term aged

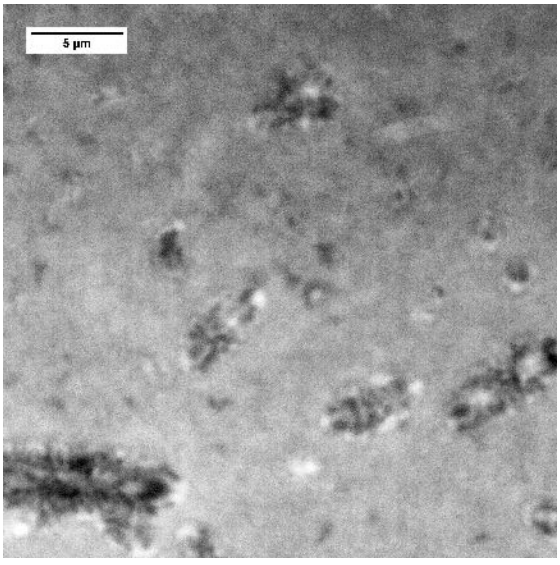

(d) G70-22 100× short-term aged

Figure 4.24: 20× and 100× Microstructure images of G70-22 in two aging conditions

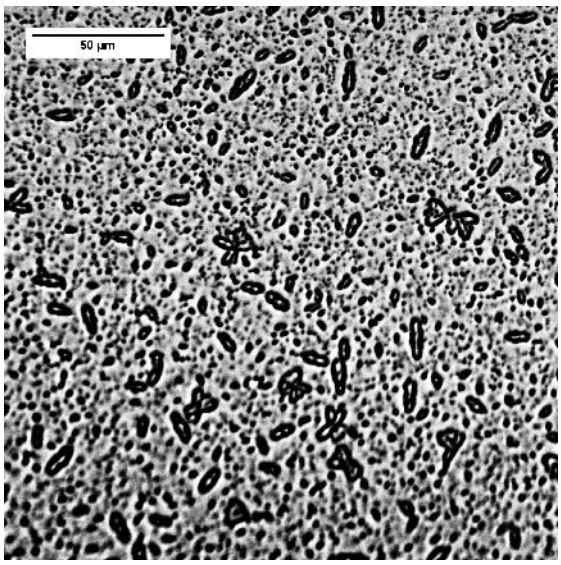

(a) G76-22 20× unaged

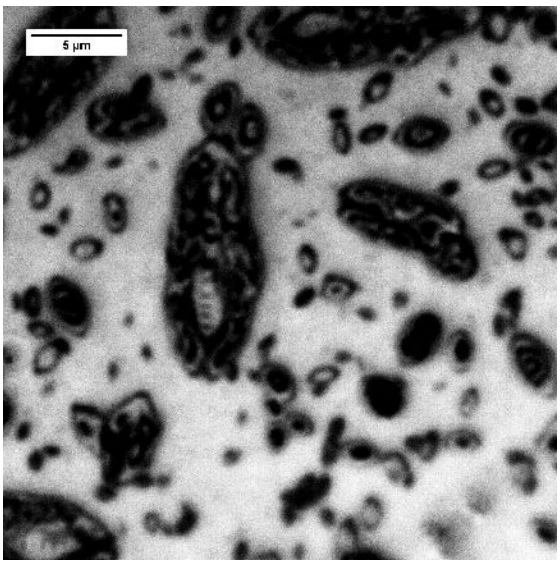

(b) G76-22 100× unaged

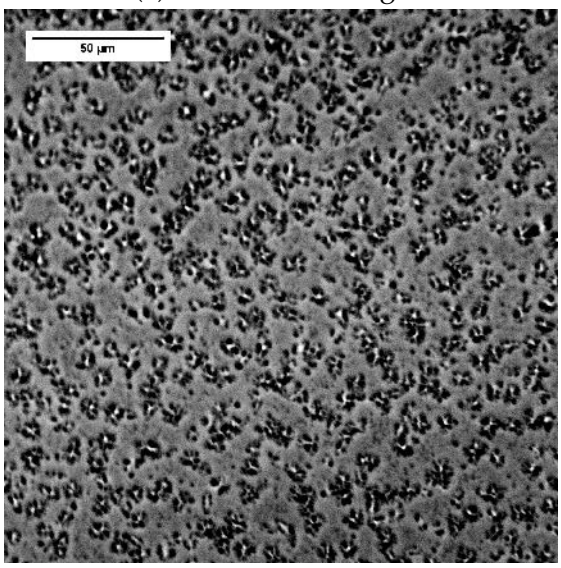

(c) G76-22 20× short-term aged

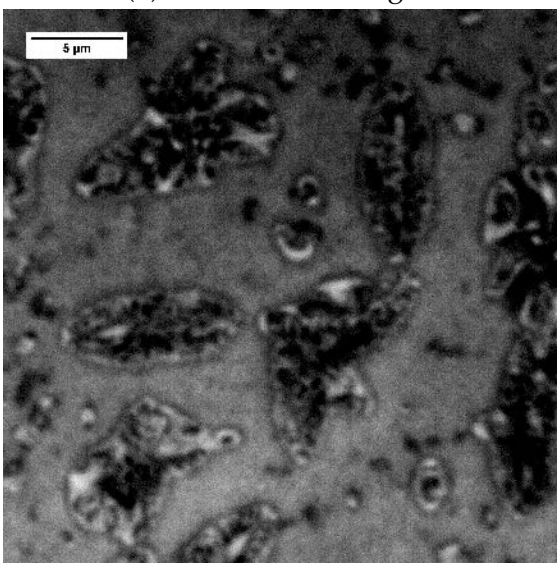

(d) G76-22 100× short-term aged

Figure 4.25: 20× and 100× Microstructure images of G76-22 in two aging conditions

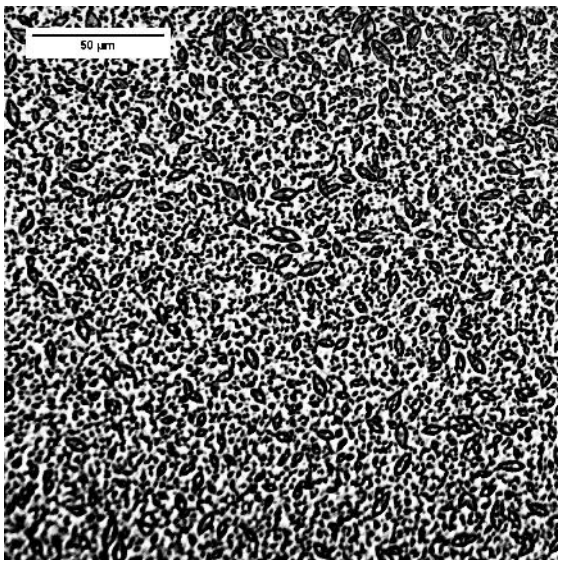

(a) H64-22 20× unaged

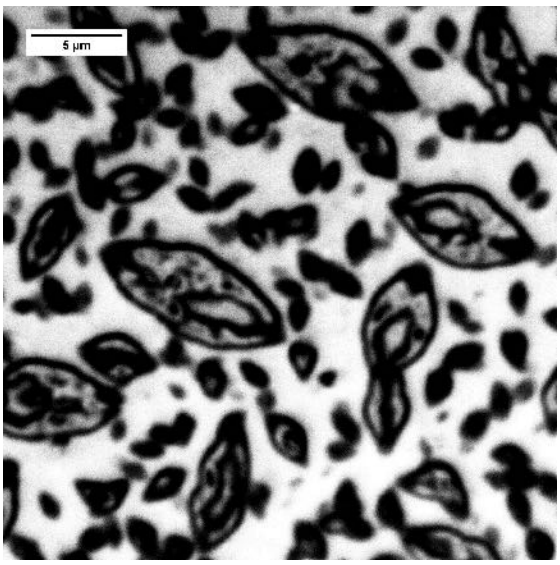

(b) H64-22 100× unaged

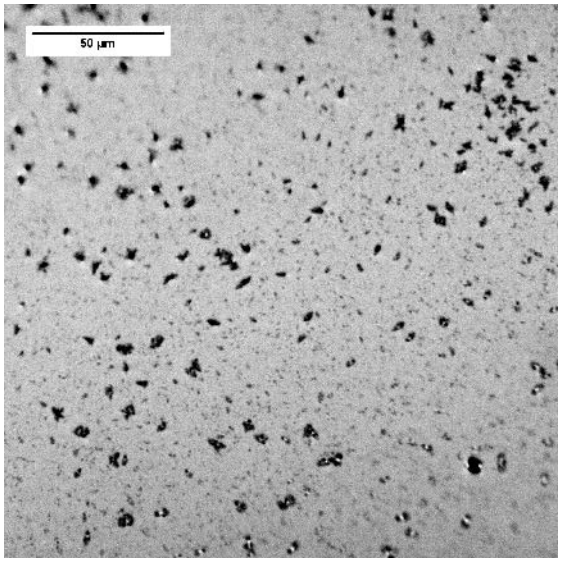

(c) H64-22 20× short-term aged

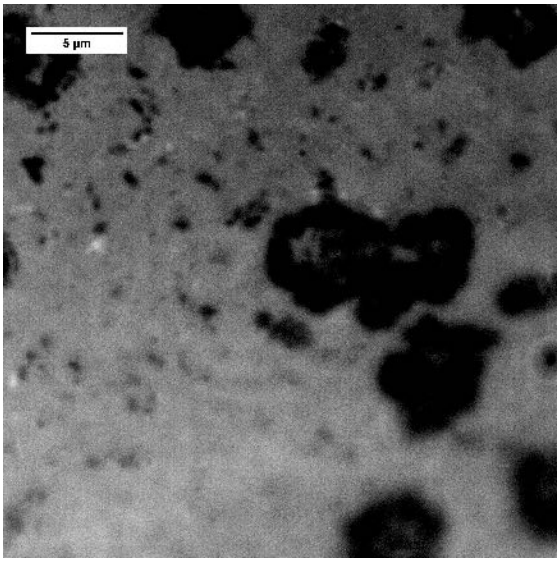

(d) H64-22 100× short-term aged

Figure 4.26: 20× and 100× Microstructure images of H64-22 in two aging conditions

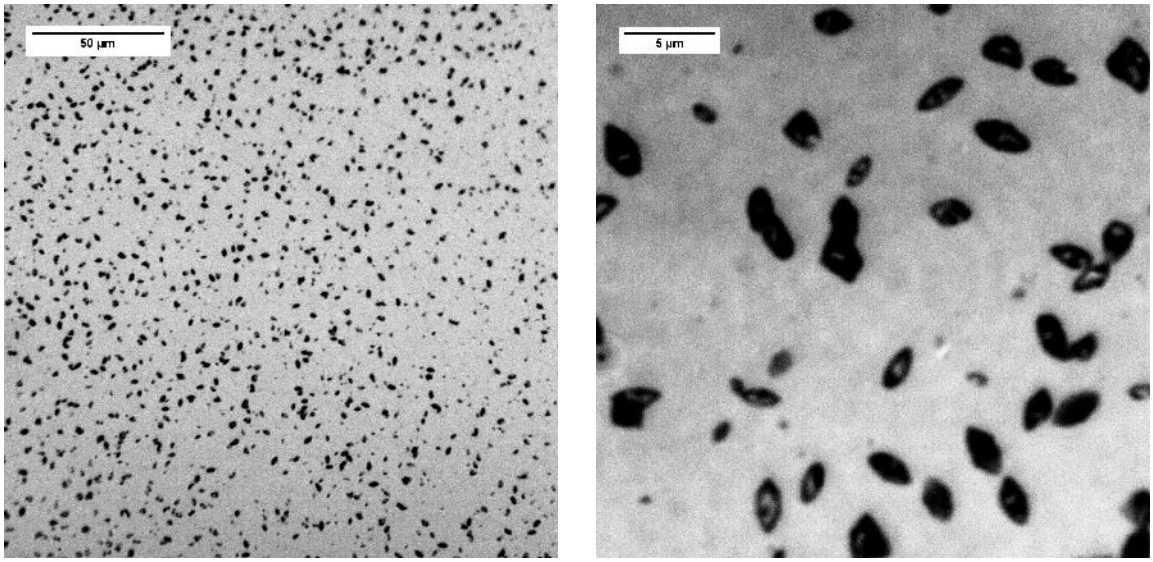

(a) I58-28 20× unaged

(b) I58-28 100× unaged

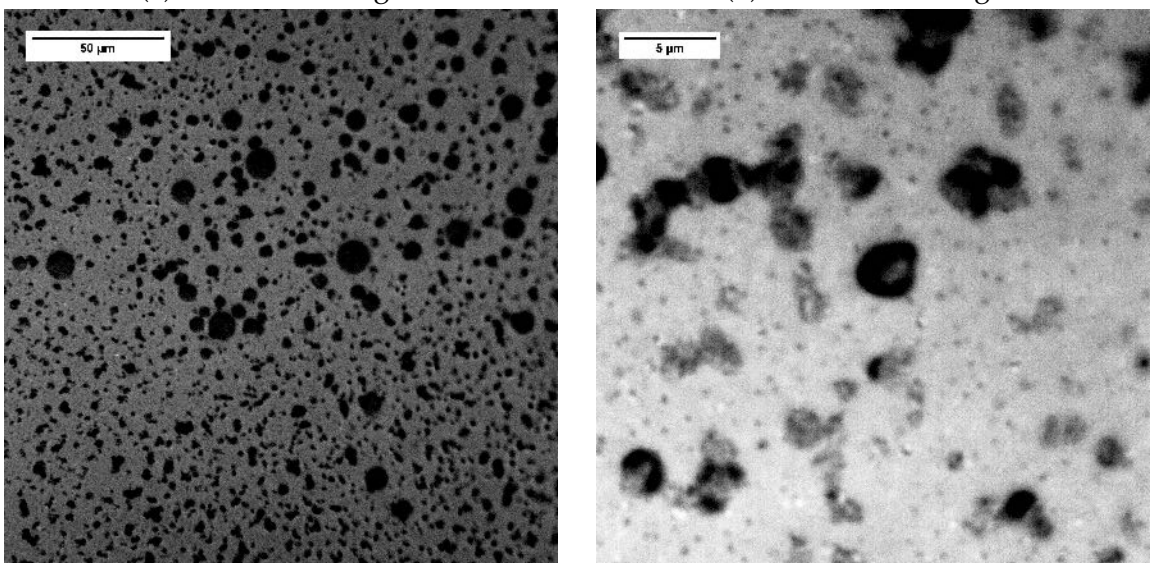

(c) I58-28 20× short-term aged

(d) I58-28 100× short-term aged

Figure 4.27: 20× and 100× Microstructure images of I58-28 in two aging conditions

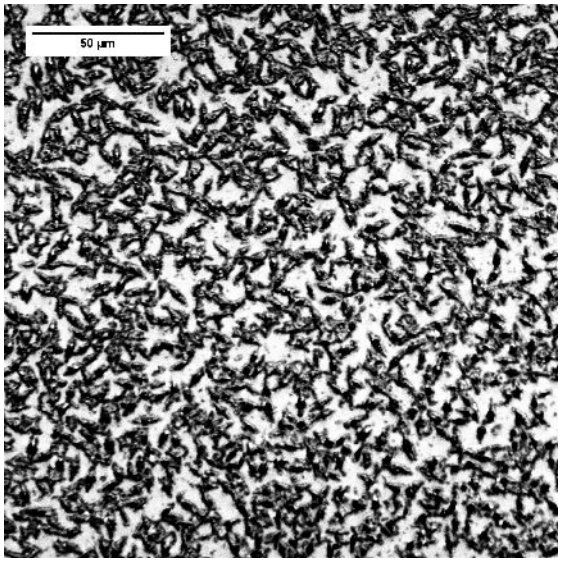

(a) I64-22 20× unaged

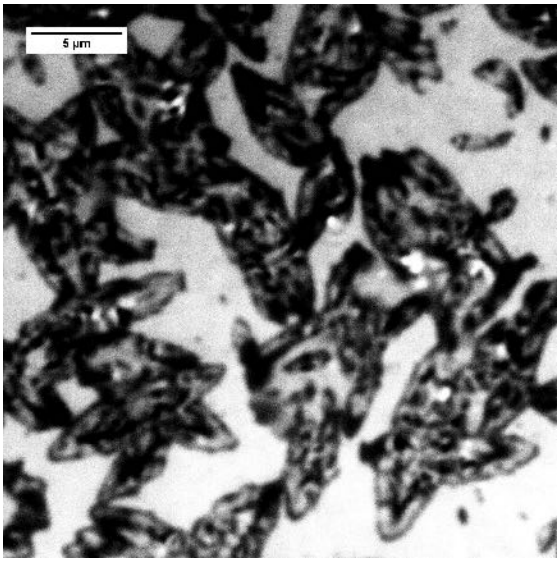

(b) I64-22 100× unaged

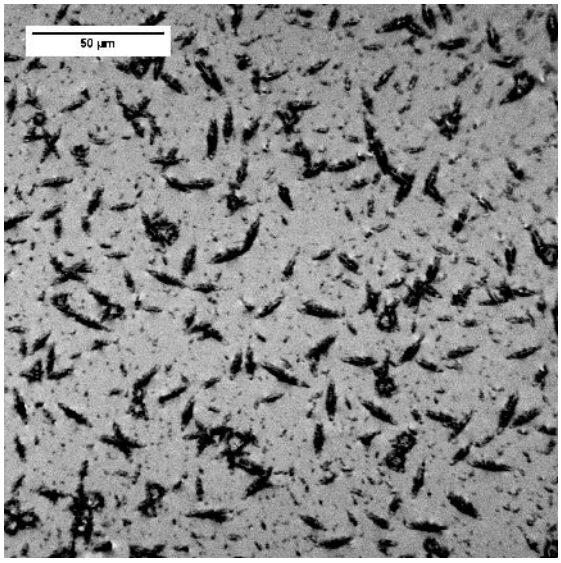

(c) I64-22 20× short-term aged

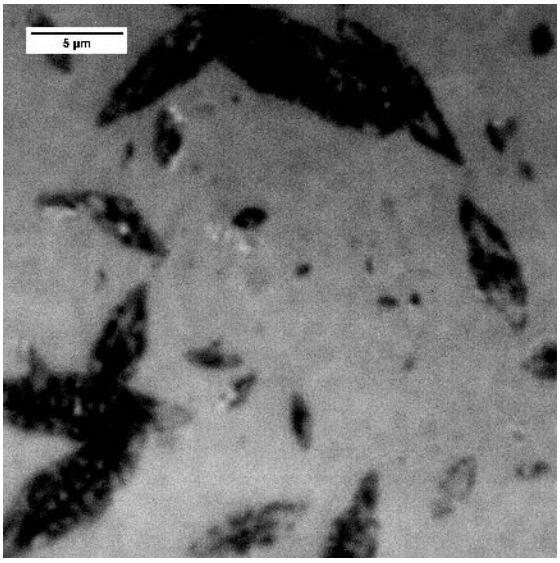

(d) I64-22 100× short-term aged

Figure 4.28: 20× and 100× Microstructure images of I64-22 in two aging conditions

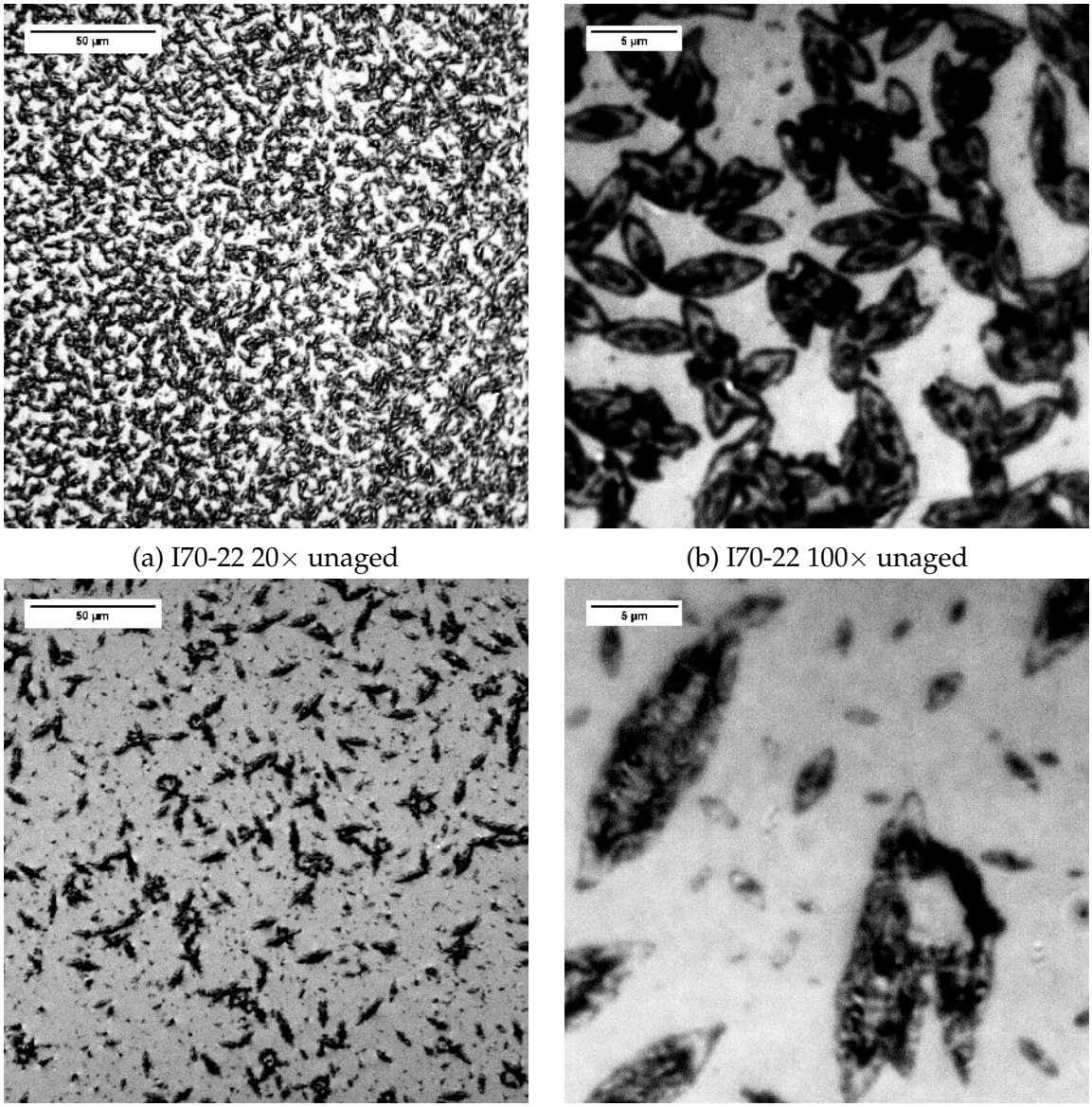

(a) I70-22 20× unaged

(b) I70-22 100× unaged

(c) I70-22 20× short-term aged

(d) I70-22 100× short-term aged

Figure 4.29: 20× and 100× Microstructure images of I70-22 in two aging conditions

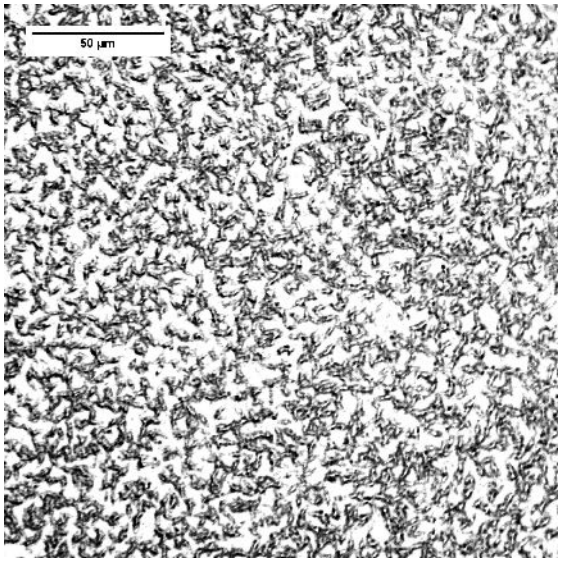

(a) I76-22 20× unaged

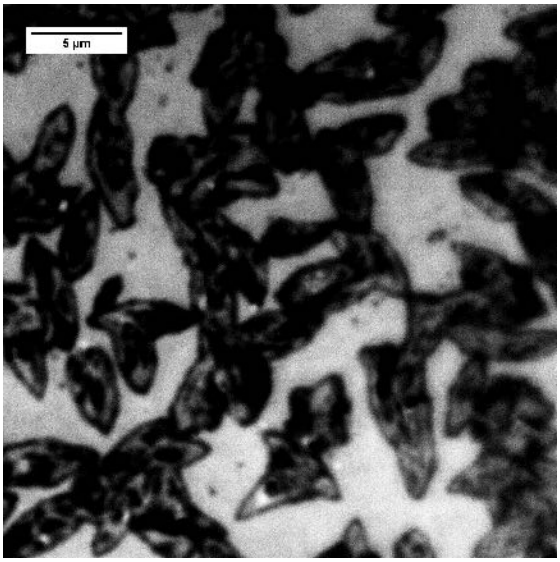

(b) I76-22 100× unaged

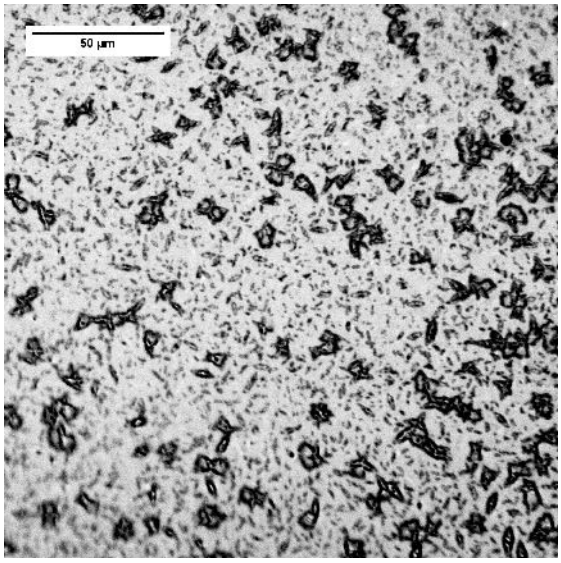

(c) I76-22 20× short-term aged

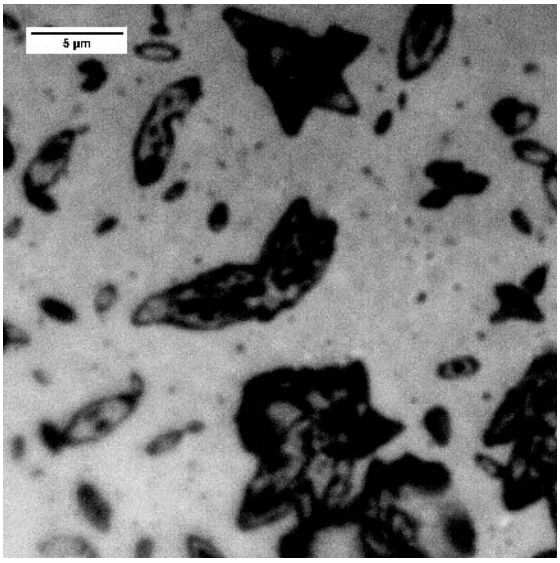

(d) I76-22 100× short-term aged

Figure 4.30: 20× and 100× Microstructure images of I76-22 in two aging conditions

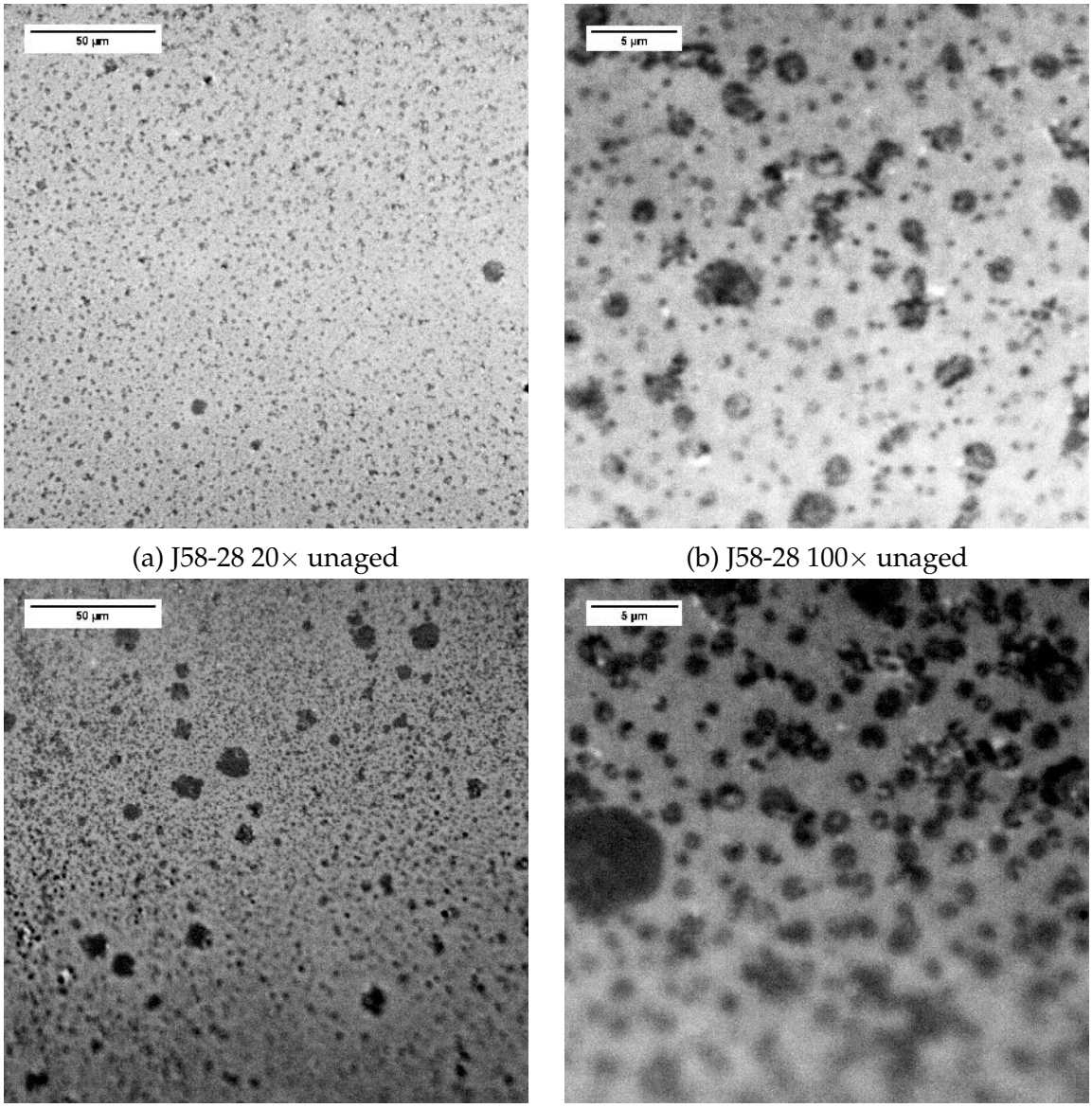

(a) J58-28 20× unaged

(b) J58-28 100× unaged

(c) J58-28 20× short-term aged

(d) J58-28 100× short-term aged

Figure 4.31: 20× and 100× Microstructure images of J58-28 in two aging conditions

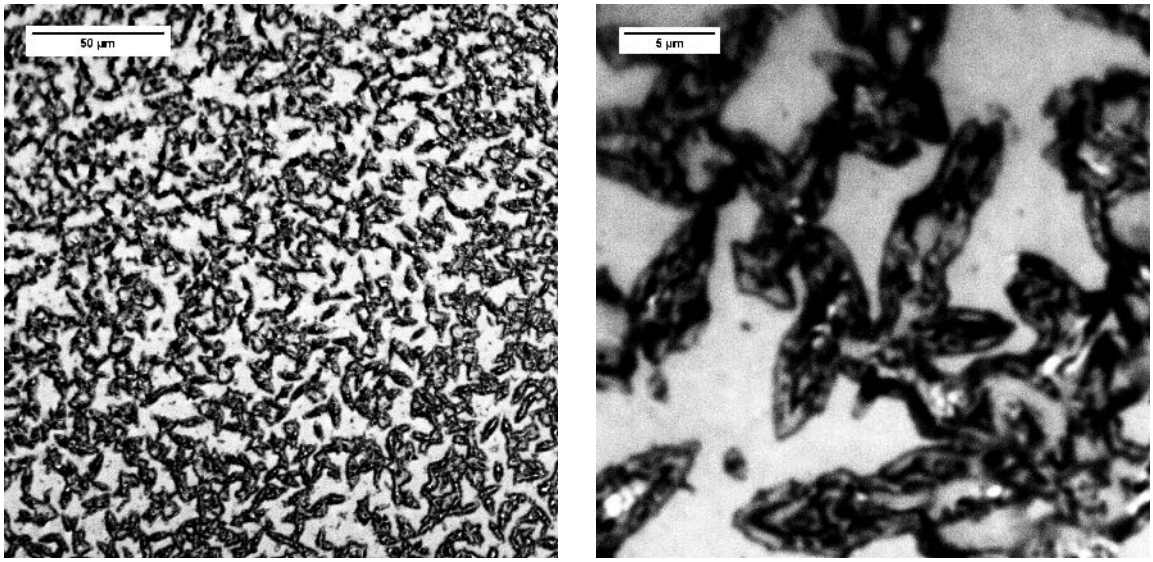

(a) J64-22 20× unaged

(b) J64-22 100× unaged

Figure 4.32: 20× and 100× Microstructure images of J64-22 in unaged condition (short-term aged sample unavailable)

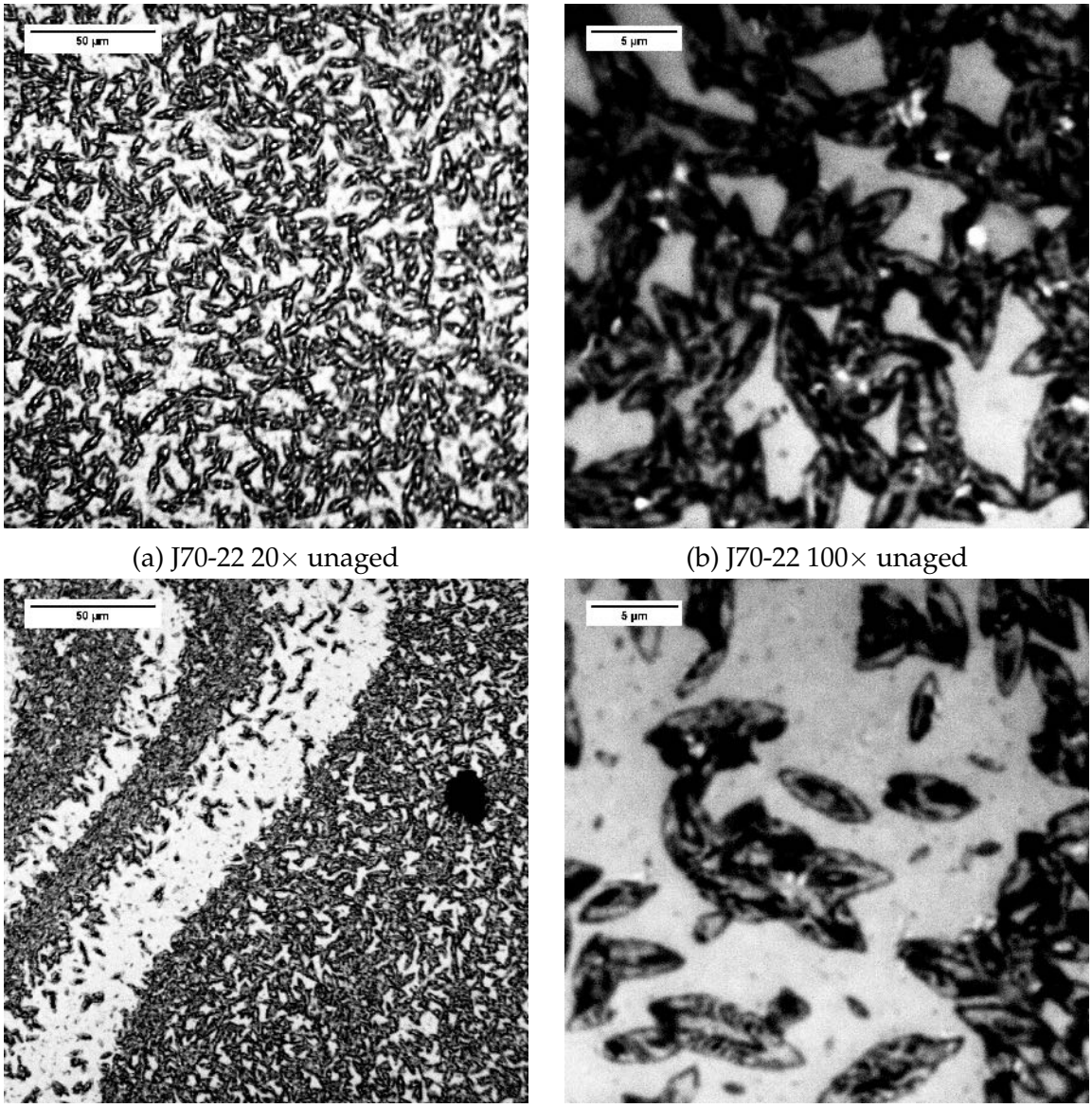

(a) J70-22 20× unaged

(b) J70-22 100× unaged

(c) J70-22 20× short-term aged

(d) J70-22 100× short-term aged

Figure 4.33: 20× and 100× Microstructure images of J70-22 in two aging conditions

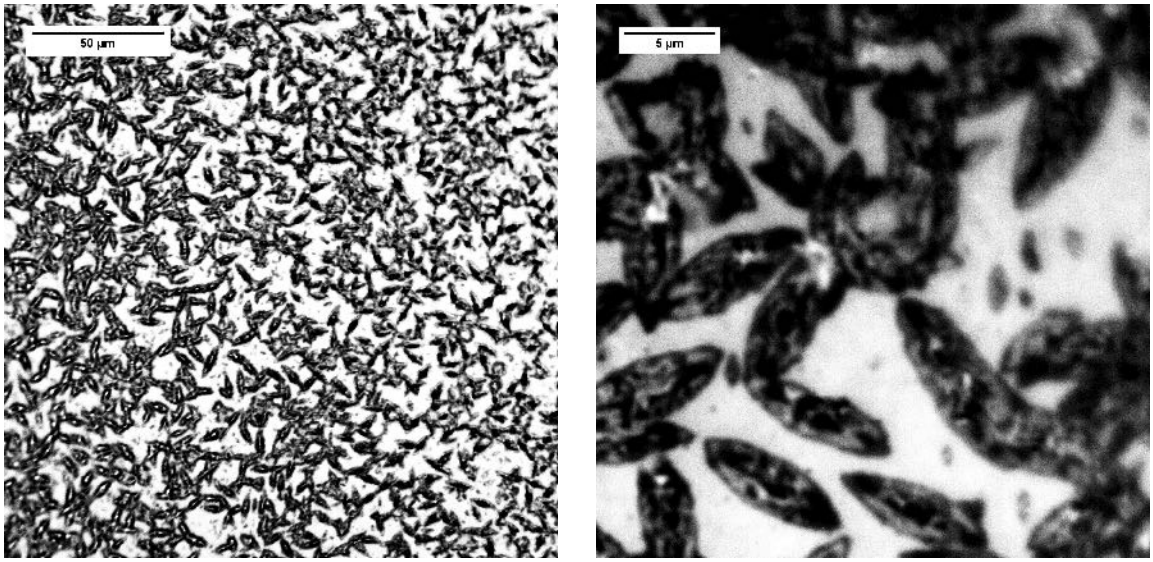

(a) J76-22 20× unaged (b) J76-22 100× unaged

Figure 4.34: 20× and 100× Microstructure images of J76-22 in unaged condition (short-term aged sample unavailable)

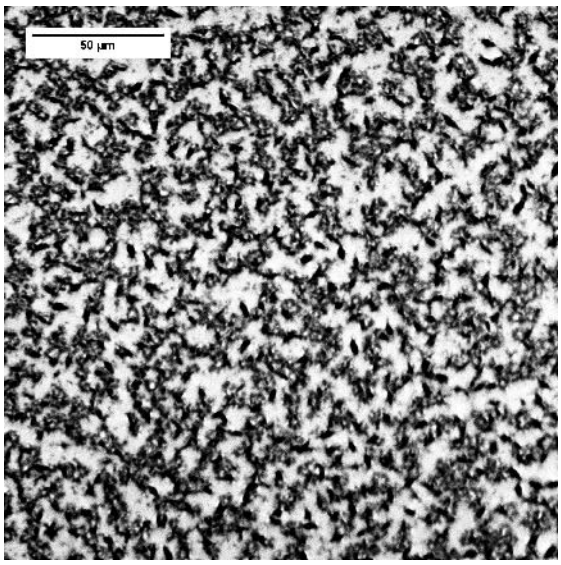

(a) K64-22 20× unaged

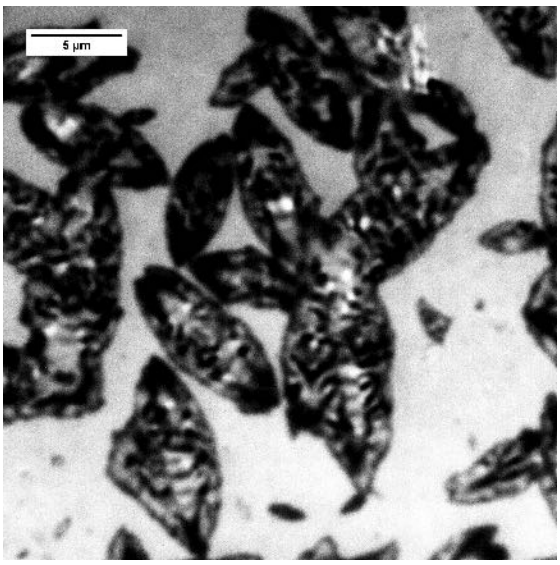

(b) K64-22 100× unaged

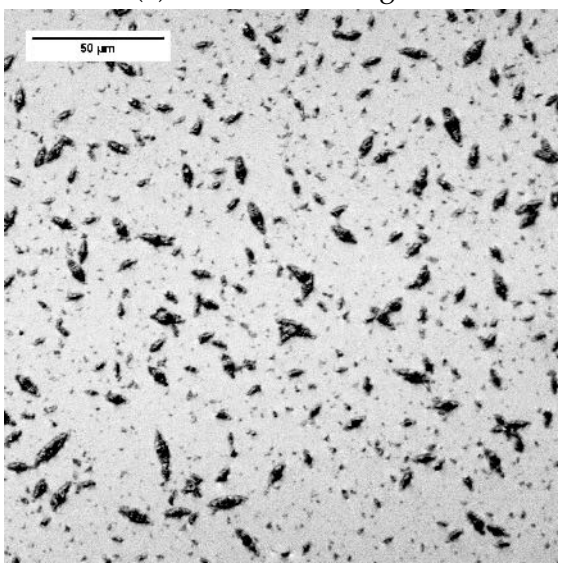

(c) K64-22 20× short-term aged

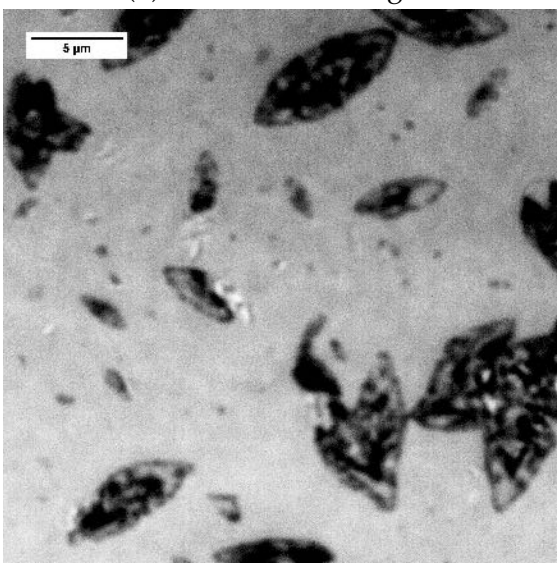

(d) K64-22 100× short-term aged

Figure 4.35: 20× and 100× Microstructure images of K64-22 in two aging conditions

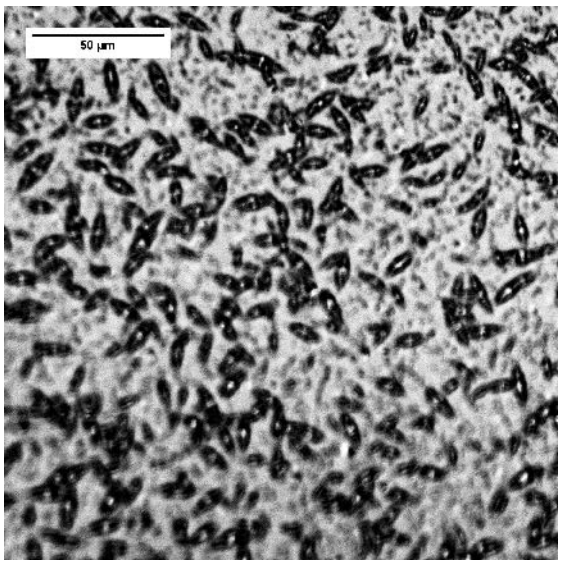

(a) K70-22 20× unaged

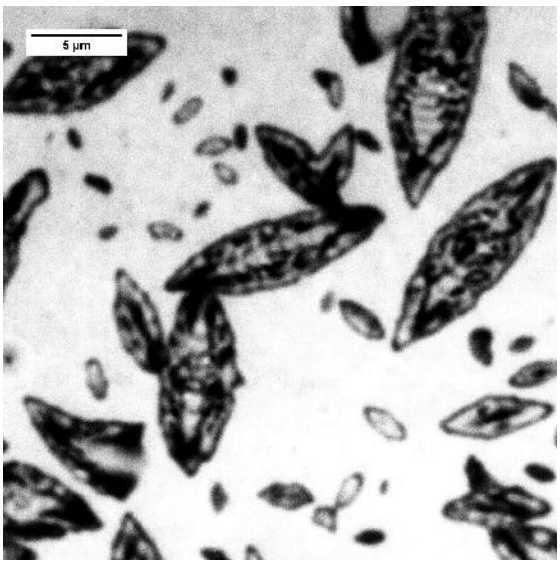

(b) K70-22 100× unaged

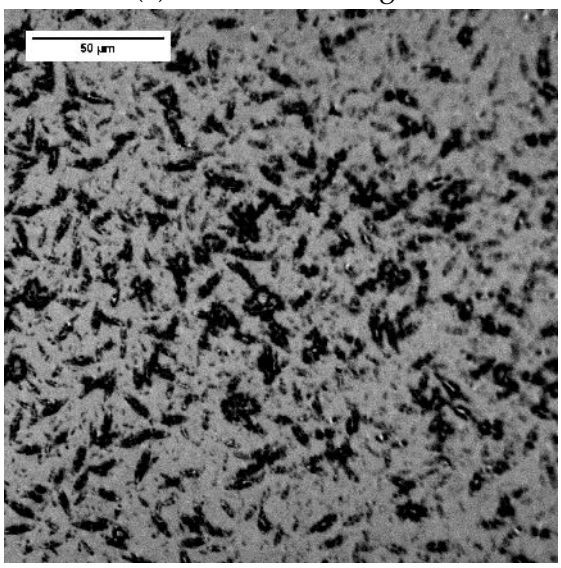

(c) K70-22 20× short-term aged

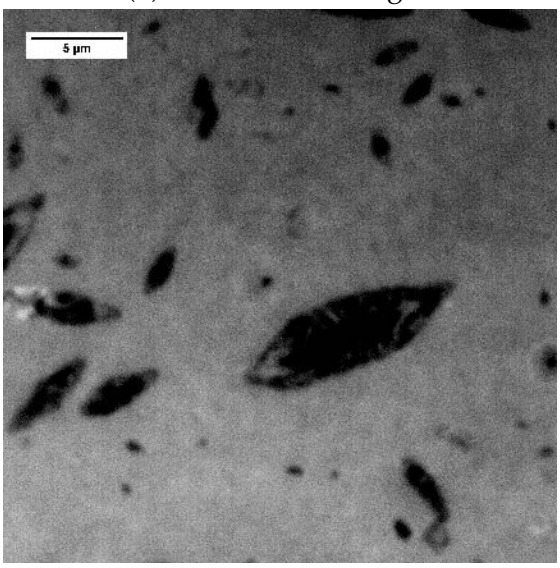

(d) K70-22 100× short-term aged

Figure 4.36: 20× and 100× Microstructure images of K70-22 in two aging conditions

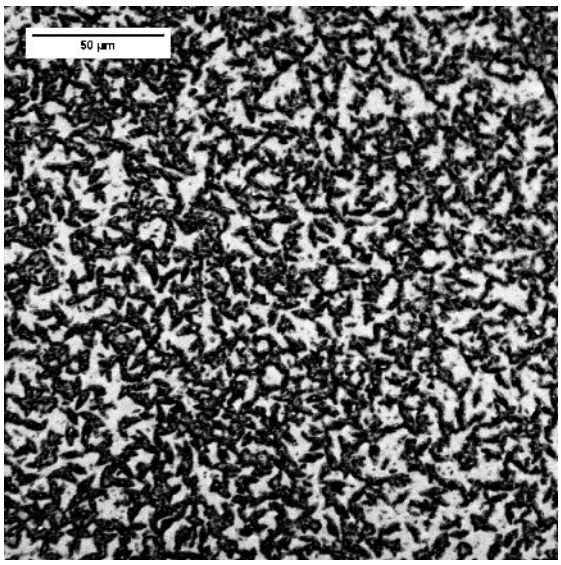

(a) K76-22 20× unaged

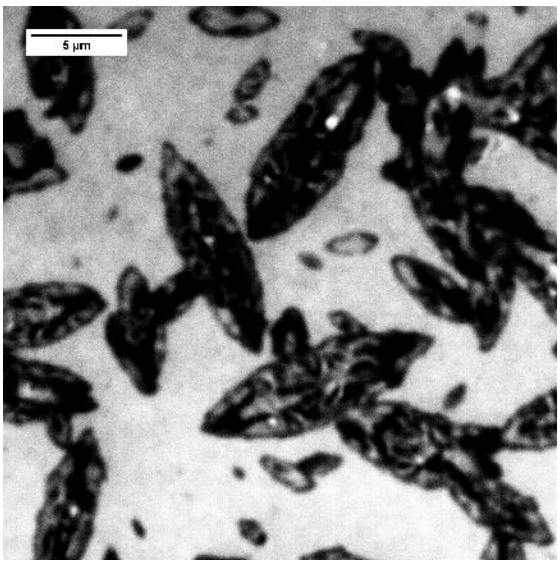

(b) K76-22 100× unaged

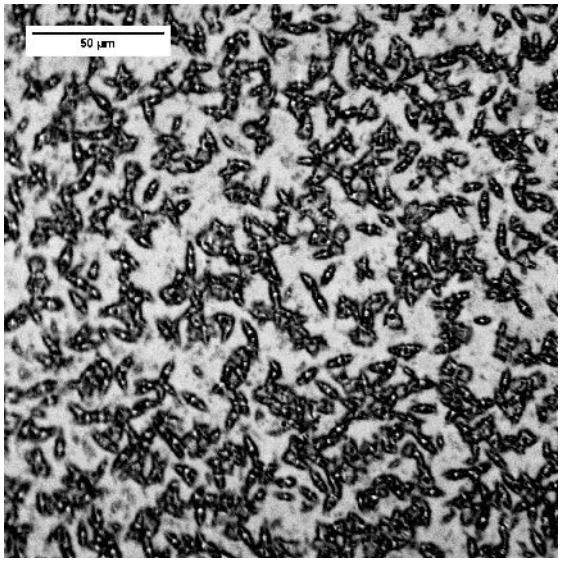

(c) K76-22 20× short-term aged

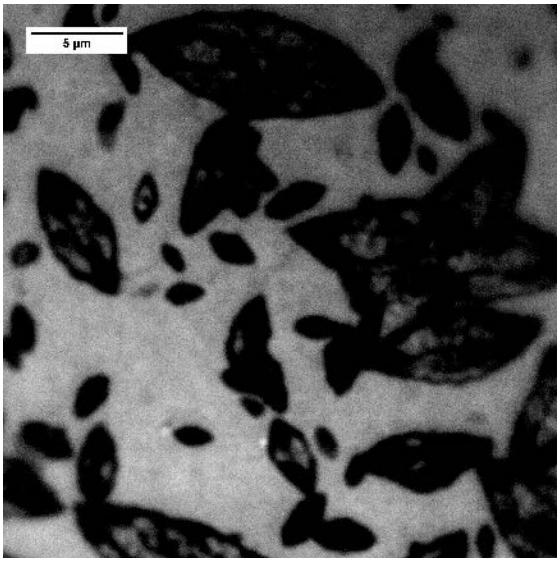

(d) K76-22 100× short-term aged

Figure 4.37: 20× and 100× Microstructure images of K76-22 in two aging conditions

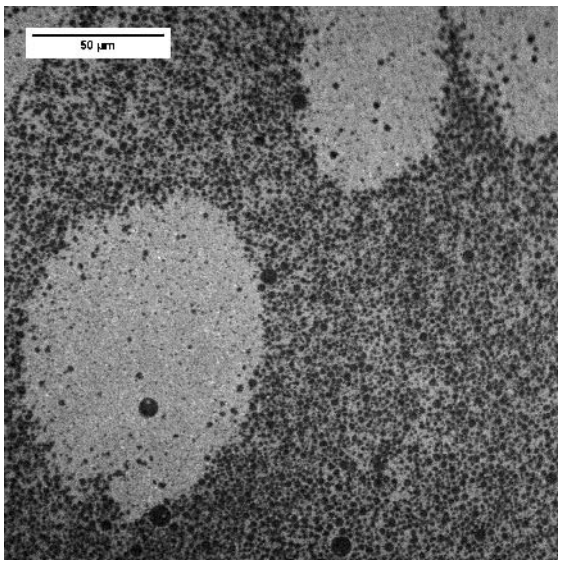

(a) L58-28 20× unaged

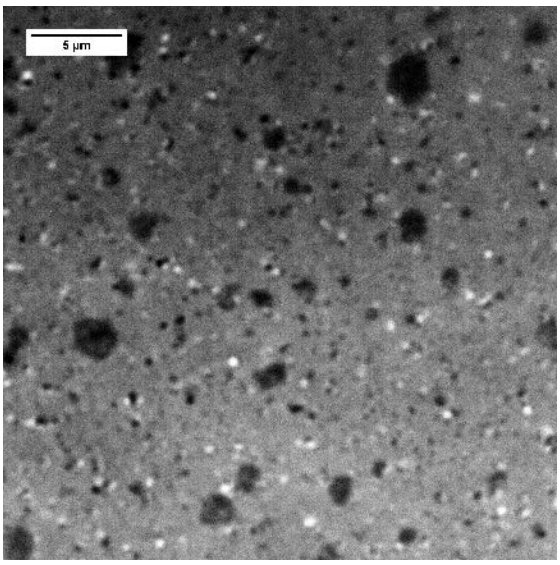

(b) L58-28 100× unaged

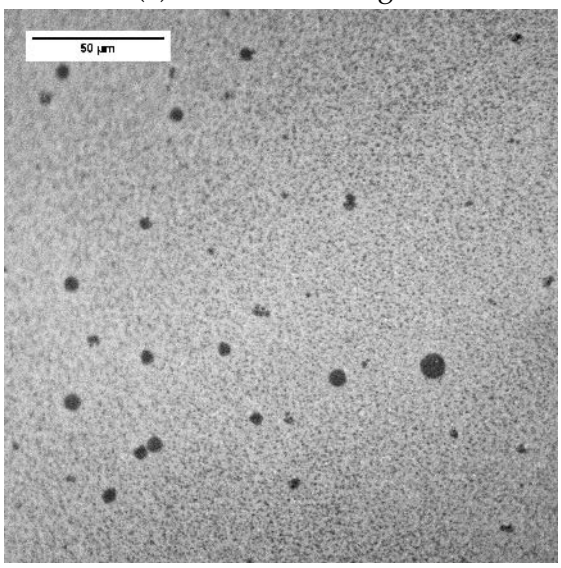

(c) L58-28 20× short-term aged

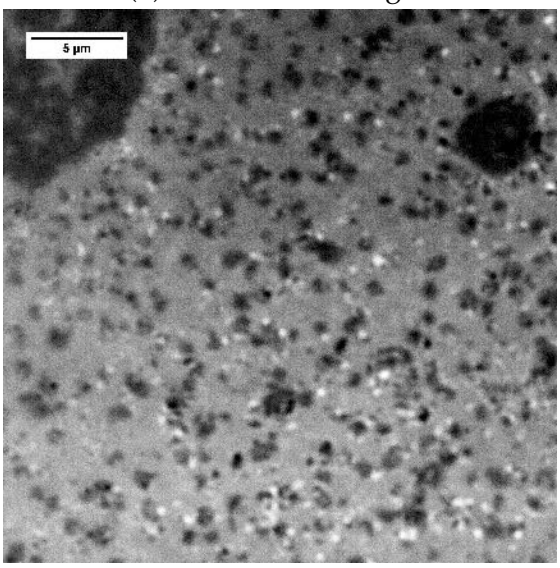

(d) L58-28 100× short-term aged

Figure 4.38: 20× and 100× Microstructure images of L58-28 in two aging conditions

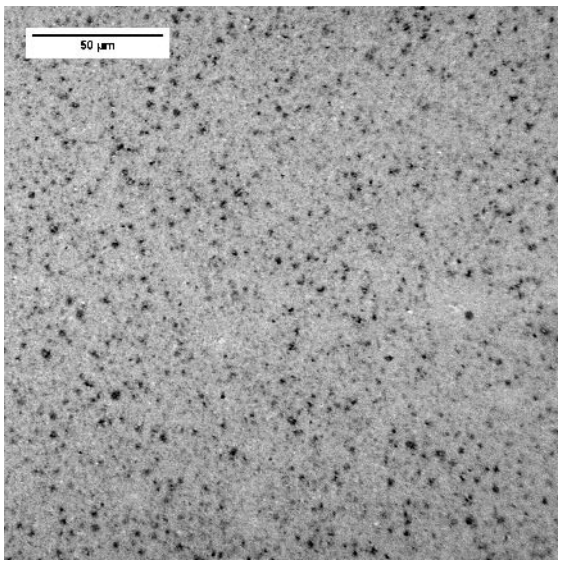

(a) L64-22 20× unaged

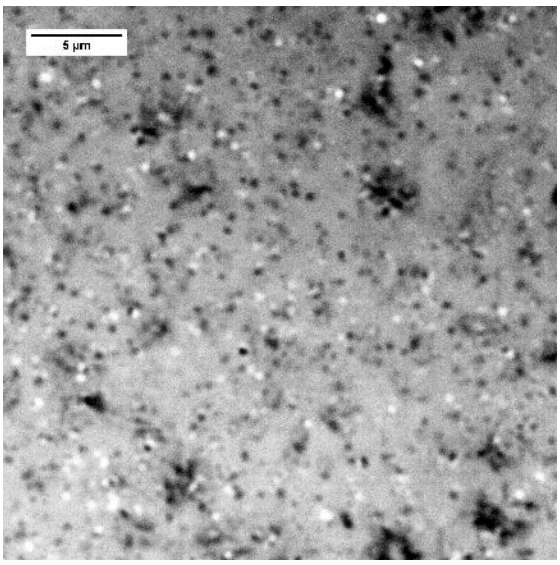

(b) L64-22 100× unaged

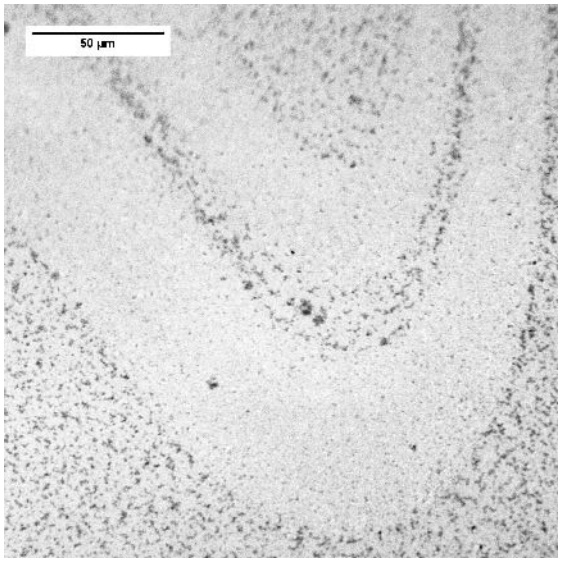

(c) L64-22 20× short-term aged

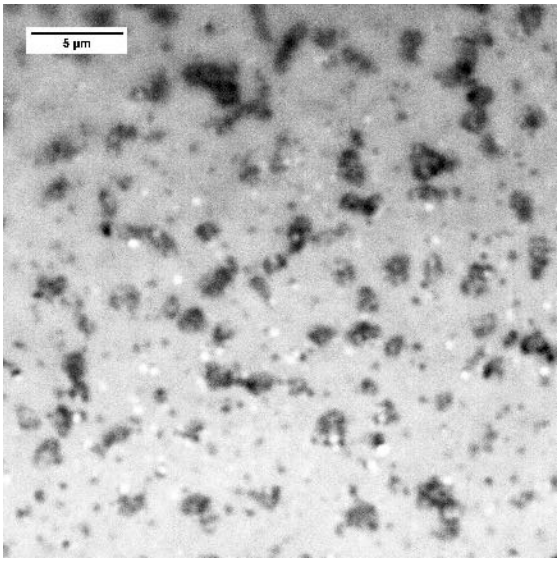

(d) L64-22 100× short-term aged

Figure 4.39: 20× and 100× Microstructure images of L64-22 in two aging conditions

Chapter 5

Conclusions

It is generally agreed that chemistry of bitumen, like any other material, dictates the macroscopic and engineering properties of the material. However, owing to the complex and heterogenous nature of the chemical makeup, it is challenging to establish the mechanism and extent of this relationship. This study offers a new methodology for separation of chemical fractions (based on polarity) which was utilized to evaluate a significant number of bitumen samples. The chemical fractions correlated with several rheological and strength properties. With the help of recent methods developed for bitumen imaging, the surface microstructure of these bitumen showed interesting similarity with respect to source and aging. Quantitatively, surface microstructures on bitumens showed some correlation with chemical fractions. The findings from this study can be summarized as follows:

1. Two fast and inexpensive SARA fractionation methods were developed and semi-quantitatively validated to equip the researchers with tools to incorporate chemical fractionation as a routine test. The sensitivity and repeatability of these methods was demonstrated to be reasonable, particularly for the liquid chromatography (TexSARA) method. Inter-laboratory results are also expected to be better than ASTM D4124 due to less variability in column packing, as SPE cartridges are commercially prepared. These methods offer chemical fractionation to be used as a routine test due to their favorable cost, simplicity and processing time. Easiness of the methods would potentially encourage researchers to opt for chemical fractionation for bitumen fingerprinting and thereby develop a large database of chemical information to understand bitumen chemistry more thoroughly.

2. About 100 bitumen samples were chemically fractionated using TexSARA. Subsets of these samples were also subjected to routine specification type tests as well as other diagnostic tests (e.g. tensile strength, spot test, and metal content analysis). Results from measurements of rheological properties were compared with parameters related to the chemical fractions based on the TexSARA method.

3. Parameters, such as complex modulus at high temperature, stiffness or S-value at low temperature, and tensile strength measured using a poker chip test at intermediate temperature, correlated well with TexSARA fractions when examined using multiple linear regression.

4. Metrics that are more influenced by loading time showed relatively weaker relationship. These parameters include Elastic recovery and m-value obtained using a Bending Beam Rheometer. It is possible that time-dependent deformation (or recovery) are driven by additional factors. However, this conclusion is also somewhat limited because of the lack of diversity in some of these parameters in the sample of materials selected.

5. In most cases bitumen samples that departed from a predicted relationship with TexSARA fraction also showed inconsistent response compared to similar bitumens using tests or parameters beyond the standard PG tests (e.g. spot test, XRF, ΔT_c). However, some other bitumens that showed anomalous behavior in other tests did not exhibit anomaly in TexSARA results.

6. Microscopic images of bitumen surface show that surface microstructure features are similar for the bitumens from same producer, even when the grades are different.

7. Quantitative analysis of the bitumen microstructure from same source showed good relationship with TexSARA fractions, although each source had a different relationship and there was not a global trend. While the relationship appeared compatible to visual observation, it should be noted that data used to establish these relationships is much smaller than the full data set considering all bitumens.

8. Bitumen samples which did not appear similar (in terms of surface microstructure) to the bitumens from the same source also showed irregular results in other tests compared to other similar bitumens.

From the observations made in this study, several recommendations can be made for future studies. First, TexSARA method can be readily integrated in a typical engineering bituminous lab. Combining TexSARA as a routine test, along

with other mechanical properties, will help develop a database of both material compositional characteristics and mechanical properties for bitumens from varied sources. Second, the influence of other attributes that define that chemical characteristics of the bitumens must also be incorporated in such a database. This will be particularly useful to address the gap that was observed in the microstructure from different producers (possibly indicating different crude sources) as well as the gap in the apparent lack of relationship between the bitumen chemistry and the more time dependent properties.

Appendix A
TexSARA: A Test method for separation of bitumen into four fractions using pre-packaged cartridges

1. The proposed method offers separation of bitumen into four (or more) fractions based on the relative polarity of the constituent molecules. The four fractions are termed as saturates, aromatics, resins and asphaltenes (commonly known as SARA fractions) with recognition of the fact that these are discrete and arbitrary divisions in the polarity-based distribution of bitumen constituents.

2. The proposed method is divided into two parts. The first part is the solubility based separation of asphaltenes and extraction of maltenes. The second part is chromatography-based fractionation of maltenes into saturates, aromatics and resins.

3. *This procedure does not address all safety concerns that can arise with its use. The user of this procedure must identify and address appropriate safety and health issues and consider the regulatory limitations as applicable to their respective institutions or regions.*

A.1 Referenced Documents

1. ASTM Standard

    1.1. D4124-09: Standard test method for separation of asphalt into four fractions.

2. IP Test Method

    2.1. IP 469: Determination of saturated, aromatic and polar compounds in petroleum products by thin layer chromatography and flame ionization detection.

A.2 Terminology

The following is a list of terms and their definitions in the context of this procedure.

1. Asphaltene: insoluble portion of bitumen when the bitumen is dissolved in n-heptane.
2. Maltene: portion of bitumen that is soluble in n-heptane.
3. S-A-R: constituents of maltene, i.e. saturates, aromatics and resins in order of increasing relative polarity.
4. Elution: passing of the mobile phase (solvent) through the stationary phase (adsorbent/silica gel) and washing a portion of analyte in the process.
5. Saturates: bitumen fraction that is eluted with n-heptane in the specified conditions.
6. Aromatics: bitumen fraction that is eluted with 80% Toluene- 20% n-heptane wash under specified conditions.
7. Resins: polar bitumen fraction that is eluted with 90% dichloromethane-10% methanol under specified conditions.

A.3 Summary of Test Method

A small amount of bitumen is dissolved in n-heptane by stirring at room temperature. The undissolved asphaltene is filtered using PTFE-based syringe filters. Separated maltenen (in the n-heptane solution) is applied on a solid phase extraction (SPE) cartridge which contains silica gel. In three steps, in increasing order of polarity, three solvents of given volume are used to elute three fractions of bitumen. The solvents are pushed through SPE cartridges by action of gravity and vacuum. Each elute is collected in pre-weighed bottles, dried, and weighed again for quantitative analysis.

A.4 Significance and Use

The test method separates four fractions of bitumen. It offers fast and repeatable results with minimal supervision time from operator. Compared to traditional liquid chromatography, relatively smaller amounts of solvents are consumed in this process. The accessories used in this procedure are inexpensive, space-friendly and commercially available in a ready-to-use form.

A.5 Apparatus and Materials

1. Hardware / equipment

    1.1. *Laboratory balance:* Any scale with 0.01 mg accuracy. Example: Sartorius Secura 225D-1S.

    1.2. *Vacuum manifold:* Any make/model/capacity should work as long as it accepts regular size syringe tip. Example: Supelco Visiprep™ SPE Vacuum Manifold 12-port model (Item: 57030-U). A manifold with at least 4 ports is required for processing one bitumen. However, a manifold with additional ports (12 or 24) is preferable for more efficient testing of multiple bitumen samples.

    1.3. *Vacuum pump:* A vacuum source to drive the vacuum manifold. Example: Pilot Chemical Resistant Diaphragm Vacuum Pump TLD5000. An oil free and chemical resistant vacuum pump is preferable.

    1.4. *Drying oven* (preferably with nitrogen purge capability): An air-tight oven that can be flooded with nitrogen with the outgas port can be used.

    1.5. *Solvent trap:* A solvent trap appropriate for the drying oven. Example: Graham condenser with cold water pump. A trap used with typical bitumen recovery apparatus (for extraction and recovery) can be used. While all solvents used in the proposed method are volatile and thus easy to boil, the amount of vapor may exceed fume hood capacity if only hotplate is used without solvent collection system.

2. Other minor hardware

2.1. A Magnetic stirring plate, example: Apera Instruments 801 Magnetic Lab Stirrer. Temperature control not required for this method; expensive magnetic stirrers with temperature control are not required. Stirring plates without temperature control are typically around $75 each. Although only one stirring plate is required, additional stirring plates will allow multiple bitumen samples to be processed and analyzed simultaneously.

2.2. Magnetic stirrer bar, 50 mm or appropriate size for the bottle to be used.One stirrer is required for each plate. The most important requirement is for the bar to have a PTFE coating.

2.3. Wide-mouth round bottle with septa closure. Example: Thermo Scientific™ Wide-mouth septa jars; (for dissolution, item 05-719-452). Having septa closures is important. One bottle is required for each stirring plate.

2.4. Silicone strip, $\approx$ 1"$\times$ 2" rectangle for preparing bitumen drops. Silicone mold used to prepare Dynamic Shear Rheometer (DSR) sample for bitumen testing can be used.

2.5. Metal measuring spoon, at least 0.4 ml capacity to take (molten liquid) bitumen from container.

2.6. Blunt tip pipetting needle 4-6 inch in length, 14 gauge or less. Length should be such that it reaches bottom of the bottle when pushed through the septa. It is necessary to have blunt tips and wider stem-dia (<14ga). Example: `http://a.co/h16216U`.

2.7. Pipettes with 0.1 mL resolution that can be used with the solvents.

2.8. Gloves compatible with the solvents.

3. Supplies and consumables (can be purchased in bulk)

3.1. Syringe, at least 10 ml capacity. Syringes can be PPE disposable type. Do not use syringes with a rubber seal.

3.2. Sharp/bevel needles, 1.5-2", 20 gauge or higher.

3.3. Syringe filters (four filters are required per typical test resulting in two asphaltene measurements and two samples for S-A-R analysis); PTFE,

0.2 or 0.22 μm, 25-30 mm diameter, preferably hydrophobic. The pore size and material for the syringe filter are extremely important and should be maintained for compatible analysis between different laboratories. Example: Thermo Scientific™ Titan3™ PTFE (Hydrophobic) Syringe Filters (item 14-823-288).

3.4. Solid phase extraction (SPE) cartridges (two cartridges are required per test resulting in two measurements), 5 g silica gel with 20 ml capacity. Specifications for the cartridges should be maintained thoroughly for compatible analysis. Example: Supelco Supelclean™ LC-Si SPE Tube (item 57133).

3.5. Vials with septa top; Example: Thermo Scientific™ Vials with Septa (Item 12-100-108).

4. Solvents (all HPLC grade)

4.1. n-Heptane

4.2. Toluene

4.3. Dichloromethane (DCM)

4.4. Methanol

A.6 Safety Precautions

The solvents used in this procedure are flammable, have fast evaporation rate at room temperature and toxic in some cases. MSDS should be consulted prior to use and appropriate measures to ensure safety of personnel and property must be followed.

A.7 Separation of bitumen into asphaltenes and maltenes

1. Dissolution of bitumen in n-Heptane:

1.1. Melt the bitumen sample to be tested until it is of the consistency of a liquid that can easily be poured. Use a metal spoon to stir and homogenize the sample. Deposit a dollop of the bitumen sample on to

the pre-weighed silicone sheet or mold. The weight of the bitumen should be 400±40 mg. If necessary, trim the sample with clean spatula to achieve desired weight. Determine the amount of the bitumen sample ($M_{bitumen}$).

1.2. In a wide mouth glass bottle of appropriate size, pour 40 mL of n-Heptane. Place the magnetic stirrer bar into the bottle and put the bottle on the stirring plate adjusting the stirring speed close to 200 RPM. Take the pre-weighed dollop of bitumen from the silicone sheet and gently drop it into the bottle with stirring n-Heptane. Special care should be taken so that no part of bitumen remains behind on the sheet. Minimize the time between pouring the solvent and dropping the bitumen solvent to prevent evaporation of n-Heptane.

(a) Sample weighing to 0.01 mg accuracy.

(b) Preparation for bitumen dissolution in

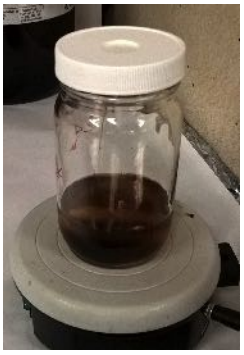

(c) Bitumen with n-Heptane on stirrer.

Figure A.1: Bitumen dissolution setup for separation of asphaltene and maltenes

1.3. Close the lid immediately and use a syringe with a sharp bevel needle to draw air out of the bottle through the septa. Draw approximately 1.25 times the volume of the air space in the bottle after filling it with heptane. This will ensure that the solution is exposed to n-Heptane vapors and not air. The stirrer should run for 24±2 hour.

1.4. During the process of dissolution, bitumen may create 'streaks' on the wall of the bottle. Also particles may get stuck above fluid level due to stirring. Dark specks that get deposited on the walls are asphaltene particles. However, lighter colored streaks are maltenes or partially dis-

Figure A.2: Set-up for asphaltene filtration.

solved bitumen. Manually tilting or swirling the bottle can help to redissolve the bitumen and maltenes stuck to the walls above the fluid level. However, this may not always remove the specks of dark asphaltenes. It is important to ensure that all the maltene and bitumen is dissolved and remains in the bulk.

2. Filtration of undissolved asphaltene:

   2.1. Take four syringes and remove their plungers. Attach a syringe filter (25-30 mm dia, PTFE, 0.2-0.22 μm pore size) to the tip of each syringe and push it into a vacuum manifold port. Ensure that a pre-weighed vial is placed under each port in the manifold.

   2.2. Push the thick blunt needle (<14 gauge) through the septa into the bottle with the solution while it is still on the stirrer. Also insert a sharp bevel needle through the septa to prevent creation of vacuum in the bottle

when drawing the solution. Attach a PPE syringe to the blunt needle. Draw 10 ml of maltene-asphaltene solution into a syringe while the solution is being stirred. Gently pull the needle to a point where it is above the liquid level. Draw a a very small amount of air into the syringe (to prevent solution from dripping out from the tip when the needle is removed).

2.3. Gently remove the syringe from the blunt end needle. Discharge the contents of the syringe into one of the empty syringes (without the plunger) on the vacuum manifold.

2.4. Repeat the above process three more times and discharge 10 mL of the solution into each syringe/port. The last draw may be less than 40 mL due to evaporation losses of n-Heptane. Record the exact volume of this last draw from the syringe ($V_{maltene4}$).

2.5. Turn on the vacuum pump and discharge the solution from the mounted syringes via the filter as seen in Figure A.3 (only one syringe is shown in the Figure for clarity). NOTE: Most vacuum manifolds allow you to open and adjust the level of vacuum on each vial; use this adjustment to control the flow of the solution so that the solution does not splash and takes at least two to three minutes to slowly discharge. Once all the solution has discharged, add an additional 5 mL of n-Heptane to each syringe to dissolve and remove any remaining maltene from the filter into the vial below.

2.6. Dry two of the vials containing 10 mL maltene solution in an oven to a constant weight, preferably under a nitrogen purge. The n-Heptane vapor produced during this process should be condensed through a Graham condenser-cold water setup or any other suitable solvent recovery process. The other two vials must be sealed and set aside for S-A-R measurement.

2.7. Dried maltene from the vials should be weighed after cooling to room temperature. Note that for accurate measurement the samples, vials, etc. being weighed must be in close proximity to the balance for a few minutes and at the same temperature. The maltene content in percentage is

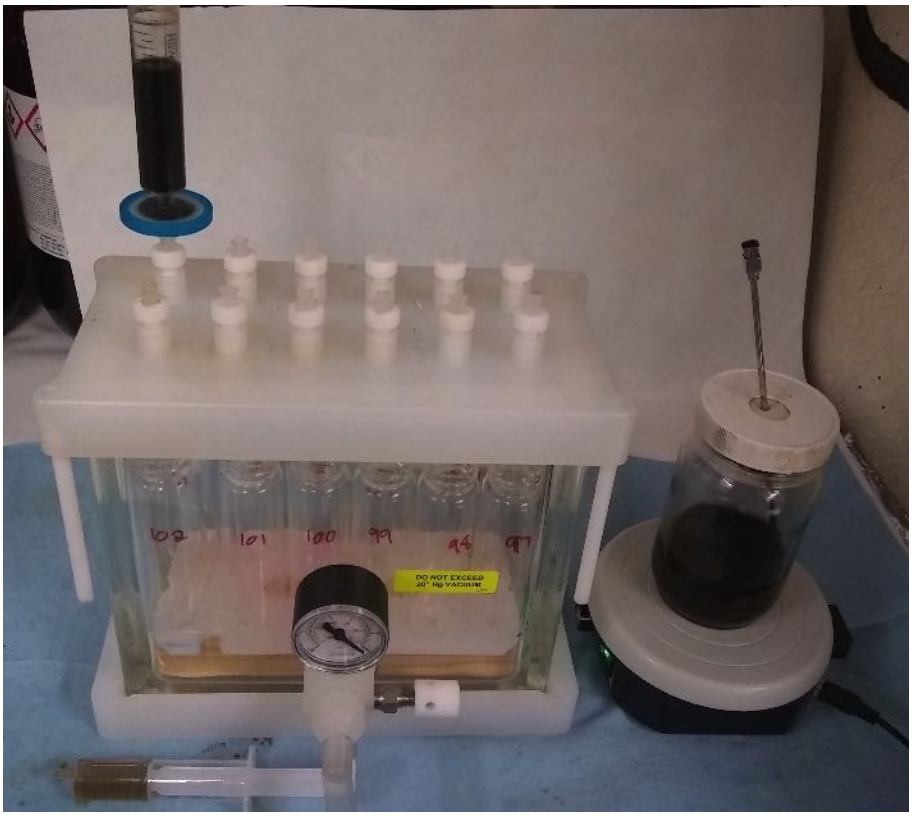

Figure A.3: Collection of maltene filtrate

determined as (100*$M_{maltene}$)/$\frac{M_{bitumen}*10}{30+V_{maltene4}}$, where $M_{maltene}$ is the mass of maltene in a single vial.

A.8 Separation of maltenes into S-A-R fractions

1. Take the third and fourth vials with the maltene-n-Heptane solution for further separation. Using the known maltene concentration from the previous step, dilute each vial with n-Heptane to achieve a 3.33 mg/mL solution. Draw 15 mL of this solution ($\approx$ 50 mg maltene) from each vial in separate syringes.

2. Prepare solutions of pure n-Heptane (20 mL and 10 mL in two different syringes or beakers), 80% Toluene- 20% n-Heptane (total 25 mL), and 90% DCM- 10% Methanol (total 40 mL). The solutions must be in syringes or beakers; while using latter ensure that the beakers are covered to minimize evaporation.

3. Prepare vacuum manifold by connecting it to a vacuum source. Place pre-weighed vials (each 40 ml capacity) below the ports and ensure that liner coming from the port discharges directly into the desired vial. At least 4 ports are necessary to be used for collection of pre-wash, saturates, aromatics, and resins, respectively. Place the cover on the manifold ensuring vacuum lock.

4. Mount a fresh SPE cartridge (5 g silica gel, 20 ml capacity) on the pre-wash location of the manifold while keeping the nozzle/vacuum closed. Pour 20 mL of n-Heptane into the SPE cartridge and turn on the vacuum. Adjust the port nozzle so that the flow of the solvent is in form of continuous drops (about 3-4 per second). Stop the flow immediately using the port nozzle when there is no more free liquid being discharged into the vial (at this time the liquid mixes with air and starts to sputter). Care should be taken not to leave the port open for too long which may dry the cartridge. The typical duration for this step is approximately 3-4 minutes.

5. Transfer the cartridge over to the next port/vial for collection of saturates. Completely close the port nozzle. Introduce 15 mL of maltene-heptane solution from one of the prepared syringes and slowly open the port nozzle to

apply vacuum as in the previous step. When there is no more free liquid at the top of the silica in the cartridge, immediately add 10 mL of n-heptane. As before, close the port nozzle and stop vacuum when no drops are visible at the exit for 3 seconds (liquid sputtering is typically seen at this time).

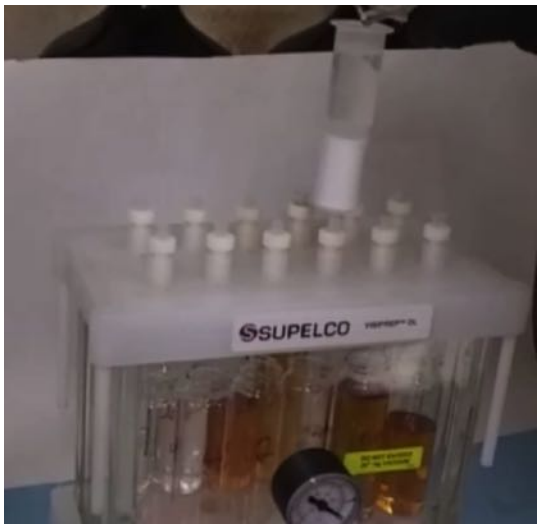

(a) Pre-washing the cartridge with n-heptane.

(b) Addition of maltene and saturates fractionation.

Figure A.4: Preparing the cartridge and addition of maltene for saturates separation

6. Transfer the cartridge to the next vial to separate aromatics. Stir and pour 25 mL of the 80% Toluene- 20% n-Heptane solution and apply vacuum as in the previous step. Solvent can be gradually added while vacuum is being applied if the volume of solvent exceeds the free capacity of the cartridge. Close the port nozzle and stop vacuum if no drops are visible for 3 seconds.

7. Move the cartridge to the next vial to separate and collect resins. Pour 40 mL of 90% DCM- 10% Methanol and apply vacuum as done in previous steps. Stop vacuum when the cartridge appears uniform and dry. The solvents, their amount and sequence are summarized in Table A.1.

8. (Optional step for consistency check) Combine and pour 15 mL of the remaining maltene-n-Heptane solution using a syringe into a pre-weighed vial.

Figure A.5: Elution of aromatics through SPE cartridges at three different phases.

Figure A.6: Elution of resins through SPE cartridges at different phases.

(a) Fractionation products and SPE cartridges after elution.

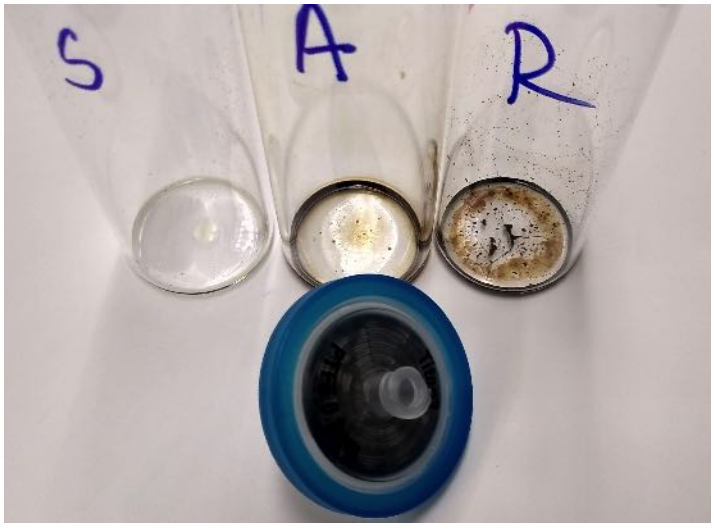

(b) Collected bitumen fractions after drying.

Figure A.7: Final fractionation products after elution and drying.

Table A.1: Solvent Schedule of S-A-R separation using SPE cartridge.

Elutant Solvent	mL	Collected Fraction
n-Heptane	20	Pre-wash
maltene solution + n-Heptane	15 + 10	Saturates
80% Toluene - 20% n-Heptane	25	Aromatics
90% DCM - 10% Methanol	40	Resins

9. Dry all bottles except pre-wash in the same way as the maltene solution was dried after asphaltene separation process. Weigh the bottles after being cooled and gravimetrically measure the S-A-R fraction ($M_{saturate}$, $M_{aromatics}$, M_{resins}, respectively).

10. (For optional step) Weigh the amount of maltene from the 15 mL solution ($M_{maltene_{15ml}}$) and compare this to the sum of the S-A-R mass fractions from the step above to verify that there was no loss during the separation process. The difference is typically less than 2%.

A.9 Calculation

1. $\%Maltene = \frac{M_{maltene}}{M_{bitumen}}$
2. $\%Asphaltene = 100\% - \%Maltene = \frac{M_{asphaltene}}{M_{bitumen}} = \frac{M_{bitumen} - M_{maltene}}{M_{bitumen}}$.
3. Check: $M_{maltene_{15ml}} = (1 \pm 0.02) \times (M_{saturates} + M_{aromatics} + M_{resins})$
4. $\%Saturates = \frac{M_{saturates}}{M_{maltene_{15ml}}} \times \frac{\%Maltene}{100}$
5. $\%Aromatics = \frac{M_{aromatics}}{M_{maltene_{15ml}}} \times \frac{\%Maltene}{100}$
6. $\%Resins = \frac{M_{resins}}{M_{maltene_{15ml}}} \times \frac{\%Maltene}{100}$

A.10 Precision and Bias

Not established.

Appendix B: Effect of filter pore size on asphaltene content

To study the effect of filter pore size, syringe filters of three different porosity were selected along with medium porosity fritted glass filter on buchner funnel. These filters were PTFE-made 0.2 μm pore, glass microfiber made 1μm and glass microfiber made 2.2 μm while the medium porosity fritted glass is known to have 10 to 15 μm pores. These syringe filters are small in size (25-35 mm dia) and commercially available. The fritted glass filter was 50 mm dia and about 5-6 mm thick.

1g of bitumen is placed into 100 ml n-heptane solvent in a glass jar. The solution was stirred for 1 day. Pre-weighted bottles were arranged and filters were placed appropriately. There were two filters for each filter type except for a single fritted glass filter. Each syringe filters processed 10 ml of solution whereas 20 ml solution was filtered using the only fritted glass filter.

The filtrate from each type of filters were collected in a single bottle which was then dried under nitrogen blanket and weighted. The measured weight indicates the weight of the maltene which is then subtracted from the total asphalt content to measure asphaltene. The measured asphaltene content is presented in the table B.1 below:

Table B.1: Filter types and respective Asphaltene content for n-heptane and iso-octane

Filter Type	Asphaltene Content (% w/w)
0.2μm PTFE	24.3
1μm GMF	23.5
2.2μm GMF	21.2
Fritted Glass	16.4
Fritted Glass with iso-octane (Sultana et al. 2014)	18.2

Bibliography

Allen, R., Little, D., Bhasin, A., and Glover, C. (2014). The effects of chemical composition on asphalt microstructure and their association to pavement performance. *International Journal of Pavement Engineering*, 15(1):9–22.

Allen, R. G., Little, D. N., and Bhasin, A. (2012). Structural Characterization of Micromechanical Properties in Asphalt Using Atomic Force Microscopy. *Journal of Materials in Civil Engineering*, 24(10):1317–1327.

Arnold, T. and Shastry, A. (2015). Analysis of asphalt binders for recycled engine oil bottoms by x-ray fluorescence spectroscopy. In *Transportation Research Board 94th Annual Meeting*, Washington DC, USA.

ASTM D2007 (2016). Standard Test Method for Characteristic Groups in Rubber Extender and Processing Oils by Clay-Gel Adsorption Chromatography Method. *ASTM International*.

ASTM D3279 (1997). Standard Test Method for n-Heptane Insolubles. *ASTM International*.

ASTM D4124 (2009). Standard Test Methods for Separation of Asphalt into Four Fractions. *ASTM International*.

ASTM D6560 (2012). Standard Test Method for Determination of Asphaltenes (Heptane Insolubles) in Crude Petroleum and Petroleum Products. *ASTM International*.

Batista, F., Hofko, B.and De Visscher, J., Tanghe, T., and da Costa, M. (2017). Towards improved correlations between bitumen properties and rutting resistance of bituminous mixtures: Fundbits literature review. *IOP Conference Series: Materials Science and Engineering*, 236(1).

Baumgardner, G. L. (2012). Why and how of polyphosphoric acid modification. Technical Report Transportation Research Circular E-C160, Transportation Research Board.

Bhasin, A. and Ganesan, V. (2015). Preliminary investigation of using a multi-component phase field model to evaluate microstructure of asphalt binders. *International Journal of Pavement Engineering*, 0(0):1–8.

Boysen, R. and Schabron, J. (2015). Automated HPLC SAR-AD Separation. Technical Report FP01, Western Research Institute.

Branthaver, J., Petersen, J., Robertson, R., Duvall, J., Kim, S., Harnsberger, P., Mill, T., Ensley, E., Barbour, F., and Scharbron, J. (1993). Binder characterization and evaluation. volume 2: Chemistry. Technical Report SHRP-A-368, Strategic Highway Research Program.

Cebolla, V. L., Lazaro, M. J., and Herod, A. A. (2016). Petroleum Products-Thin Layer (Planar) Chromatography. In *Reference Module in Chemistry, Molecular Sciences and Chemical Engineering*. Elsevier.

Cebolla, V. L., Matt, M., Galvez, E. M., Membrado, L., Domingo, M. P., Vela, J., Beregovtsova, N., Sharypov, V., Kuznetsov, B. N., Marin, N., and Weber, J. V. (2002). Application of thin-layer chromatography with fluorescence scanning densitometry for analysing saturates in heavy liquids derived from Co-pyrolysis of biomass and plastics. *Chromatographia*, 55(1-2):87–93.

Cebolla, V. L., Membrado, L., Domingo, M. P., Henrion, P., Garriga, R., Gonzalez, P., Cossio, F. P., Arrieta, A., and Vela, J. (1999). Quantitative applications of fluorescence and ultraviolet scanning densitometry for compositional analysis of petroleum products in thin-layer chromatography. *Journal of chromatographic science*, 37(6):219–226.

Cebolla, V. L., Membrado, L., Matt, M., Galvez, E. M., and Domingo, M. P. (2003). Thin-layer chromatography for hydrocarbon characterization in petroleum middle distillates. In *Analytical Advances for Hydrocarbon Research*, pages 95–112. Springer.

Claudy, P., Letoffe, J., King, G., and Plancke, J. (1992). Characterization of asphalts cements by thermomicroscopy and differential scanning calorimetry: Correlation to classic physical properties. *Journal of microscopy*, 10(4-6):735–765.

Corbett, L. W. (1969). Composition of Asphalt Based on Generic Fractionation, Using Solvent Deasphaltening, Elution-Adsorption Chromatography, and Densimetric Characterization. *Analytical Chemistry*, 41(4):576–579.

Daly, W. (2017). *NCHRP 511: Relationship Between Chemical Makeup of Binders and Engineering Performance*. National Academy of Sciences.

D'Angelo, J. (2009). Current status of superpave binder specification. *Road Materials and Pavement Design*, 10(1).

Das, P. K., Kringos, N., Wallqvist, V., and Birgisson, B. (2013). Micromechanical investigation of phase separation in bitumen by combining atomic force microscopy with differential scanning calorimetry results. *Road Materials and Pavement Design*, 14(sup1):25–37.

Delgadillo, R., Nam, K., and Bahia, H. (2006). Why do we need to change g/sin(delta) and how? *Road Materials and Pavement Design*, 7.

Eberhardsteiner, L., Fussl, J., Hofko, B., Handle, F., Hospodka, M.and Blab, R., and Grothe, H. (2015). Influence of asphaltene content on mechanical bitumen behavior: experimental investigation and micromechanical modeling. *Materials and Structures*, 48(10).

Fan, T. and Buckley, J. S. (2002). Rapid and Accurate Sara Analysis of Medium Gravity Crude Oils. *Energy and Fuels*, 16:1571–1575.

Fan, T., Wang, J., Buckley, J. S., and others (2002). Evaluating crude oils by SARA analysis. In *SPE/DOE Improved Oil Recovery Symposium*. Society of Petroleum Engineers.

FHWA (2016). Highway statistics 2016. Technical report, Federal Highway Administration.

Glaser, R., Planche, J., Turner, F., Boysen, R., Schabron, J., Delfossa, F., Drouadaine, I., Faucon-Dumont, S., Largeaud, S., and Eckmann, B. (2016). Relationships between solubility and chromatographically defined bitumen fractions and physical properties. *6th Eurasphalt and Eurobitume Congress*.

Gocan, S. (2005). Sample application in TLC. In *Encyclopedia of Chromatography, Second Edition*, pages 1480–1486. CRC Press.

Guo, M., Bhasin, A., and Tan, Y. (2017). Effect of mineral fillers adsorption on rheological and chemical properties of asphalt binder. *Construction and Building Materials*, 141:152–159.

Guzman, R., Ancheyta, J., Trejo, F., and Rodriguez, S. (2017). Methods for determining asphaltene stability in crude oils. *Fuel*, 188.

Hajj, R. and Bhasin, A. (2017). The search for a measure of fatigue cracking in asphalt binders âĂŞ a review of different approaches. *International Journal of Pavement Engineering*, 19(3).

Hajj, R., Hure, R., and Bhasin, A. (2017). Evaluation of stiffness, strength, and ductility of asphalt binders at an intermediate temperature. *Transportation Research Record: Journal of the Transportation Research Board,*, 2632.

Hansen, C. M. (1967). The three dimensional solubility parameter. *Copenhagen Denmark: Danish Technical*, page 14.

Hansen, C. M. (2007). *Hansen solubility parameters: a user's handbook*. CRC press.

Hildebrand, J. H. (1936). *Solubility of non-electrolytes*. Chapman & Hall, Ltd, 2nd edition.

Hofko, B., Eberhardsteiner, L., Fussl, J., Grothe, H., Handle, F., Hospodka, M., Grossegger, D., Nahar, S., Schmets, A., and Scarpas, A. (2016). Impact of maltene and asphaltene fraction on mechanical behavior and microstructure of bitumen. *Materials and Structures*, 49(3).

Hure, R. (2017). *Beyond the PG Specification for Asphalt Binders*. The University of Texas at Austin.

IP469 (2006). Determination of saturated, aromatic and polar compounds in petroleum products by thin layer chromatography and flame ionization detector. *Energy Institute*.

Isacsson, U. and Zeng, H. (1997). Relationships between bitumen chemistry and low temperature behaviour of asphalt. *Construction and Building Materials*, 11(2):83–91.

Jahangir, R., Little, D., and Bhasin, A. (2015). Evolution of asphalt binder microstructure due to tensile loading determined using afm and image analysis techniques. *International Journal of Pavement Engineering*, 16(1):337–349.

Jarne, C., Cebolla, V. L., and Membrado, L. (2015). Gradient-based high performance thin-layer chromatography for an expanded SARA analysis of heavy petroleum products. In *250th Americal Chemical Society National Meeting and Exposition Proceedings*. American Chemical Society, Division of Energy and Fuel.

Jewel, D. M., Weber, J. H., Bunger, J. W., Plancher, H., and Latham, D. R. (1972). Ion-Exchange, Coordination, and Adsorption Chromatographic Separation of Heavy-End Petroleum Distillates. *Analytical Chemistry*, 44(8):1391–1395.

Karlsen, D. A. and Larter, S. R. (1991). Analysis of petroleum fractions by TLC-FID: applications to petroleum reservoir description. *Organic Geochemistry*, 17(5):603–617.

Kharrat, A. M., Zacharia, J., Cherian, V. J., and Anyatonwu, A. (2007). Issues with Comparing SARA Methodologies. *Energy and Fuels*, 21:3618–3621.

Loeber, L., Sutton, O., Morel, J., Valleton, J.-M., and Muller, G. (1996). New direct observations of asphalts and asphalt binders by scanning electron microscopy and atomic force microscopy. *Journal of Microscopy*, 182(1):32–39.

Lyne, Ã., Wallqvist, V., Rutland, M., Claesson, P., and Birgisson, B. (2013). Surface wrinkling: the phenomenon causing bees in bitumen. *Journal of materials science*, 48(20):6970–6976.

Masson, J., Price, T., and Collins, P. (2001). Dynamics of Bitumen Fractions by Thin-Layer Chromatography/Flame Ionization Detection. *Energy and Fuels*, 15:955–960.

Masson, J.-F., Leblond, V., and Margeson, J. (2006). Bitumen morphologies by phase-detection atomic force microscopy. *Journal of Microscopy*, 221(1):17–29.

Matt, M., Galvez, E., Cebolla, V., Membrado, L., Vela, J., and Gruber, R. (2002). Planar chromatography for the hydrocarbon group type analysis of petroleum middle distillates and coal-derived products. *Fuel Processing Technology*, 77-78:245–253.

Matt, M., Galvez, E. M., Cebolla, V. L., Membrado, L., Bacaud, R., and Pessayre, S. (2003). Improved separation and quantitative determination of hydrocarbon types in gas oil by normal phase high-performance TLC with UV and fluorescence scanning densitometry. *Journal of Separation Science*, 26(18):1665–1674.

Menapace, I., Masad, E., and Bhasin, A. (2016). Menapace, i., masad, e. and bhasin, a., 2016. effect of treatment temperature on the microstructure of asphalt binders: insights on the development of dispersed domains. *Journal of microscopy*, 262(1):12–27.

Motamed, A., Bhasin, A., and Liechti, K. (2014). Using the poker-chip test for determining the bulk modulus of asphalt binders. *Mechanics of Time-Dependent Materials*, 18(1).

Nahar, S. (2016). *Phase-separation characteristics of bitumen and their relation to damage-healing*. PhD thesis, Delft University of Technology.

Pauli, A. and Branthaver, J. (1998). Relationships between asphaltenes, heithaus compatibility parameters, and asphalt viscosity. *Petroleum science and technology*, 16(9-10).

Pauli, A., Branthaver, J., Robertson, R., Grimes, W., and Eggleston, C. (2001). Atomic force microscopy investigation of shrp asphalts: Heavy oil and resid compatibility and stability. *Preprints-American Chemical Society. Division of Petroleum Chemistry*, 46(2):104–110.

Pauli, A. T., Grimes, R. W., Beemer, A. G., Turner, T. F., and Branthaver, J. F. (2011). Morphology of asphalts, asphalt fractions and model wax-doped asphalts studied by atomic force microscopy. *International Journal of Pavement Engineering*, 12(4):291–309.

Poole, C. F. (2015). Solvent Selection and Method Development. In *Instrumental Thin-Layer Chromatography*, pages 313–350. Elsevier.

Popovic, N. and Sherma, J. (2014). Comparative study of the quantification of thin-layer chromatograms of a model dye using three types of commercial densitometers and image analysis with ImageJ. *Trends in Chromatography*, 9:21–28.

Radenberg, M., Nytus, N., and Gehrke, M. (2014). Chemische und physikalische eigenschaften der in deutschland verwendeten strabenbaubitumen. *Strabe und Autobahn*, 65(11).

Ramm, A., Sakib, N., Bhasin, A., and Downer, M. (2016). Optical characterization of temperature and composition dependent microstructure in asphalt binders. *Journal of microscopy*, 262(3).

Ramm, A., Sakib, N., Bhasin, A., and Downer, M. (2018). Correlated time variation of bulk microstructure and rheology in asphalt binders. *Journal of microscopy*, 271(3).

Redelius, P. (2004). Bitumen Solubility Model Using Hansen Solubility Parameter. *Energy & Fuels*, 18(4):1087–1092.

Redelius, P. and Soenen, H. (2015). Relation between bitumen chemistry and performance. *Fuel*, 140:34–43.

Redelius, P. G. (2000). Solubility parameters and bitumen. *Fuel*, 79(1):27–35.

Robertson, R., Branthaver, J.F.and Harnsberger, P. P. J. D. S. M. J., Turner, T., Pauli, A., Huang, S., Huh, J., and Tauer, J. (2001). Fundamental properties of asphalts and modified asphalts, volume i: Interpretive report. Technical Report FHWA-RD-99-212, Western Research Institute.

Rogel, E., Ovalles, C., Vien, J., and Moir, M. (2016). Asphaltene content by the in-line filtration method. *Fuel*, 171:203–209.

Sakib, N. and Bhasin, A. (2018). Measuring polarity-based distributions (sara) of bitumen using simplified chromatographic techniques. *International Journal of Pavement Engineering*, pages 1–14.

Santagata, E., Baglieri, O., Dalmazzo, D., and Tsantilis, L. (2009). Rheological and chemical investigation on the damage and healing properties of bituminous binders. *Asphalt Paving Technology-Proceedings*, 28:567.

Schabron, J. F. and Rovani, J. F. (2008). On-Column Precipitation and Re-Dissolution of Asphaltenes in Petroleum Residua. *Fuel*, 87:165–175.

Schabron, J. F., Rovani, J. F., and Sanderson, M. M. (2010). Asphaltene Determinator Method for Automated On-Column Precipitation and Redissolution of Peri-condensed Aromatic Asphaltene Components. *Energy and Fuels*, 24:5984–5996.

Schmets, A., Kringos, N., Pauli, T., Redelius, P., and Scarpas, T. (2010). On the existence of wax-induced phase separation in bitumen. *International Journal of Pavement Engineering*, 11(6):555–563.

Sepulveda, J., Bonilla, J., and Medina, Y. (2017). Prediccion de la estabilidad de los asfaltenos mediante lautilizacion del analisis sara para petroleos puros. *Revista Ingenieria y Region*, 7.

Soenen, H., Besamusca, J., Fischer, H., Poulikakos, L., Planche, J., Das, P., Kringos, N., Grenfell, J., Lu, X., and Chailleux, E. (2014). Laboratory investigation of bitumen based on round robin dsc and afm tests. *Materials and structures*, 47(7):1205–1220.

Soenen, H., Visscher, J. D., Vanelstraete, A., and Redelius, P. (2006). Influence of thermal history on rheological properties of various bitumen. *Rheologica Acta*, 45(5):729–739.

Stangl, K. (2010). *Linking chemical and physical characteristics with mechanical performance of bitumen*. PhD thesis, Vienna University of Technology.

Sultana, S. (2014). *Tensile strength of asphalt binder and influence of chemical composition on binder rheology and strength*. PhD thesis, The University of Texas at Austin.

Sultana, S. and Bhasin, A. (2014). Effect of chemical composition on rheology and mechanical properties of asphalt binder. *Construction and Building Materials*, 72:293–300.

Sultana, S., Bhasin, A., and Liechti, K. M. (2014). Rate and confinement effects on the tensile strength of asphalt binder. *Construction and Building Materials*, 53:604–611.

Suzuki, Y. (1972). Studies on Quantitative TLC by means of a Hydrogen FID. II Rapid Analysis of Fuel Oil Constituents,âĂIJ. In *21st Annual Meeting of the Japan Society for Analytical Chemistry*, volume 47.

Vela, J., Cebolla, V. L., Membrado, L., and Andres, J. M. (1995). Quantitative hydrocarbon group type analysis of petroleum hydroconversion products using an improved TLC-FID system. *Journal of chromatographic science*, 33(8):417–425.

Wan, C. C., Waters, T. H., and Wolever, R. D. (1992). Development of a Reproducible Iatroscan Method to Chemically Characterize Asphalt. *American Chemical Society, Division of Fuel Chemistry Preprints*, pages 1350–1359.

Weigel, S. and Stephan, D. (2018). Relationships between the chemistry and the physical properties of bitumen. *Road Materials and Pavement Design*, 19(7).

Yu, H., Le, H. M., Kaale, E., Long, K. D., Layloff, T., Lumetta, S. S., and Cunningham, B. T. (2016). Characterization of drug authenticity using thin-layer chromatography imaging with a mobile phone. *Journal of Pharmaceutical and Biomedical Analysis*, 125:85–93.